RF-3103-A1

Institute of Polar Studies

Report No. 56

Glacial Geology and Late Cenozoic History of the Transantarctic Mountains, Antarctica

by

Paul A. Mayewski
Institute of Polar Studies

November, 1975

The Ohio State University
Research Foundation
Columbus, Ohio 43212

Institute of Polar Studies

Report No. 56

GLACIAL GEOLOGY AND LATE CENOZOIC HISTORY OF THE TRANSANTARCTIC MOUNTAINS, ANTARCTICA

by

Paul A. Mayewski

Institute of Polar Studies
The Ohio State University

November 1975

The Ohio State University
Research Foundation
Columbus, Ohio 43212

ABSTRACT

A glacial geology for the Transantarctic Mountains is determined, based on a comparison of glacial deposits in the Queen Maud Mountains and along the nunataks at the heads of the ice-free valleys of southern Victoria Land with deposits studied by other workers in southern Victoria Land. Based on the terminology adopted in the Queen Maud Mountains and on correlations with deposits dated by Behling, Denton, Fleck and others in southern Victoria Land, the glacial chronology of the Transantarctic Mountains includes the:

Event	Maximum Time Span
Amundsen Glaciation	< 9,490 y. B.P.
Shackleton Glatiation	49,000 y. to 1.6 m.y. B.P.
Scott Glaciation	2.1 m.y. to 2.4 m.y. B.P.
"Interglacial"	
Queen Maud Glaciation	> 4.2 m.y. B.P.

The deposit used to define the Queen Maud Glaciation is the Sirius Formation which is composed of two members: (1) lodgement till and (2) stratified ice-contact deposits. This formation is dintinguished and interpreted by the investigation of the elevation of outcrop, underlying striae and grooves, structure, fabric of elongate clasts, particle size distribution, lithologic and mineralogic components, and rounding and freshness of contained clasts.

Fluvial features including channels and potholes are used as evidence of the "interglacial" period which followed the Queen Maud Glaciation. These features represent far more extensive amounts of meltwater than are presently noted in the Transantarctic Mountains during even the height of the ablation season.

The Scott, Shackleton and Amundsen Glaciations are differentiated by three sets of lateral moraines which can be traced throughout the Transantarctic Mountains. These moraines are named from oldest to youngest: High, Middle and Low Moraines. They are distinguished by the investigation of the elevation and continuity relative to present ice surface, morphology, thickness of drift, presence or lack of an ice core, and weathering of surficial clasts. In addition, several characteristics of the soils developed in these moraines are also used: particle size distribution, color, secondary salt content, acidity - alkalinity, and clay mineral content.

Ice surface reconstructions are developed for the former glaciations recorded in the Transantarctic Mountains. These reconstructions are generated from a study of the distribution of the glacial deposits

used to determine the glacial chronology since these deposits record former ice levels in the Transantarctic Mountains. The ice surfaces of former glaciations in these mountains are extrapolated inland to generate former ice sheet surface profiles and out onto the Ross Ice Shelf to determine former grounding lines and ice thicknesses in this area.

The ice surface reconstructions indicate that during the Queen Maud Glaciation the Transantarctic Mountains were almost completely covered by ice. The East Antarctic sheet was as much as 350 meters thicker in the area of the present ice divide. A grounding line in the Ross Sea area extended 225 kilometers north of the present terminus of the Ross Ice Shelf.

During the "interglacial" period which followed the Queen Maud Glaciation, the Antarctic ice sheet shrank to possibly less than its present dimensions. Three readvances follow this interglacial corresponding to the Scott, Shackleton and Amundsen Glaciation. Each readvance is marked by progressively less ice cover over the Transantarctic Mountains. The elevation of the ice sheet at the ice divide probably never exceeded 100 meters more than the present elevation during these glaciations. Grounding lines in the Ross Ice Shelf area were situated closer to the coast during each successive glaciation, finally resulting in the present, or Amundsen Glaciation grounding line.

Ice volumes are determined from the ice surface profiles of the former glaciations. These ice volumes are extrapolated over the area of Antarctic grounded ice and ice shelves, assuming the Transantarctic Mountains reflect glacial events over the whole continent. The ice volumes are converted to sea level equivalents to determine the effect of Antarctic glaciations on worldwide sea level.

ACKNOWLEDGMENTS

This report is part of a continuing investigation in the Trans-antarctic Mountains, Antarctica, undertaken by the Institute of Polar Studies at The Ohio State University. It is the result of work completed during the 1968-69, 1970-71 and 1971-72 field seasons.

I would like to thank Dr. Richard P. Goldthwait for his support and guidance at The Ohio State University and Dr. Parker E. Calkin, State University of New York at Buffalo, for introducing me to Antarctic research.

Mr. Stephen D. Etter and Robert S. Wilkinson were of great assistance in both the scientific and logistic aspects of the field work. Antarctic Development Squadron Six, U.S. Navy, provided invaluable helicopter support. In particular I am grateful to Lieutenant Commanders "Doc" Kinsey, G. Skaar, L. McKay, A. Dyer, V. Mizner and Chief L. Trail. H. Mehrling, at the Institute of Polar Studies, prepared the necessary scientific equipment to conduct field research.

Several individuals contributed to the lab analyses referred to in this report: J.M. Schopf, U.S. Geological Survey Coal Laboratory at The Ohio State University (microflora studies), P.N. Webb and B. Burt, New Zealand Geological Survey (scanning electron microscopy), G. Faure, J. Muskopf, and S. Derksen, Department of Geology and Mineralogy, The Ohio State University (x-ray diffraction studies), and D. Drees and L. Jones, Department of Agronomy, The Ohio State University (x-ray diffraction, electrical conductivity and acidity-alkalinity studies).

Dr. R.P. Goldthwait, C. Bull, K. Everett, T. Hughes, J. Mercer, H. Noltimier of The Ohio State University, and A. Weidick, Greenland Geological Survey, Copenhagen, Denmark, reviewed this manuscript. H. Ehrenspeck designed and drafted the figures. Judy Hower edited the final manuscript which was prepared for publication by Jean Cothran and Peter Anderson.

This research was made possible by National Science Foundation grants GA-4029 and GV-26652 to the Institute of Polar Studies and The Ohio State University Research Foundation.

CONTENTS

CONTENTS

CONTENTS

LIST OF ILLUSTRATIONS

LIST OF ILLUSTRATIONS (cont'd)

LIST OF ILLUSTRATIONS (cont'd)

LIST OF ILLUSTRATIONS (cont'd)

LIST OF ILLUSTRATIONS (cont'd)

LIST OF TABLES

LIST OF TABLES (cont'd)

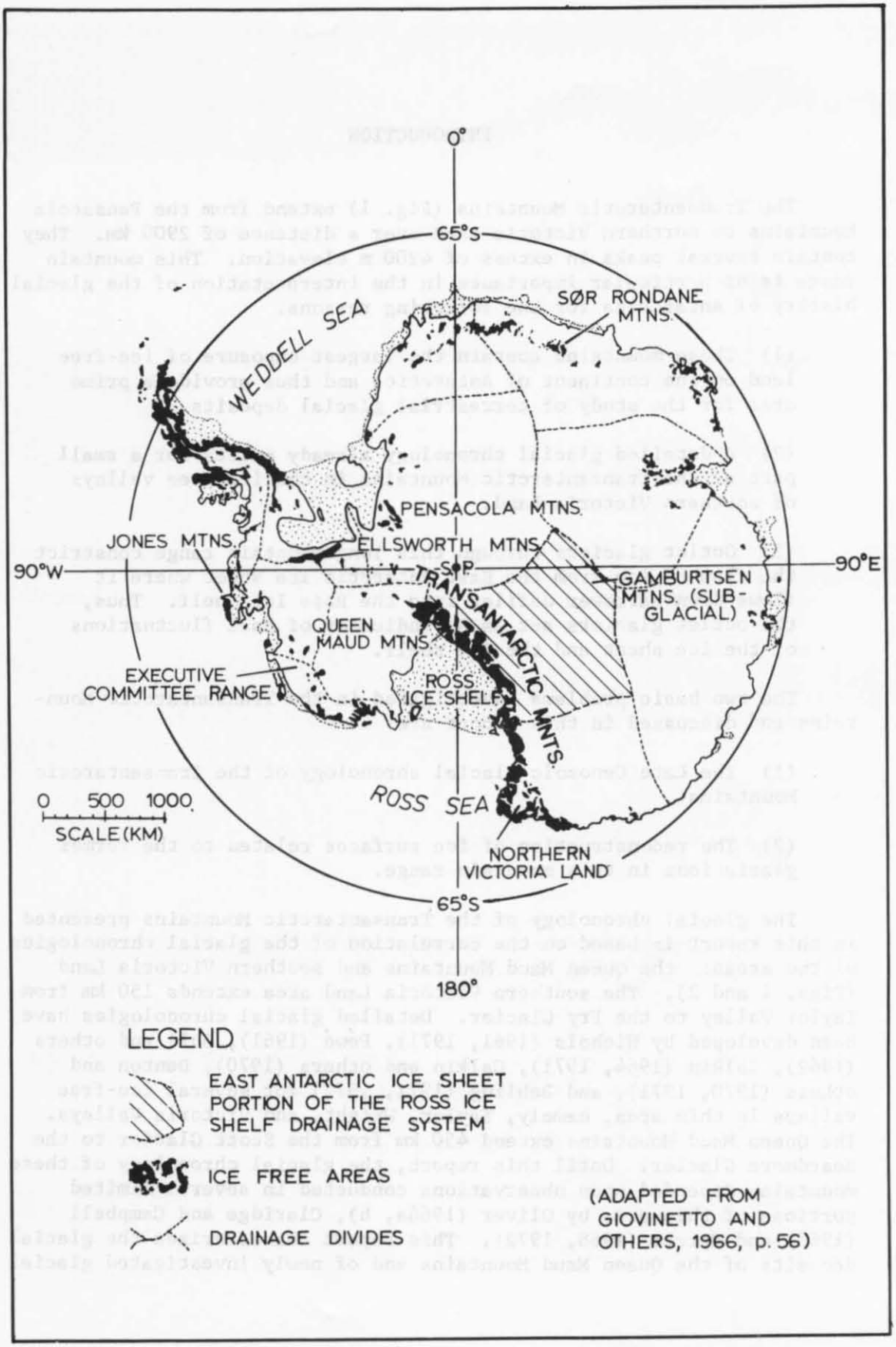
0°
65°S
SØR RONDANE MTNS.
WEDDELL SEA
PENSACOLA MTNS.
JONES MTNS.
ELLSWORTH MTNS.
90°W
S.P.
90°E
GAMBURTSEN MTNS. (SUB-GLACIAL)
TRANSANTARCTIC MNTS.
QUEEN MAUD MTNS.
EXECUTIVE COMMITTEE RANGE
ROSS ICE SHELF
0 500 1000
SCALE (KM)
ROSS SEA
NORTHERN VICTORIA LAND
65°S
180°
LEGEND
EAST ANTARCTIC ICE SHEET PORTION OF THE ROSS ICE SHELF DRAINAGE SYSTEM
ICE FREE AREAS
DRAINAGE DIVIDES
(ADAPTED FROM GIOVINETTO AND OTHERS, 1966, p. 56)

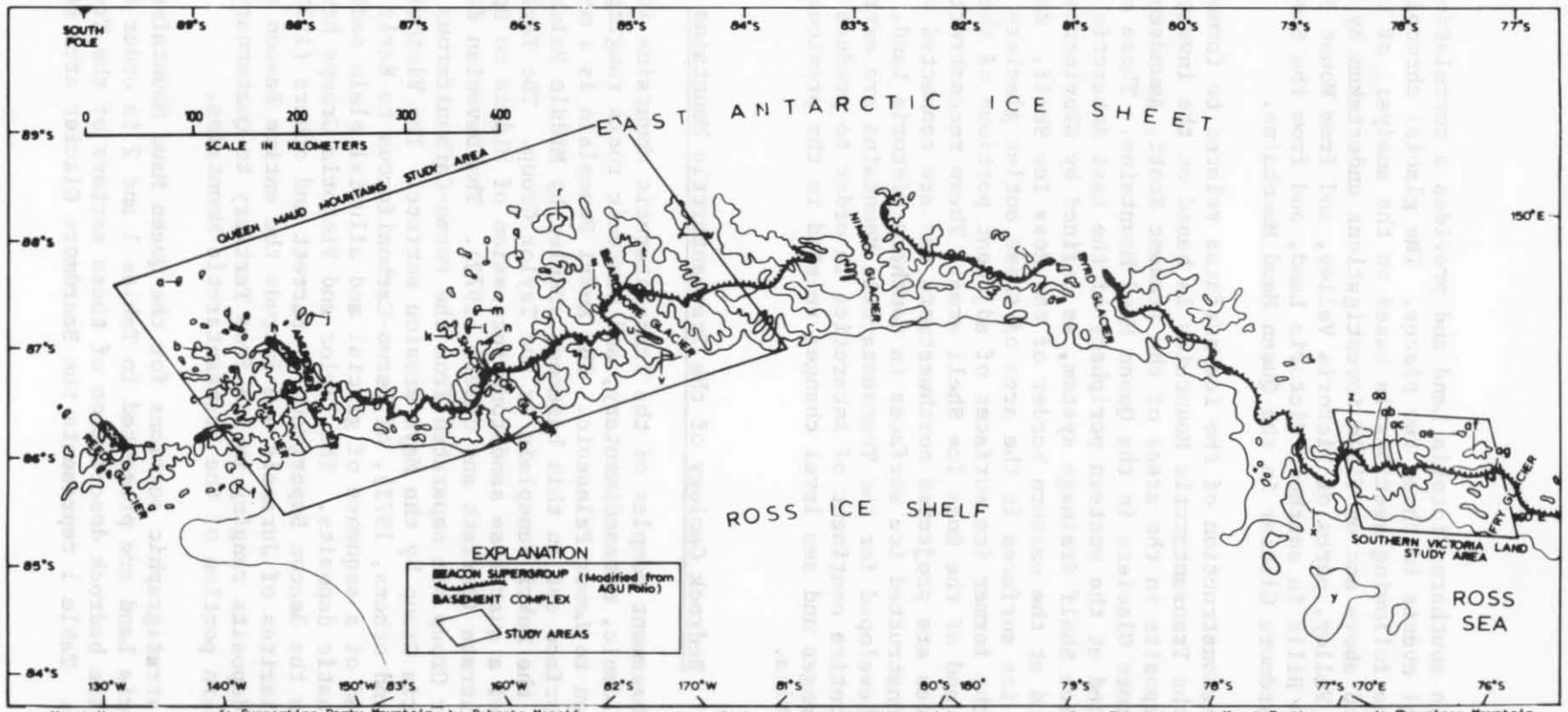

a: Mount Howe
b: La Gorce Mountains
c: Mount Blackburn
d: Mount Saltonstall
e: Mount Innes-Taylor
f: Supporting Party Mountain
g: Mount Crockett
h: Nilsen Plateau
i: Mount Pulitzer
j: Mount Wisting
k: Roberts Massif
l: Dismal Buttress
m: Half Century Nunatak
n: Bennett Platform
o: Mount Block
p: Mount Roth
q: Otway Massif
r: Dominion Range
s: Mount Deaken
t: Mount Kirkpatrick
u: Mount Kyffin
v: Mount Robert Scott
w: Mount Sirius
x: Cape Chocolate
y: Ross Island
z: Mount Feather
aa: Taylor Valley
ab: Wright Valley
ac: Victoria Valley
ad: Shapeless Mountain
ae: Carapace Nunatak
af: Allan Nunatak
ag: Coombs Hills

deposits in southern Victoria Land and provides a correlation between the glacial events in these two places. The glacial chronology developed in the following sections is based on the analysis of the previous works noted above and on field investigations undertaken by this author in Wright Valley, parts of Victoria Valley, and from Mount Feather to the Coombs Hills in southern Victoria Land, and from the Scott Glacier to the Beardmore Glacier in the Queen Maud Mountains.

The reconstruction of the ice surfaces related to former glaciations in the Transantarctic Mountains is based on the investigation of glacial deposits in the areas of the present Scott, Amundsen, Shackleton, and Beardmore Glaciers in the Queen Maud Mountains. These outlet glaciers are situated at the western periphery of the East Antarctic portion of the Ross Ice Shelf drainage system, as defined by Giovinetto and others (1966), and at the eastern border of the Ross Ice Shelf. Reconstruction of former ice surfaces in the area of these outlet glaciers directly reflects the former ice surfaces of adjacent portions of the continental ice sheet and of the Ross Ice Shelf area. These reconstructed former ice surfaces are projected northwestward and are connected with correlative reconstructed ice surfaces in southern Victoria Land. The ice surfaces developed for the Transantarctic Mountains are extrapolated over the entire continent of Antarctica in order to produce the ice volume changes and sea level changes related to the previous glaciations in Antarctica.

Bedrock Geology of the Transantarctic Mountains

The basement complex of the Transantarctic Mountains is composed of metavolcanic, metasedimentary, and plutonic rocks ranging in age from Precambrian to Lower Paleozoic. The Kukri Peneplain is a moderately smooth erosion surface cut in this basement complex by Middle Paleozoic time. Overlying the Kukri Peneplain is the Taylor Group. The Taylor Group consists of a quartzose sandstone succession of Middle to Upper Devonian or older strata (Barrett and others, 1972). The Devonian deposits of the Taylor Group are separated from the Permo-Carboniferous deposits of the Victoria Group by the Maya erosion surface. The Victoria Group (Barrett and others, 1972), of Permo-Carboniferous to Early Jurassic age, is composed of a sequence of glacial and alluvial plain sediments as well as pyroclastic deposits. The Taylor and Victoria Groups have been combined into the Beacon Supergroup by Barrett and others (1972). The Ferrar Dolerites of Jurassic age intrude the entire Beacon sequence. Volcanic deposits ranging in age from Tertiary to Quaternary occur in the northern portion of the Transantarctic Mountains.

The stratigraphic sections for the Queen Maud Mountains and southern Victoria Land are presented in Tables 1 and 2 in order to provide a more precise bedrock description of these sectors of the Transantarctic Mountains. Table 1 represents the Beardmore Glacier area stratigraphic

Table 1

Queen Maud Mountains Bedrock Geology
(from the Beardmore Glacier Area)

Group	Age	Formation	Description
Beacon Supergroup	Jurassic	Kirkpatrick Basalt	Tholeiitic flows
		Ferrar Dolerite	Sills and dikes
	Triassic	Prebble Fm.	Volcanic mudflows, agglomerate, tuff
		Falla Fm.	Sandstone, shale, tuff
		Fremouw Fm.	Sandstone, mudstone, coal
		DISCONFORMITY	
Victoria	Permian	Buckley Fm.	Lithic sandstone, shale, coal
		Fairchild Fm.	Arkosic sandstone
		MacKellar Fm.	Shale and sandstone
	Permo-Carboniferous	Pagoda Fm.	Tillite, sandstone, shale
		DISCONFORMITY (MAYA)	
	Mid-Upper Devonian	not present	
Taylor	Devonian and older	Alexandra Fm.	Orthoquartzite and sandstone
		UNCONFORMITY (KUKRI)	
	Ordovician	Hope Granite	Granite, granodiorite, quartz-diorite, pegmatite, lamprophyre
Byrd	Lower-Middle Cambrian	Shackleton Limestone	Limestone, shale, conglomerate
Beardmore	Uppermost Precambrian	Goldie Fm.	Graywacke, phyllite, quartzite, marble, schist, hornfels
Nimrod			High-grade metasediment marbles, amphiboles

Table 2 Southern Victoria Land Bedrock Geology

Group	Age	Formation	Description
	Jurassic	Kirkpatrick Basalt	Tholeiitic flows
		Ferrar Dolerite	Sills and dikes
		Mawson Fm.	Volcanic mudflows, agglomerates, tuffs
		DISCONFORMITY	
	Triassic	Lashly Fm.	Sandstone and siltstone
		Fleming Fm.	Quartzose sandstone and mudstone
Victoria		Feather Fm.	Pebbly quartzose sandstone and mudstone
	Permian	Wellar Coal Measures	Carbonaceous strata
		DISCONFORMITY	
	Permo-Carboniferous	Metschel Tillite	Tillite and pebbly mudstone
		DISCONFORMITY (MAYA)	
	Mid-Upper Devonian	Aztec Siltstone	Siltstone and sandstone
Taylor		Beacon Heights Orthoquartzite	Sandstone
	Devonian and older	Arena Sandstone	Sandstone
		Altar Mountain Fm.	Sandstone
		DISCONFORMITY	
		New Mountain Sandstone	Conglomerate, sandstone, siltstone, claystone
		UNCONFORMITY (KUKRI)	
Granite Harbour Intrusives	Lower Paleozoic		Granite, granodiorite, microdiorite, granite-gneiss
Skelton	Cambrian & older	Koettlitz Marble	
		Anthill Limestone	
		Teall Graywacke	

Beacon Supergroup

section and is intended to be a generalization for the stratigraphy of the Queen Maud Mountains. This section is based on stratigraphies developed by Grindley (1963), Barrett and others (1968), Barrett (1969), Gunner (1969) and Lindsay (1969) for the Beacon Supergroup and by Gunner (1969) for the basement complex. Table 2, representing southern Victoria Land, is based on stratigraphies developed by McElroy (1969) and McKelvey and others (1970) for the Beacon Supergroup and by Gunn and Warren (1962) for the basement complex.

The dividing line between Beacon Supergroup and basement complex outcrops in the Transantarctic Mountains is indicated in Figure 2. The basement complex occupies the coastward portion of the range and the inland portion of the range is composed primarily of the Beacon Supergroup and the Ferrar Dolerites. The area of outcrop of the Beacon Supergroup and of the Ferrar Dolerites is typified by broad platforms and more gentle slopes than those near the Ross Ice Shelf and the Ross Sea which are developed on the basement complex material. Moraine and talus are almost totally absent from the slopes of the basement complex because these slopes are so steep.

Climate of the Transantarctic Mountains

The Queen Maud Mountains and southern Victoria Land are similar climatically in that both are characterized by:

(1) Predominant wind directions from the inland East Antarctic ice sheet as a result of downslope (katabatic) winds funneling along ice surface contours (Schwerdtfeger, 1968).

(2) Predominant precipitation directed from the open ocean and the Ross Ice Shelf which results in frequent cloud cover along the coast.

(3) A secondary precipitation source derived from blowing snow transported by the katabatic winds.

(4) Major ablation in the form of sublimation (Bull, 1971).

The similarities noted above are modified by the fact that:

(1) The Queen Maud Mountains lie in the range of 84° to 87° south latitude while southern Victoria Land lies between 76° to 78° south latitude. Thus, the amount of direct solar radiation reaching the Queen Maud Mountains is less than that reaching southern Victoria Land because of the decrease in angle of incidence of direct solar radiation with increasing latitudes.

(2) The predominant elevation of glacial deposits in the Queen Maud Mountains ranges between 1400 to 2000 m above sea level, whereas most glacial deposits in southern Victoria Land are at an elevation of 0 to 1200 m above sea level. Assuming a dry-adiabatic lapse rate of 1°C per 100 m, this implies a 2 to 14°C mean annual difference in temperature between the Queen Maud Mountains and southern Victoria Land.

(3) The Queen Maud Mountains lie between 600 and 900 km from open ocean water, whereas all of southern Victoria Land is within 100 km of open ocean water during, at least, part of the year while pack ice is at a minimum. Thus, moisture originating from the open ocean and the moderating effect of ocean temperatures are more pronounced in southern Victoria Land than in the Queen Maud Mountains.

The Development of a Thick Ice Sheet in Antarctica

The separation of Antarctica and Australia began approximately in the Early Cretaceous (Elliot, 1972) or the Late Eocene (Heirtzler and others, 1968; Le Pichon, 1968). As early as Middle to Late Cretaceous (Elliot, 1972), Antarctica may have moved into its present position.

The first Antarctic glaciers were probably temperate mountain glaciers situated on the highest mountains of the continent (Mercer, 1972), namely, the Ellsworth Mountains, the Transantarctic Mountains, the Sør Rondane Mountains, and the presently subglacial Gamburtsev Mountains. Drewry (1972), conducting a radio-echo sounding survey of part of the Transantarctic Mountains, has located several subglacial troughs and ridges on the inland side (southwest) of these mountains which may have been sculptured during this early mountain glacier period.

The earliest record of glaciation in Antarctica is marked by quartz grains which display glacial imprinting (Geitzenauer and others, 1968; Rex and Margolis, 1969). These quartz grains have been recovered from southern ocean deep sea cores and dated by foraminiferal associations as Lower Eocene, Middle Eocene, and Oligocene. These dates represent the earliest record for the initiation of glaciation in Antarctica. In addition, Webb (personal communication) has recently examined cores from the Ross Sea which contain ice-rafted debris which dates as early as Late Oligocene. Thus, by no later than the Oligocene, glaciers were calving into Antarctic coastal waters and icebergs carried glacial debris north.

By Late Miocene to Middle Pliocene an extensive Antarctic ice sheet had built up in Antarctica according to the following information:

(1) In the Jones Mountains Rutford and others (1972) discovered a striated erosion surface cut in granite and overlain by till lenses. Basalt flows overlying the till yielded a potassium-argon date of 7 to 10 million years. Rutford (personal communication to Denton and others, 1971) has also noted that the clasts within the till are apparently derived from the Ellsworth Mountains, thus implying transport by a thick ice sheet which covered the Jones and the Ellsworth Mountains.

(2) In northern Victoria Land Hamilton (1969) has evidence of an ice sheet that was at least 2 km thick associated with volcanic ice-contact breccias that date by potassium-argon at 7.4, 6.8, and 5.5 million years.

(3) North-south trending glacial grooves in volcanic rocks dated by potassium-argon at 6 million years in the Executive Committee Range by Doumani (1963) are situated 500 m above the present ice surface. Both the elevation and direction of these grooves indicate a thick continental ice sheet.

(4) Dates between 5.7 and 2.8 million years are presented by Anderson (1972) for the occurrence of dry-based glaciers calving into the Weddell Sea based on combined foraminifera, sediment and paleomagnetic studies from deep sea cores. These early dry-base glaciers extended 75 km farther out onto the continental shelf than at present, suggesting that extensive inland ice was necessary to maintain this enlarged ice shelf in the Weddell Sea.

Several features on and surrounding the Antarctic continent attest to the existence of an ice sheet and ice shelves which exceeded the dimensions of the present Antarctic ice cover:

(1) Crary (1959), Crary and others (1962) and Lepley (1964) have noted depressions, kilometers wide and hundreds of meters deep, in the Antarctic continental shelf. These depressions occur both perpendicular to and parallel to the Antarctic coastline. Zhivago (1962), Guilcher (1963) and Lepley (1964) attribute these depressions to glacial sculpture. Only floating ice, incapable of substantial erosion, exists over these areas at present. Glacial sculpturing in these areas requires grounded ice and thus an oceanward extension and a thickening of the present Antarctic ice sheet.

(2) Taylor (1930) has suggested that vast submarine terminal moraines can be found off the Queen Mary Coast, the Adelié Coast, and in the Ross Sea. Lepley (1964), although disputed by Houtz and Meijer (1972), has noted submarine ridges off Edward VII Peninsula in the Ross Sea which he terms end and lateral moraines. If present these features imply an oceanward extension and a thickening of the Antarctic ice sheet.

(3) Frakes (1970), investigating the distribution of continentally derived till deposited in the Ross Sea, estimates that the Ross Ice Shelf must have at one time extended 300 km farther north than its present terminus. An extension of this magnitude may imply an increase in the dimensions of the ice sheet feeding the Ross Ice Shelf.

(4) Nichols (1960), studying glacial deposits and glacial sculpturing in the Marguerite Bay area of West Antarctica, estimates that in the past as much as 2 km of ice covered this area. Similar conclusions have been drawn by John (1972) in the South Shetland Island area of West Antarctica.

(5) U-shaped valleys, benches, glaciated and polished high level surfaces, particularly in the presently ice-free valleys of southern Victoria Land, all indicate a more extensive ice cover in this portion of Antarctica.

Glacial History of the Transantarctic Mountains

The Transantarctic Mountains provide abundant evidence for the history of the Antarctic ice sheet. Although the first glaciers in the Transantarctic Mountains were probably high mountain glaciers as proposed by Mercer (1972), deposits derived from these glaciers have probably been eradicated by the erosive action of the ice sheet which followed. The maximum recorded extent of this ice sheet is represented throughout the Transantarctic Mountains by the deposits of the Sirius Formation. The glaciation during which this formation was deposited is here referred to as the Queen Maud Glaciation. The Sirius Formation was originally interpreted by Mercer (1972) as being the result of deposition by local temperate glaciers. However, further investigation of this formation by this author indicates that it is more likely the result of deposition by an enlarged version of the present Antarctic ice sheet. The recession of this ice sheet is marked by some "interglacial" evidence in the Transantarctic Mountains. The characterization and interpretation of the Sirius Formation and the following "interglacial" are discussed later in this report.

Lateral moraines flanking the outlet glaciers of the Transantarctic Mountains record three readvances of the ice in this area. These readvances correspond to glaciations of successively lower extent here named the Scott, Shackleton, and Amundsen Glaciations. The youngest of these, the Amundsen Glaciation, corresponds to the present ice surface. The lateral moraines marking these glaciations have been investigated by this author in the Queen Maud Mountains and have been correlated with similar moraines studied by other workers in southern Victoria Land to produce an overall glacial chronology for the Transantarctic Mountains. The lateral moraines in the Queen Maud Mountains and their correlation with those in southern Victoria Land are discussed elsewhere in this report.

THE SIRIUS FORMATION

As first described by Mercer (1972, p. 427) from his studies on Mount Sirius and in the Dominion Range, the Sirius Formation is a "compact glacial drift that unconformably covers pre-Tertiary rocks". Mercer interpreted this deposit as the result of deposition by a temperate ice cover situated on the Transantarctic Mountains and predating the formation of the Antarctic ice sheet.

Investigations by the author of this report throughout the Transantarctic Mountains indicate several amendments and additions to Mercer's interpretation. The Sirius Formation is a widespread deposit found throughout the Transantarctic Mountains and is nearly identical at the 24 sites (Fig. 3, Table 3) presently known. Nearly all of these sites have been investigated in detail by this author.

This deposit is composed of two members: a till member and an overlying stratified member.

The till member is the lower and most common of the two members. It overlies pre-Tertiary rocks unconformably and is composed primarily of semi-lithified till and sparsely scattered stratified lenses. The till contains clasts of many lithologies including: metasediments, granite, dolerite, sandstone, shale, siltstone, and volcanics. The proportion of these lithologies seems to vary as a function of the distance to the source material and the size of the source of glacial transport. The clasts within the till are predominantly angular or subangular and some are faceted and striated. The strong fabric produced by the elongate clasts in the till and the compactness of the clasts and the matrix in this till suggest deposition from the base of a glacier. Till deposited in this manner is referred to as lodgement till (Flint, 1971, p. 171) or basal till (Goldthwait, 1971, p. 15).

The stratified member of the Sirius Formation has undergone far more extensive post-depositional erosion than the underlying till member. Therefore, it crops out in far fewer localities. The stratified member is composed almost entirely of stratified lenses, ranging in length from several centimeters to several meters intercalated with sparsely scattered lenses of till. The stratified lenses are composed of gravel, sand, silt and clay and range from well-sorted to unsorted. Clasts are similar in lithology to those of the till member, but show an increase in rounding. The stratified member is interpreted as an ice-contact deposit because of its: (1) extreme range and abrupt changes in grain size, (2) included bodies of till, and (3) deformation as required by the definition of Flint (1971, p. 184).

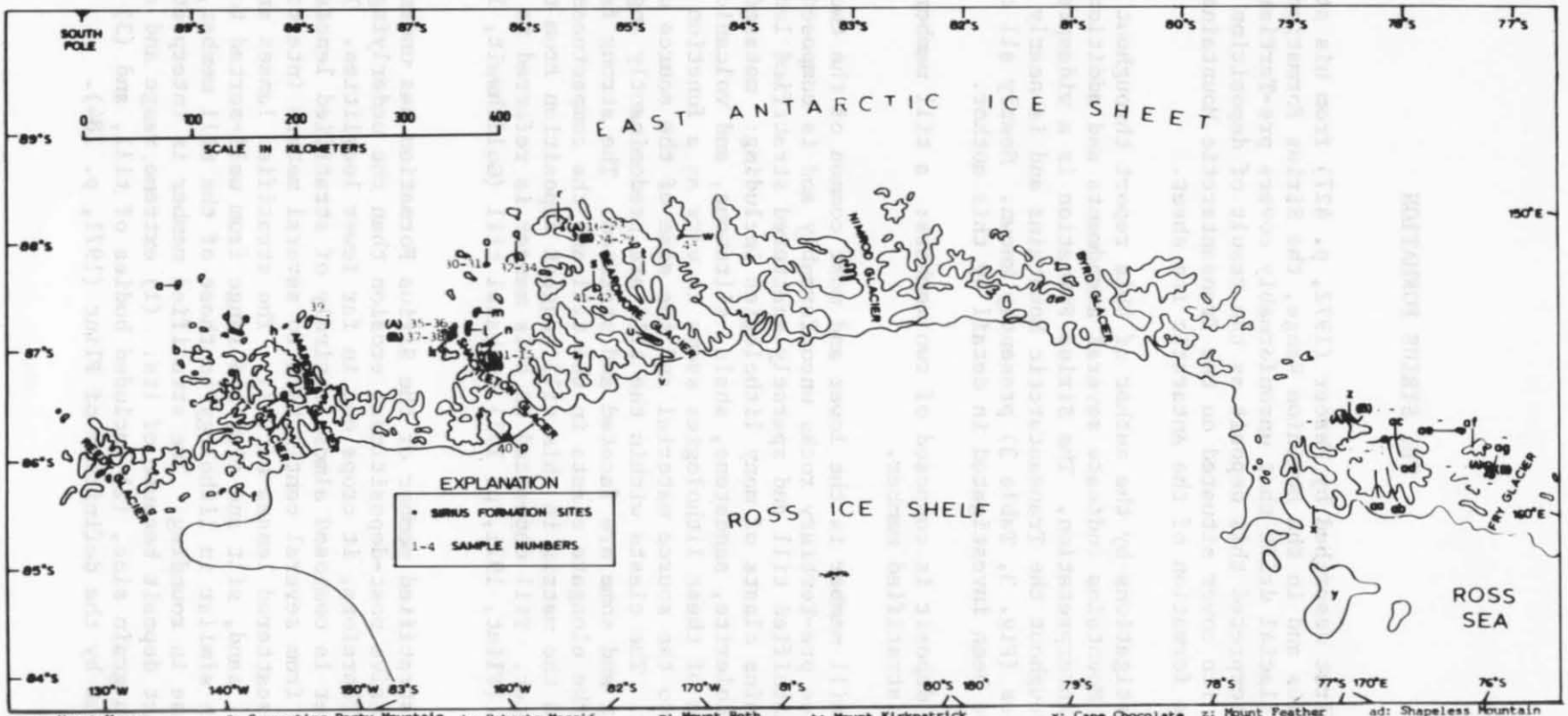

a: Mount Howe
b: La Gorce Mountains
c: Mount Blackburn
d: Mount Saltonstall
e: Mount Innes-Taylor
f: Supporting Party Mountain
g: Mount Crockett
h: Nilsen Plateau
i: Mount Pulitzer
j: Mount Wisting
k: Roberts Massif
l: Dismal Buttress
m: Half Century Nunatak
n: Bennett Platform
o: Mount Block
p: Mount Roth
q: Otway Massif
r: Dominion Range
s: Mount Deaken
t: Mount Kirkpatrick
u: Mount Kyffin
v: Mount Robert Scott
w: Mount Sirius
x: Cape Chocolate
y: Ross Island
z: Mount Feather
aa: Taylor Valley
ab: Wright Valley
ac: Victoria Valley
ad: Shapeless Mountain
ae: Carapace Nunatak
af: Allan Nunatak
ag: Coombs Hills

Table 3

List of Sirius Formation Sites
(For Map Position See Fig. 2)

Location	Elevation at Top of Deposit
+Mt. Innes-Taylor (Doumani & Minshew, 1965)	2200 m
+Mt. Saltonstall (Doumani & Minshew, 1965)	2200
Mt. Blackburn Area (Doumani & Minshew, 1965)	3000
+Mt. Wisting	2000
Mt. Roth (E. Stump & V. Wendland, pers. comm.)	800
Bennett Platform (A) (Wade and others, 1965)	2150
Bennett Platform (B) (Wade and others, 1965)	1600
Half Century Nunatak	2600
Dismal Buttress (McGregor, 1965)	2300
Roberts Massif (A) (Claridge & Campbell, 1968)	2100
Roberts Massif (B)	2050
Mt. Block (D. Elliot, pers. comm.)	2700
Mt. Deaken (S. Etter & D. Coates, pers. comm.)	2800
Mt. Sirius (P. Barrett, pers. comm.)	2300
Otway Massif (D. Elliot, pers. comm.)	2400
Dominion Range (A) (Oliver, 1946)	2200
Dominion Range (B) (Oliver, 1946)	1800
Mt. Feather (A) (D. Elliot, pers. comm.)	2800
Mt. Feather (B)	2750
Shapeless Mtn. (P. Barrett, pers. comm.)	2400
+Carapace Nunatak (H. Borns & B. Hall, pers. comm.)	2000
Allan Nunatak (H. Borns & B. Hall, pers. comm.)	1750
Coombs Hills (A) (P. Barrett, pers. comm.)	1900
Coombs Hills (B)	

+ Deposit not in situ

The high elevation (Table 3) at which the Sirius Formation is usually found and the orientation of elongate clasts in the till member indicate deposition by an ice mass of continental proportions, i.e. an ice sheet. This ice sheet is envisioned as an enlarged version of the present Antarctic ice sheet. This interpretation does not coincide with Mercer's in which localized temperate glaciation in the Transantarctic Mountains is believed to be responsible for the deposition of the Sirius Formation. To substantiate these conclusions the characteristics of the Sirius Formation are analyzed and interpreted.

Characteristics

The Sirius Formation is composed primarily of till. A description of this deposit can, therefore, be analyzed in terms of the characteristics of till. The characteristics investigated in this chapter are those developed by both Goldthwait (1971, p. 4-5) and Flint (1971, p. 192):

(1) "a striated surface on the rock or sediment basement beneath" (Goldthwait, 1971); "whaleback (streamline) form of the upper surface of the diamict or that of the underlying bedrock" (Flint, 1971)

(2) "thickness and lateral extent variable" (Flint, 1971)

(3) "a homogeneous mix lacking any smooth lamination or regular bedding...." (Goldthwait, 1971)

(4) "compactness or close packing contrasted to neighboring sediments" (Goldthwait, 1971)

(5) "lack of complete sorting.... presence of some pebbles or boulders much larger than the dominant clay, silt, or sand..." (Goldthwait, 1971)

(6) "lithology of clasts generally variable...." (Flint, 1971)

(7) "coarse particles not rounded; some faceted, some pentagonal, conspicuous basal facet" (Flint, 1971); "subangularity in clasts of all sizes" (Goldthwait, 1971); "...clasts predominantly fresh...." (Flint, 1971); "at least a small proportion of striated stones and microstriated grains" (Goldthwait, 1971)

(8) "common orientation of the long axes of elongated grains and pebbles" (Goldthwait, 1971)

(9) "upper surface possessing constructional features" (Flint, 1971)

Basal Contact

The till member of the Sirius Formation is underlain by a fresh, relatively smooth striated and/or grooved erosion surface. The fluid soaked state of the till member during deposition is demonstrated by the thin stringers of till which fill small fractures in the underlying erosion surface. The similar basal contacts noted for the Sirius Formation throughout the areas investigated indicate equivalent depositional environments. The orientation of striae and grooves in the underlying erosion surface with the fabric of the overlying till indicate that erosion and deposition were both the result of similar ice flow directions. The direction of this ice flow converging into "through valleys" indicates that the ice mass present at this time surmounted many bedrock highs which are currently ice-free. This indicates that the erosion prior to the deposition of the Sirius Formation, and the following deposition of the Sirius Formation, were produced by an ice mass which had a higher surface level than the present Antarctic ice sheet and which was less dependent on local bedrock configuration than the present ice sheet. Furthermore, both erosion and deposition date from the same glaciation, as shown by the unweathered underlying surface. Four basal contacts were investigated in detail (Fig. 3): (1) Roberts Massif (a), (2) Dominion Range (A), (3) Allan Nunatak, and (4) Coombs Hills (B).

Roberts Massif

The large bedrock basin developed on the northwest side of Roberts Massif contains a small roughly circular deposit of the Sirius Formation (Fig. 4). The maximum dimensions of the deposit are 100 m in diameter by 1-2 m in thickness. The bedrock basin in which the deposit rests is divided into eastern and western halves by outcrops of fine- to medium-grained dolerite and coarse-grained dolerite, respectively. The Sirius Formation covers a small segment of the fine- to medium-grained dolerite outcrop.

The Shackleton Glacier presently partially invades the open northwest side of the basin. Former invasions by the Shackleton Glacier into the basin from the northwest are noted by rubbly belts of moraine which outline former lateral margins of this glacier. To the southeast a bedrock threshold (2400 m a.s.l.) presently protects the basin from invasion by the East Antarctic ice sheet.

Grooves developed in the fine- to medium-grained dolerite bedrock on the eastern half of the basin record the overriding of the bedrock threshold by ice of the East Antarctic ice sheet. The grooves (Fig. 5) are parallel to each other and have a bearing of 171°. They have a maximum length of approximately 50 m and in cross section form an undulating surface with up to 3 m in relief. The ridges between the

Figure 4. Example of till member outcrop (light patch in foreground), Roberts Massif.

Figure 5. Glacial grooves developed in bedrock basin, Roberts Massif. Shackleton Glacier in the distance. Grooves formed by ice flowing from foreground toward the Shackleton Glacier.

Figure 6. Close-up of grooves noted in previous figure. Arrow indicated direction of ice-flow. Ridges between grooves are smoothed toward the south.

the grooves are rounded and smoothed and the grooves themselves are sparsely filled with fines. In long section the ridges are smoothed toward the south (Fig. 6) and jagged toward the north. The form of the grooves and ridges and their orientation both indicate that the scouring agent traversed from south to north across the basin at right angles to the outlet glacier just south of it today. During the development of these grooves the East Antarctic ice sheet must have attained a great enough thickness or high enough surface to surmount the bedrock threshold and enter the basin directly.

The fabric of the elongate clasts in the deposit of the Sirius Formation which overlies the fine- to medium-grained dolerite is parallel to the trend of the grooves. Thus, the Sirius Formation must have been deposited by ice flowing in the same direction as that which scoured the grooves, or more specifically by the East Antarctic ice sheet.

The western half of the basin contains a system of dead-end "channels" similar in form to the controversial "channels" developed in the Labyrinth in the western or inland abutment of Wright Valley. The coarse-grained dolerite portion of the basin is more highly fractured than the fine- to medium-grained dolerite portion. The increased velocity of the ice as it slipped off the bedrock threshold into the bedrock basin and the thickness required to overrun the threshold may have allowed pressure-melting at the base of the glacier. Water at the base of the ice created by this pressure-melting will tend to freeze into the fractured coarse-grained dolerite of the bedrock basin as the velocity of the ice decreases after its entry into the basin. As the water freezes large coarse-grained dolerite blocks are plucked from the bedrock basin resulting in the formation of dead-end "channels". Furthermore, basal debris picked up in this manner and plastered to the underlying bedrock provides a mechanism for the deposition of the till member deposit overlying these grooves.

Dominion Range

At the site labeled (A) in the Dominion Range the Sirius Formation overlies a sandstone unit of the Fremouw Formation. Along the approximately 50-m lateral extent of the basal contact the sandstone maintains a nearly horizontal plane (Fig. 7). The sandstone surface is cleanly scoured. Small fractures extend sporadically a few centimeters vertically into the sandstone. The overlying till member is found squeezed into the fractures, indicating the fluid nature of the till during deposition. The cleanly scoured sandstone contact allied with the lack of any increased concentration of sandstone blocks in the till at the base of the till member imply an extensive period of erosion, down to competent bedrock, prior to deposition of the till.

Figure 7. Contact between till member and underlying Fremouw Formation, Dominion Range (A).

Allan Nunatak

At Allan Nunatak a topographic situation exists similar to that at Roberts Massif. The backwall of a bedrock basin situated on the northern side of this nunatak acts as a threshold (2000 m a.s.l.) to ice invasion from the south, but the northern opening of the basin admits a lobe of thickened inland ice that has been diverted south to north around the nunatak. Unlike the cleanly scoured contact in the Dominion Range the underlying shale bedrock forms a gradational contact with the overlying till. Within the lower 0.5 m of the till, fragments of the shale comprise more than 50% (Fig. 8). The intercalated shale fragments and till corroborate the fluid nature of the till during deposition. The irregular contact results from the brittle nature of the shale bedrock which renders it incapable of being eroded down to a lithologically competent level as was the case in the Dominion Range.

Coombs Hills

At section B in the Coombs Hills the till member of the Sirius Formation overlies a sandstone unit of the Lashly Formation. The till at this site is less than 1 m thick and is easily excavated. The basal portion of this till is composed primarily of clay. Impressions formed in the clay record the shearing of basal clasts against the clay (Fig. 9) and indicate the moist condition of the lower till during deposition. Removal of the clay reveals an extremely fresh bedrock surface (Fig. 10), indicating extensive erosion prior to the deposition of the Sirius Formation. The fresh surface further implies that between the period of bedrock scouring and deposition the bedrock surface was not subaerially exposed, and therefore both erosion and deposition were the result of the same ice covering.

Extent and Dimensions

The extent and dimensions (Fig. 3) of the Sirius Formation indicate deposition by an ice sheet of continental scale. These deposits extend a maximum length along the Transantarctic Mountains of approximately 1300 km (from Mount Blackburn to the Coombs Hills) and a maximum width of approximately 165 km (from Mount Roth to Mount Block). The deposit is confined almost entirely to elevations in excess of 1750 m with the notable exception of the deposit at Mount Roth at 800 m elevation (Table 3).

The Sirius Formation differs markedly in thickness from site to site. Of the sections studied, section A in the Dominion Range was the thickest (estimated at 80 m in thickness). At this section, as with all other sections, true thicknesses could not be measured because of: (1) unknown bedrock topography beneath the deposit,

Figure 8. Basal portion of till member with intercalated shale fragments, Allan Nunatak. (photo by R. Wilkinson)

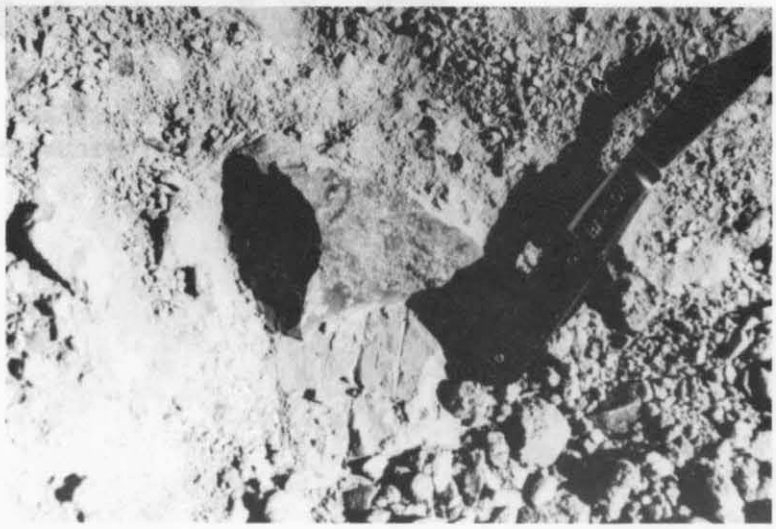

Figure 9. Clay at basal contact of till member, Coombs Hills. Note scratches next to knife formed by clasts shearing against clay. (photo by R. Wilkinson)

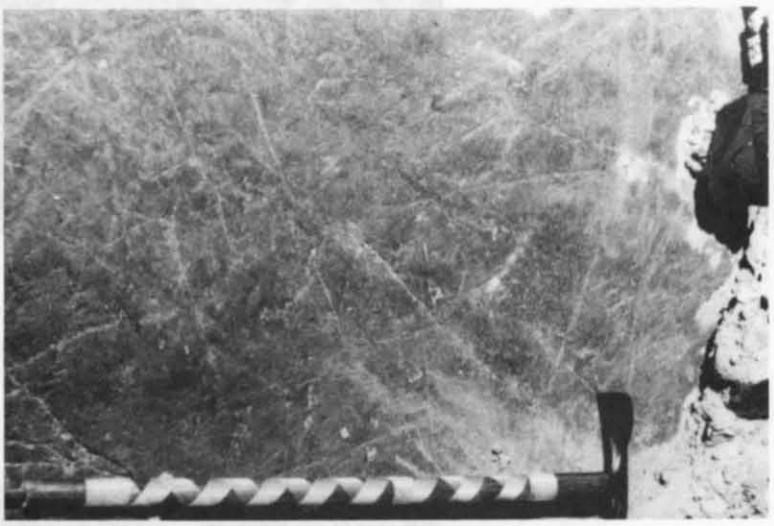

Figure 10. Striated pavement exposed after removal of clay layer noted in previous figure. (photo by R. Wilkinson)

(2) talus accumulations covering the tops of the sections, and (3) the overlap of younger moraine systems obscuring the lower edges of the deposit. Extremely small deposits were also noted. The smallest was found at Mount Block as a 1 m square chunk of till wedged in a crack on the ridge at the mountain top.

Deposits of the Sirius Formation are found as erratics at Mount Wisting, Mount Saltonstall, Mount Innes-Taylor, and Carapace Nunatak. The erratics range in size up to 1.5 m in diameter. Those found at Mount Wisting indicate a general source from the south and beneath the inland ice.

Structure

The till and the stratified members of the Sirius Formation can be differentiated by their marked differences in structure. These differences in structure are an important key to their environments of deposition.

The till member is an extremely massive or structureless deposit (Fig. 7 and 11) deposited like a sheet and moulding to the local bedrock topography (Fig. 12). This member is most commonly preserved in protected bedrock embayments and on bedrock platforms, although the best sections for study are positioned against valley walls. Scattered stratified lenses can be found within the till member. These stratified lenses are usually only crudely stratified and are almost always composed of coarse-grained material ranging in size from coarse gravel to cobbles (10-30 cm average size). The coarse texture and moderately good sorting of these lenses is in sharp contrast to the very poorly sorted texture of the till. The lenses were deposited in close proximity to the till, but represent deposition in a different environment. They result from the deposition of portions of the till into englacial and/or basal pockets and channels of meltwater. Within the ice enclosures of this meltwater environment the finer material of the till is winnowed out. The remaining coarser material settles into a crudely stratified structure representative of this turbid environment.

The stratified member observed only at one site (Bennett Platform) of the Sirius Formation contains some small till lenses. Viewed from a distance (Fig. 13) this member appears to be composed of subhorizontal, continuous layers. Closer observation, however, indicates that the unit is composed of slumped and fractured blocks, (Fig. 14) and more importantly, that the apparently continuous strata are really a composite of intermixed stratified lenses.

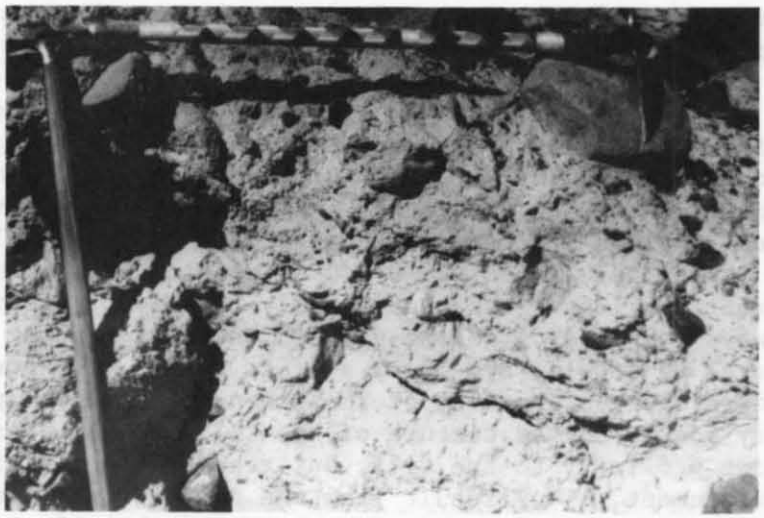

Figure 11. Example of massive structure of till member, Coombs Hills. (photo by R. Wilkinson)

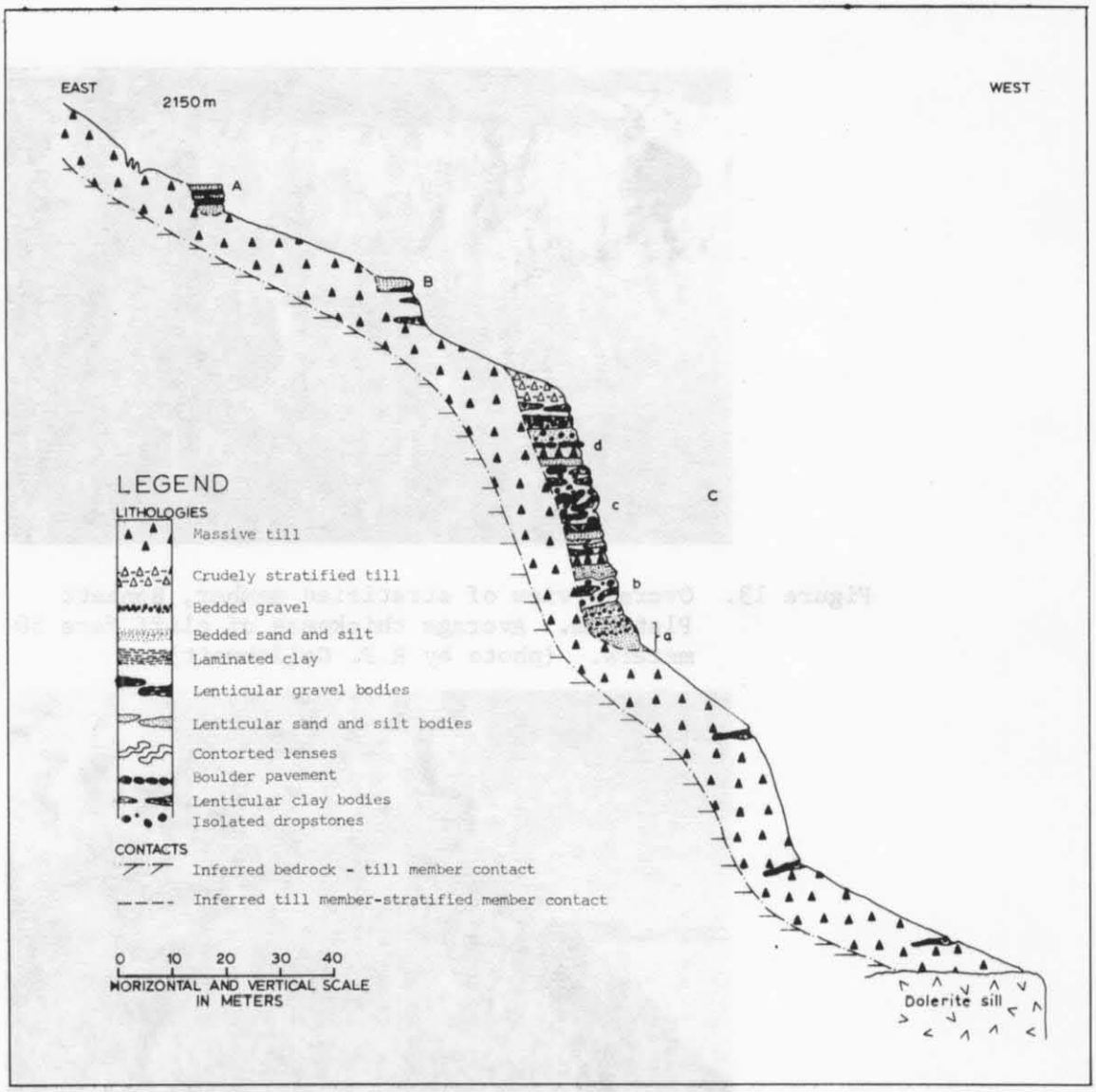

Figure 12. Generalized stratigraphic section of the Sirius Formation, Bennett Platform.

Figure 13. Overall view of stratified member, Bennett Platform. Average thickness of cliff face 50 meters. (photo by R.P. Goldthwait)

Figure 14. Close-up of stratified member noted in previous figure. Note slumping and fracturing. (photo by R.P. Goldthwait)

Figure 12 is a generalization of the most complete section of the Sirius Formation noted in the Transantarctic Mountains. The stratified member of the Sirius Formation in this figure is composed of three distinct accumulations (A, B, C in Fig. 12). The general dip of the stratified deposits in these accumulations is sub-horizontal to slightly in-slope. The slight tilt of these strata away from the Shackleton valley indicates a depositing source from within the valley. The Shackleton valley must have been filled with ice during the time of deposition of the stratified member. In order to fill the Shackleton valley, an ice mass similar in dimensions to the present Antarctic ice sheet is required inland from this valley. Furthermore, the Sirius Formation crops out above the current surface of the Shackleton Glacier indicating even greater ice thicknesses in the past than at present, as opposed to more limited extent glaciers, i.e. localized temperate glaciers.

The best stratified and finest-grained portion (Fig. 15) of any stratified member is observed at the basal portion of the stratified member accumulations. For example, the 4.2-m-thick portion, labeled a in Figure 12, is composed of alternating bands of: (1) wispy silt (0.5 to 4.0 cm thick) subdivided into laminae each less than 1.0 mm thick, (2) poorly-sorted fine gravel in a fine sand to silt matrix (0.25 to 7.5 cm thick), and (3) occasional dropstones. Mild depositional conditions appear to have initiated the onset of each of the stratified member accumulations. The fine silt laminae are the result of deposition by relatively slow-moving meltwater streams into ponds, and the fine gravel and dropstones represent more rapid fluxes of meltwater streams into them. These meltwater streams issued from within or upon a degenerating ice mass and then into stable englacial and/or superglacial meltwater ponds.

Moving upward in altitude, in each of these stratified member accumulations there is an increase in the proportion of coarse material, i.e. gravel and boulders (b in Fig. 12). Interspersed with these coarser lenses are occasional till lenses, and some scattered sorted silt and sand. The silt and sand represent occasionally milder depositional conditions, while the till may represent incorporated portions of the lower till member. In general, however, a marked increase in energy of meltwater streams is noted with a corresponding increase in altitude in each of the stratified member accumulations.

Contorted lenses appear in the middle portion of the lowest stratified accumulation (labeled c in Fig. 12). The break between contorted and overlying uncontorted lenses is marked by a boulder pavement (labeled D in Fig. 12) which overlies a thin till accumulation. This line of boulders, one boulder thick, is composed of well striated and faceted fine- to medium-grained dolerite boulders averaging

Figure 15. Example of alternating silt and fine gravel in stratified member, Bennett Platform.

approximately 0.5 m in length. It extends laterally for 15 m. This boulder pavement and the underlying till suggest a readvance of the ice sheet and a return to basal till deposition in between the degenerating stages of the ice sheet.

Several features suggesting fluvial and lacustrine deposition occur in the stratified member, such as graded bedding, cross-bedding (Fig. 16) and dropstones. In addition, minor fractures were noted in a thin-section investigation of the stratified member samples. These fractures were filled with clays. The fractures represent either desiccation cracks or brittle failure of the stratified member. These features may suggest a period of drying of portions of the stratified member followed by a renewed influx of clays in suspension. Such periodic drying may imply subaerial drying or seasonal fluxes of englacial meltwater streams.

Compaction

Both the till and stratified members of the Sirius Formation are extremely compact deposits. Except for the most gravelly end-members of both units they are so compact that sampling presents a problem. The compactness is a function of: (a) the semi-lithification of this deposit, (b) the high percentage of matrix material (medium silt to clay) which binds the deposit, (c) the deposition of the till member beneath a thick overburden of ice, and (d) the caking effect that is created during the drying of moist deposits.

Particle Size Distribution

Analysis of particle size distribution (Appendix A) in the Sirius Formation allows: (a) an indication of the equivalence of the till member samples from site to site throughout the Transantarctic Mountains, (b) an approximation of the relative amount of glacial transport of these deposits, and (c) the differentiation of the till member from the stratified member.

In general, the till member can be characterized as being poorly sorted and containing boulders up to 1.5 m in length mixed with gravel and sand, all set in a matrix of silt and clay. Stratified member samples are consistently better-sorted than till member samples. In order to investigate these generalizations more fully, samples of the Sirius Formation (Fig. 3) were collected for size analysis. Analysis of the following size distributions are discussed: (1) gravel - sand - mud (silt and clay), (2) sand - silt - clay, (3) five sand fractions - total silt - total clay, and (4) very coarse sand to coarse silt. A physical disaggregation process was used for analyses (1) to (3). Wet-sieving was used to remove particles in excess of 2 mm.

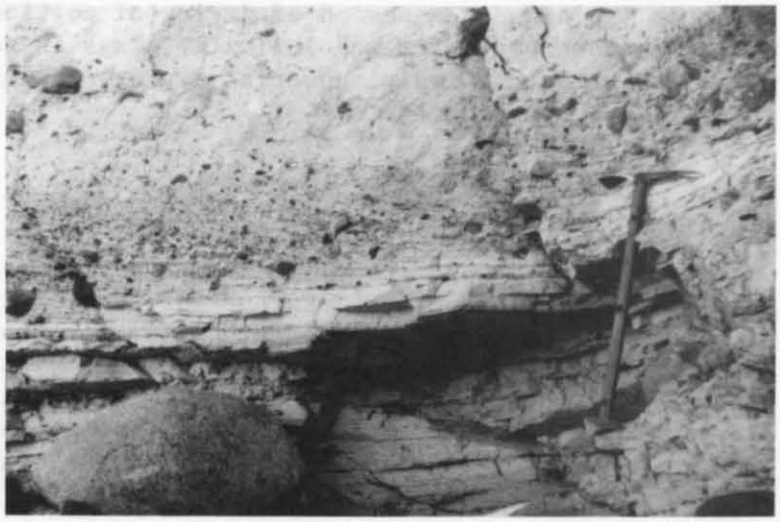

Figure 16. Example of cross-bedding in stratified member, Bennett Platform.

The remainder of the less than 2 mm size particles were dry-sieved to obtain a sand versus silt and clay separation. Total silt and total clay were separated by allowing a timed settling of these fractions in solution and drawing off the total clay. Thin-section measurements were used for the size separation in (4).

Gravel - sand - mud

A gravel (>2 mm) - sand (0.0625 to 2.0 mm) - mud (<0.0625 mm) distribution (Folk, 1968) was analyzed for 12 till member samples throughout the Transantarctic Mountains (Fig. 17). The semi-lithified state of the Sirius Formation hampered physical disaggregation of all but these 12 samples. In general, these samples fall in the size range gravelly mud to slightly gravelly muddy sand using Folk's terminology. Although three samples fall slightly outside this general range, the remaining samples, despite location, are within this range and are, therefore, equivalent on this level of size analysis.

Sand - silt - clay

Removal of the gravel fraction of the preceding samples provides a sand (0.0625 to 2.0 mm) - silt (0.0039 to 0.0625 mm) - clay (0.0039 mm) distribution analysis (Fig. 18). In general, these samples fall in the range sandy mud to muddy sand using Folk's terminology. Once again, despite location these samples fall in the same general size range and are, therefore, equivalent on another level of size analysis.

Five sand fractions - silt - clay

Analysis of these samples on a more detailed level of particle size distribution--very coarse sand (2.0 to 1.0 mm)- coarse sand (1.0 to 0.5 mm) - medium sand (0.5 to 0.25 mm) - fine sand (0.25 to 0.125 mm) very fine sand (0.125 to 0.0625 mm) - total silt (0.0625 to 0.0039 mm) - total clay (<0.0039 mm)--provides a differentiation between till member samples from the Queen Maud Mountains (Fig. 19) and those from southern Victoria Land (Fig. 20). Queen Maud Mountains samples have a primary mode around the silt fraction. Southern Victoria Land samples have a primary mode around the silt fraction and a secondary mode around the coarse to medium sand fraction. The preponderance of the silt mode in preference to coarser modes implies greater breakdown by glacial transport for Queen Maud Mountains as opposed to southern Victoria Land samples.

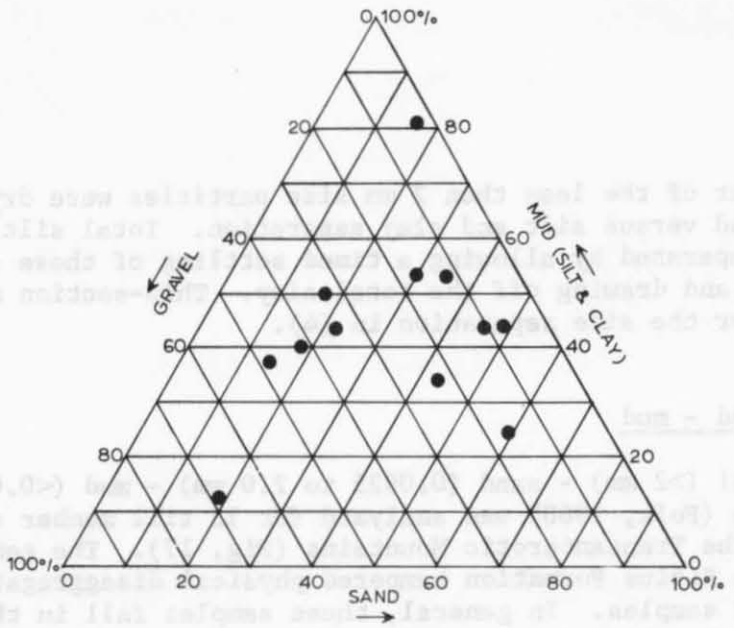

Figure 17. Gravel - sand - mud triangular diagram of selected till member samples from throughout the Transantarctic Mountains. (dots represent samples)

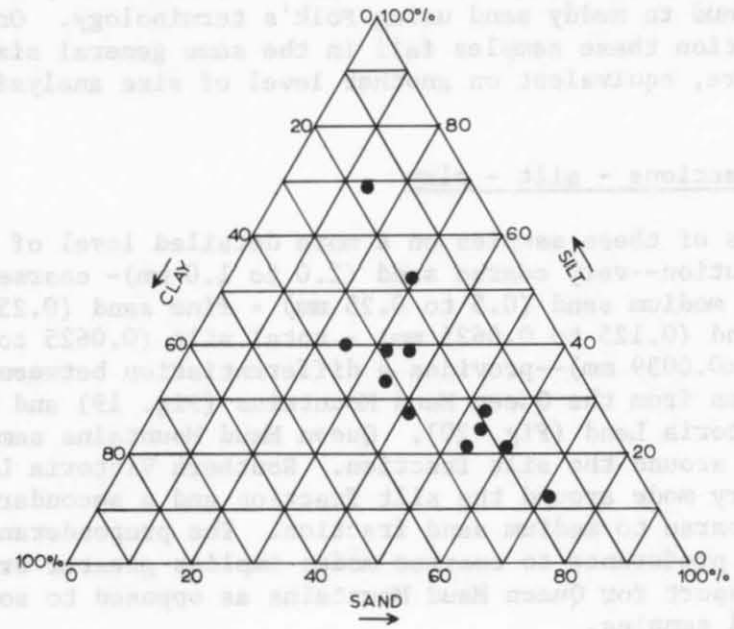

Figure 18. Sand - silt - clay triangular diagram of selected till member samples from throughout the Transantarctic Mountains.

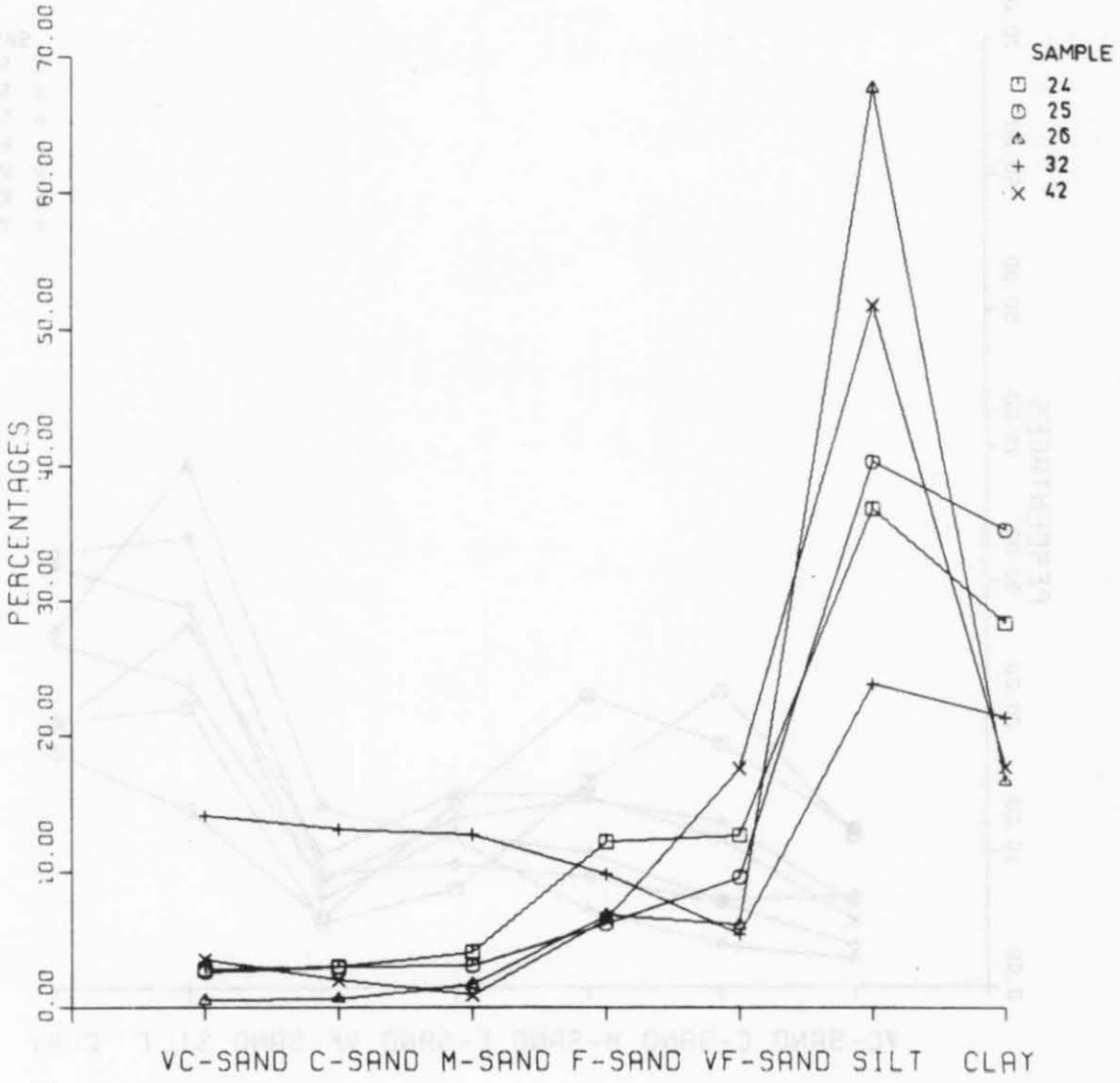

Figure 19. Particle size distribution of selected till member samples from throughout the Queen Maud Mountains.

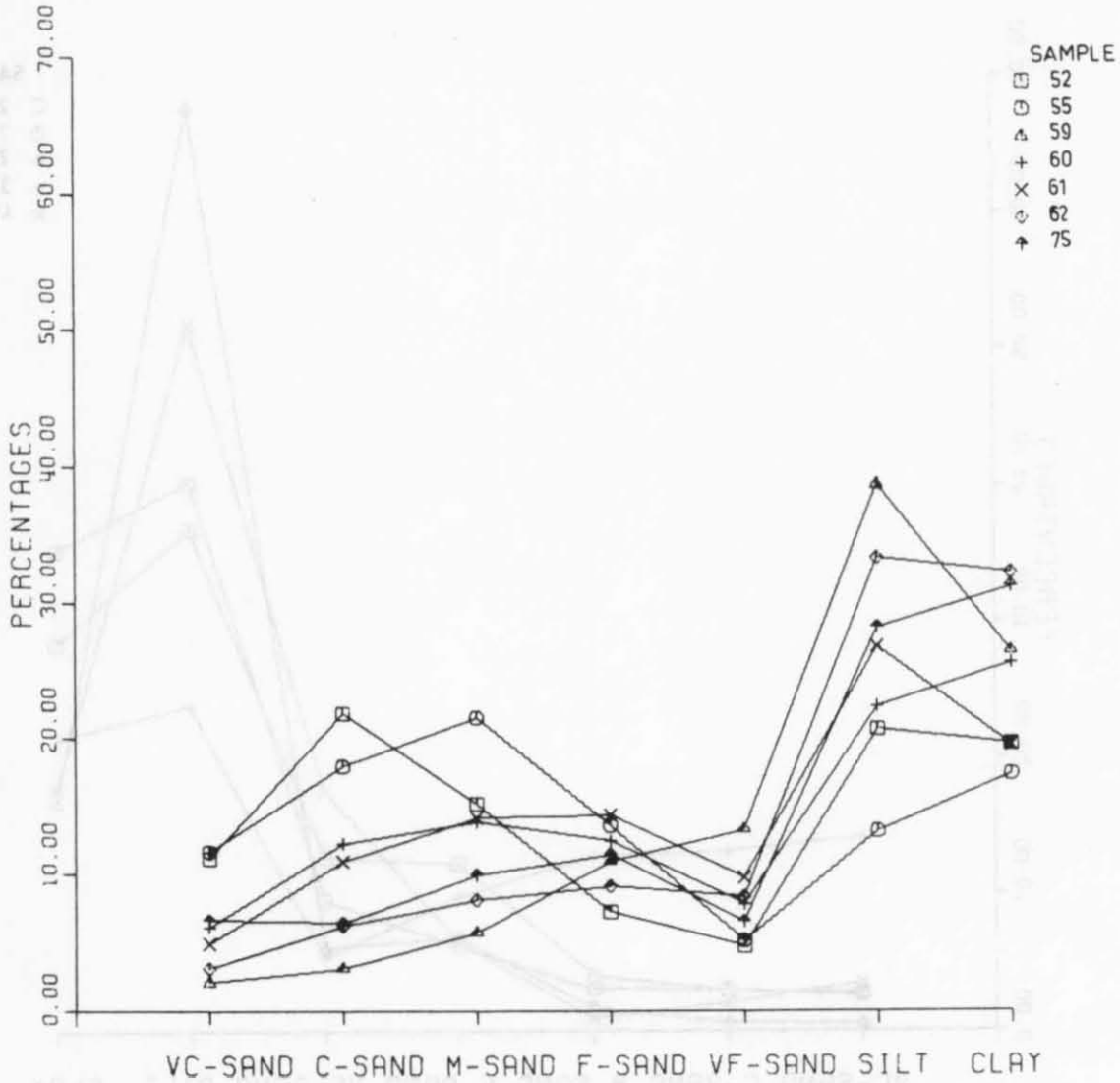

Figure 20. Particle size distribution of selected till member samples from southern Victoria Land.

Thin-section

Thin-section size analyses of 36 samples were made in order to supplement the limited preceding size analysis data. Analysis of the size distribution of till member samples by measurement in this section yields results quite comparable to the disaggregation technique, except for three potential errors: (1) particles in excess of very coarse sand (> 1 mm) tax the dimensions of the slide, and (2) those less than coarse silt (<0.031 mm) tax the magnification power of the microscope, and (3) only two dimensions, as opposed to three for sieving, can be measured in thin section. Thus, the size range 1 mm to 0.031 mm is the most realistic size range to investigate using this technique.

Size analysis of thin section samples from the Queen Maud Mountains (Fig. 21) indicates a pronounced mode in the medium sand to very fine sand (0.25 to 0.0625 mm) size range. Thin-section samples from southern Victoria Land (Fig. 22) have a pronounced mode around the medium sand fraction (0.5 to 0.25 mm) and a secondary mode around the fine sand fraction (0.25 to 0.125 mm). Although the physical disaggregation and thin-section techniques do not coincide in the presentation of modes, as a result of the different size ranges analyzed, both techniques indicate the slightly coarser state of the southern Victoria Land samples. Parent material differences and/or less extensive glacial transport of southern Victoria Land as opposed to Queen Maud Mountains samples may cause this difference.

Lithologic, Mineralogic and Organic Components

Lithologic and mineralogic components of the Sirius Formation are analyzed in order to indicate: (1) the equivalence of deposits throughout the Transantarctic Mountains, (2) differences between the till and stratified members, and (3) source area. Determination of source area is particularly important for distinguishing between local and continental scale glaciation, and for these samples indicates ice movement from the inland ice sheet. The lack of organic constituents in the samples studied implies a sterile environment prior to deposition of the Sirius Formation rather unlike that expected in an area of temperate glaciation.

Lithology and mineralogy

Stone counts made in the field at each locality corresponded closely to the distribution of bedrock in the surrounding area. Point counts were made from thin sections prepared for most of the samples collected (Fig. 3) in order to provide a more detailed analysis of lithology and mineralogy. Results of the thin section counts for Queen Maud Mountains samples are given in Tables 4 and 5, and for

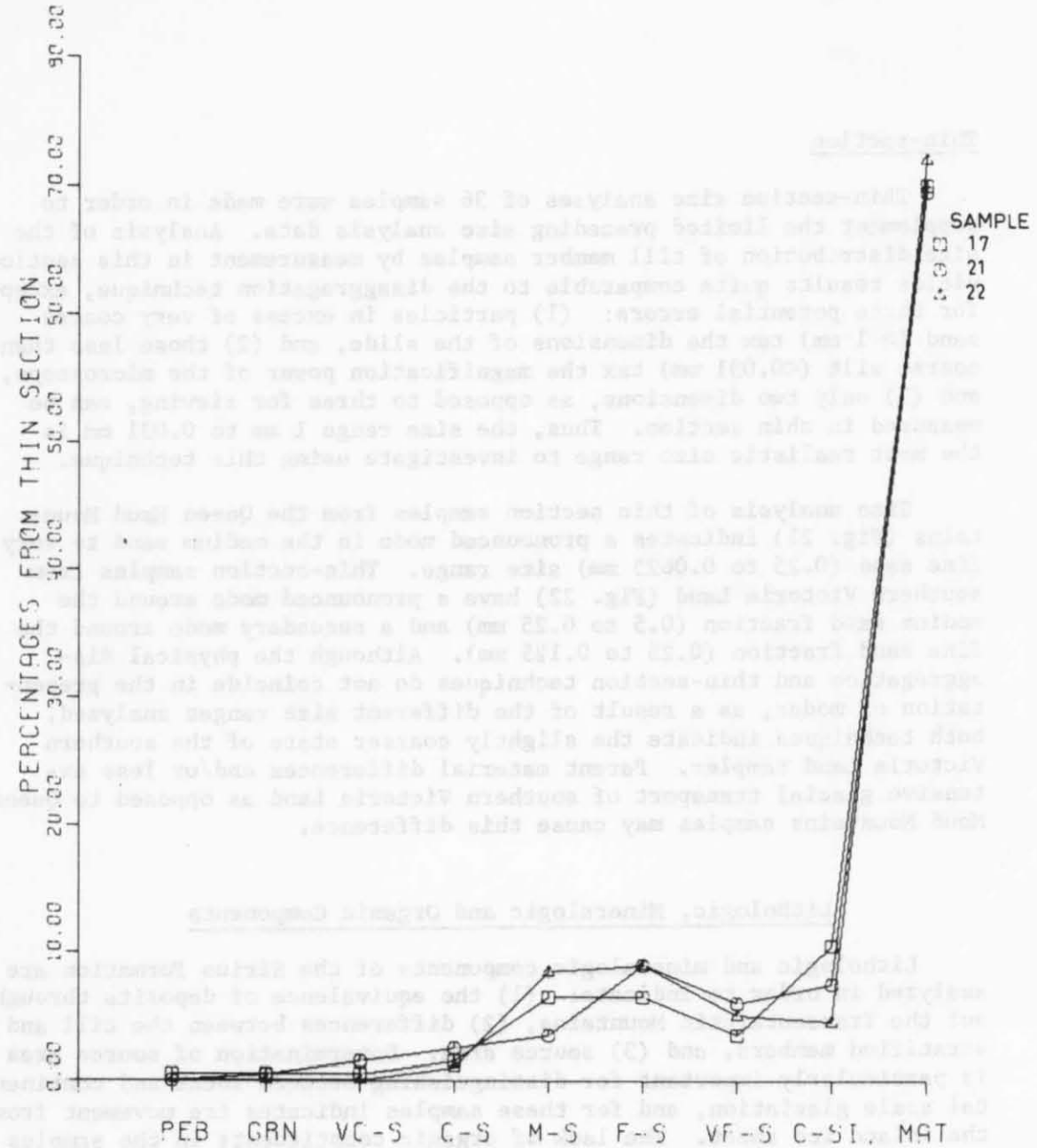

Figure 21. Particle size distribution of selected till member samples from the Dominion Range. Analysis by thin-section.

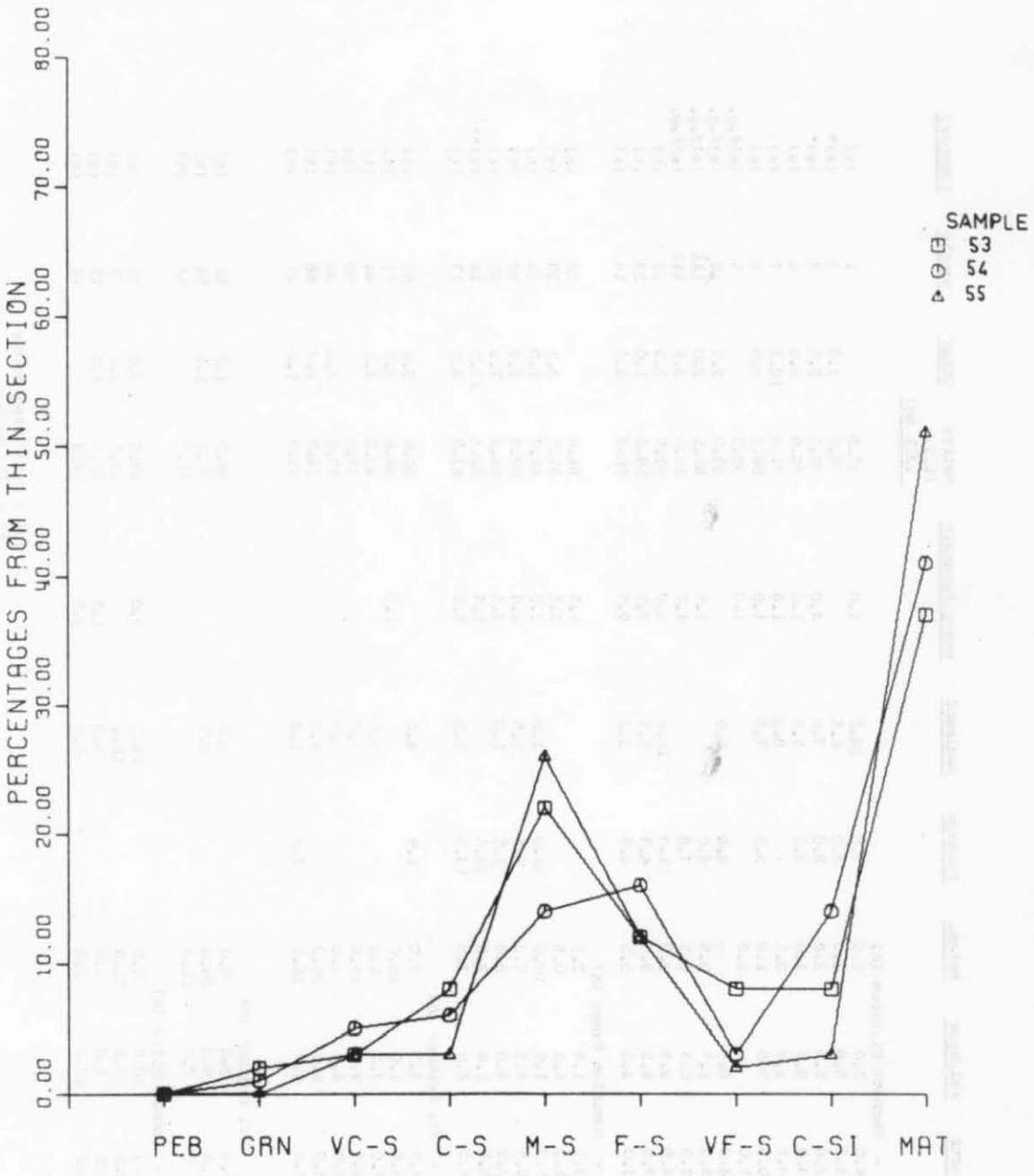

Figure 22. Particle size distribution of selected till member samples from Mount Feather. Analysis by thin-section.

	Quartz	Feldspar	Metam.	Igneous	Sediment	Heavy Minerals	Matrix (L.T. .031 mm)	Other	Sample	(Member)
Table 4 - Bennett Platform (A)										
	16.0	3.0	6.0	3.0	14.0	1.0	57.0		1	(s)
	3.5	5.0	2.0	2.0	6.5		79.0	2.0	3	(s)*
	12.0	1.0	2.0	2.0	7.0	4.0	70.0	2.0	4	(s)*
	13.0	0.5	1.0	3.0	5.5	1.0	70.0	6.0	6	(s)
	14.5	2.0	0.5		0.5	1.0	71.0	10.5	7	(s)
	10.5	3.0	1.0	5.5	7.0	1.0	66.5	5.5	8	(s)
	5.0		2.0			1.0	92.0		9	(s)f.g.
	4.0	0.5		4.0	6.0		83.0	2.5	10	(s)f.g.
	3.0	1.5	0.5	4.0		1.5	87.5	2.0	11A	(s)f.g.
	3.0	0.5	0.5	7.0		1.5	84.0	3.5	11B	(s)f.g.
	4.5	2.5	2.0	11.0	12.0	3.0	62.5	2.5	12	(t)
	7.5	4.5	9.5	4.5	2.5	2.5	68.0	1.0	13	(t)
	13.0	4.0	5.5	4.5	3.5	0.5	66.0	3.0	14	(t)
Table 5 - Dominion Range (A)										
	10.5	1.5	2.5			1.5	84.0		20	(s)
	11.5	1.5	0.5			2.5	81.5	2.5	19	(s)
	5.0	1.0	10.0	16.0	1.0	3.0	62.0	2.0	23	(t)
	10.5	3.5	7.0	0.5	0.5	4.0	69.0	5.0	22	(t)
	12.0	4.0	8.0	1.0	1.0	2.5	64.0	7.5	21	(t)
	5.5	1.0	3.5	22.5		1.5	52.5	13.5	18	(t)**
	6.0	4.0	3.5	14.5	1.0	5.0	62.0	4.0	17	(t)
Table 6 - Mt. Feather (A)										
	37.0	3.0	3.0	1.0	4.0		50.0	2.0	52	(t)
	39.0	1.0	19.0			1.0	38.0	2.0	51	(t)
	37.0	7.0	6.0		5.0		42.0	3.0	44	(t)
	38.0	9.0	15.0		1.0		37.0		50	(t)
	28.0	4.0	5.0		3.0		57.0	3.0	49	(t)
	25.0	6.0	28.0		5.0		34.0	2.0	48	(t)
	36.0	4.0	16.0	7.0	1.0		35.0	1.0	47	(t)
Mt. Feather (B)										
	45.0	3.0	4.0		1.0		46.0	1.0	55	(t)
	27.0	9.0	24.0		8.0		31.0	1.0	54	(t)
	51.0	7.0	11.0				31.0		53	(t)
Table 7 - Coombs Hills (A)										
	10.0	10.0	8.0		24.0	2.0	43.0	3.0	70	(t)
	9.0	17.0	11.0		18.0		43.0	2.0	72	(t)
	18.0	8.0	8.0		5.0	1.0	51.0	9.0	73	(t)
	25.0	12.0	2.0		5.0	2.0	54.0		74	(t)

(s) = stratified member
(t) = till member
* = till lense in stratified member
** = stratified lense in till member
f.g. = fine-grained

southern Victoria Land samples in Tables 6 and 7. Each table is partitioned into categories of percent: quartz, feldspar, lithic fragments (subdivided into metamorphic, igneous and sedimentary), heavy minerals, matrix, and other (i.e. carbonates and secondary iron accumulations).

Summarizing Tables 4 to 7, the following conclusions can be drawn:

quartz

Stratified member samples have high and consistent quartz percentages as a function of the fluvial reworking of already glacially modified particles. The notable exception to the usually high quartz content of the stratified member samples is the low quartz content in samples of the very fine-grained stratified member. This low quartz content is attributed to the longevity of the resistant mineral quartz in the coarser size grades, i.e. sand sizes, even with continued reworking (Folk, 1968).

The quartz content of samples of the till member and samples from till lenses in the stratified member varies widely, depending on the differing amounts of glacial abrasion and differing additions of parent material. The very high quartz content of the southern Victoria Land samples results from the high quartz content of the parent materials, i.e. the nearby Feather Conglomerate and the Lashly Formation (Table 2).

feldspar

Variations in percent feldspar are inversely proportional to those of quartz. Samples from the stratified member have consistently lower feldspar percentages, 2 to 3 times lower, than samples from the till member and till lenses in the stratified member. Increased reworking tends to lower the feldspar content.

lithic fragments

The metamorphic subcategory of lithic fragments is the most indicative of all of the lithic subcategories. Metamorphic fragments are far less abundant in stratified member deposits than in till member deposits in the proportion 1:3 (stratified member to till member). Igneous and sedimentary fragments appear to be less diagnostic, possibly because of their dilution during transport. Metamorphic fragments do not commonly crop out upglacier from sites of the Sirius Formation, and, therefore, are probably not available as a source of introduced fragments during travel as frequently as igneous and sedimentary rocks.

heavy minerals

Analysis of heavy minerals, predominantly iron-magnesium minerals, produced no noticeable deviation from member to member. However, a marked decrease in percent of heavy minerals was noted from the Queen Maud Mountains to southern Victoria Land and is assumed to be dependent on local source materials.

"other"

Although the category "other" in Tables 4-7 is broad, it does serve to set aside minerals which, because of local derivation, are of little value in comparing deposits from widely-separated localities. Many of these minerals are, however, important indicators of the direction from which source material was derived. These will be treated in the following list, by location, along with indicators of direction of derivation of source material derived from the categories already discussed.

Bennett Platform (sample 14): This sample was collected close to the dolerite contact at the base of the Bennett Platform section. Baked sedimentary fragments, resulting from contact metamorphism as a result of dolerite sill intrusion, are far more common in this sample than in samples higher in the section. This concentration of baked fragments indicates local derivation.

Roberts Massif (samples 35-38): These samples contain basalt fragments and, therefore, indicate transport of material from the southwest rather than from a local source, as the only known basalt outcrops are inland from Roberts Massif.

Dominion Range (samples 19-21 and 28): These samples contain abundant calcite (fragments and cement) and analcime. These two minerals are very probably derived from the Falla Formation which crops out locally.

In addition, sample 28 contains accretionary lapilli which suggest a local source such as the Falla or Fremouw Formations. In general, Dominion Range samples also contain abundant basalt fragments which imply transport of this material from under the inland ice to the south.

Mount Wisting (sample 39): This sample is part of an erratic boulder and contains basalt fragments. Both the presence of the basalt fragments and the location of the sample at the edge of the inland ice indicate that the boulder has been transported from under the inland ice south of Mount Wisting.

Mount Roth (sample 40): This very crudely stratified, pebbly sample is important because it comes from the lowest level occurrence of the Sirius Formation. It consists entirely of metasedimentary components, more than 95 percent of which are marble. This composition and the coarseness of the fragments indicate extremely local derivation.

In conclusion, the Sirius Formation has the following lithologic and mineralogic compositions:

(1) The stratified and till members of the Sirius Formation have different proportions of contained quartz, feldspar and metamorphic lithic fragments. These differences are assumed to reflect the amount of reworking of material combined with the relative resistance of the component fragments.

(2) Till member samples have differing percentages of quartz, feldspar, metamorphic fragments, and heavy minerals, reflecting different source material, amount of glacial transport, or both.

(3) Although several samples of the Sirius Formation are composed of locally derived material, samples from Roberts Massif, the Dominion Range, and Mount Wisting contained components derived from inland sources under the Antarctic ice sheet. With the present bedrock and ice surface topographies, these components could not be transported into these areas. Only if the ice surface were higher than at present would such transport be possible, which implies an enlarged version of the present Antarctic ice sheet.

Organic components

Five samples from the Queen Maud Mountains (samples, 1, 9, 14, 17, and 23) and five samples from southern Victoria Land (samples 47, 51, 59, 72, and 78) were examined by Dr. J.M. Schopf of the U.S. Geological Survey Coal Geology Laboratory at The Ohio State University for fossil flora related to the Sirius Formation. Each sample was chosen for its potential for containing preserved flora based on the occurrence of: (1) laminated, fine-grained samples related to quiet water deposition and likely entrapment of flora, (2) till member samples from near the base of the deposit which may have incorporated organic material during transport, and (3) dark-colored samples which presumably attribute their color to contained organic material. Based on the examination and interpretation of these samples by Dr. Schopf the only possible indigenous fossils noted were fragmentary cuticular flakes, brownish or yellowish in color (indicating a fossil state), which were poorly preserved. All of these fragments, however, were eventually assigned to a source from the Triassic sediments of the Beacon Supergroup.

The lack of organic material deposited contemporaneously with the Sirius Formation is an indication of: (1) the eradication and sterilization of the land surface prior to the deposition of the Sirius Formation, (2) the probable subglacial and englacial deposition of the till member, and (3) the apparent lack of vegetation either aerially or subaerially during the disintegration of the ice which deposited the Sirius Formation. On the contrary, local temperate glaciation would probably have occurred contemporaneously with a local plant cover as observed in temperate areas at present, and some evidence of this plant cover should be present in or related to the deposit.

Rounding and Freshness of Grains and Glacial Imprints on Grains

Rounding

Characterization of particle rounding was attempted on both members of the Sirius Formation as a further means of differentiation. Particles in the size range 0.5 cm and greater (long axis) were examined macroscopically and particles less than 0.5 cm (long axis) were examined microscopically. Rounding of these clasts was described using the roundness scale of Pettijohn (1957). In this system roundness is divided into roundness grades ranging from angular to subangular to subrounded to rounded to well-rounded. This system is practical because both detailed descriptions and examples of each rounding grade are available. The following roundness characteristics were observed:

(1) Clasts more than 5.0 cm (long axis) from the stratified member are predominantly subrounded to rounded. A typical example of the coarser variety of these clasts can be found by referring to the gravel lens in Figure 23.

(2) Clasts more than 5.0 cm (long axis) from the till member are predominantly (70-80 percent or more) very angular to subangular. Fine- to medium-grained dolerite fragments in the cobble to boulder size range were the one exception, ranging in roundness grade from subangular to rounded. Fine- to medium-grained dolerite fragments comprise the most resistant lithology in the Sirius Formation and thus, have probably only been modified by abrasion of corners and sides rather than complete crushing. The less resistant lithologies maintain a fairly angular grade of roundness because of repeated breakage in transport.

(3) Particles in the size range 0.5 to 5.0 cm derived from the stratified member samples are concentrated predominantly in the subangular to rounded range, whereas particles in the size range 0.5 to 5.0 cm derived from till member samples concentrate predominantly in the very angular to angular range.

Figure 23. Example of gravel lens in the stratified member, Bennett Platform

(4) Particles in the size range 0.5 cm to 0.031 mm displayed the following roundness characteristics by lithology:

(a) Quartz particles from both members were predominantly very angular to subangular.

(b) Feldspar particles in the stratified member are sub-rounded and in the till member range from angular to subangular.

(c) Lithic fragments were similar in roundness to the feldspar roundness grades for both members.

(d) Heavy minerals in all samples analyzed fell in the roundness grades of very angular to subangular.

(e) Particles less than 0.031 mm when viewed under high magnification ranged in roundness grades from very angular to angular.

In general, particles derived from the stratified member are uniformly better rounded than particles derived from the till member. Particles in the till member maintain low grades of roundness due to crushing and abrasion in glacial transport. Particles in the stratified member, although derived from the underlying till member, have rounder grades due to the added influence of fluvial action.

Freshness

All clasts examined in the field and in thin section were totally unweathered with the exception of clasts on the surface of the Sirius Formation outcrops, implying an uninterrupted ice cover. These surficial clasts are exposed to post-depositional subaerial weathering resulting in iron-staining and disintegration of coarse-textured clasts.

Glacial imprints

Scanning electron microscope studies of ten samples of the Sirius Formation (samples 1, 9, 10, 14, 17, 23, 47, 51, 59, 72 and 78) were made by Drs. P. Webb and B. Burt of the New Zealand Geological Survey. Quartz grains displaying characteristic glacial imprints are common in these samples. They further indicate the glacial origin of the Sirius Formation. In Figures 24 and 25, "the sharp angular outline, high relief, smooth featureless surfaces and straight and arc-shaped features" (Webb, 1972, p. 227) characteristic of glacial origin can be noted. In Figure 26, "a series of semi-parallel, irregular steps... (and) very high relief" (Krinsley and Takahashi, 1962, p. 1263) provide further evidence of the glacial origin of the Sirius Formation. Some rounded grains are also evident in other samples studies as a

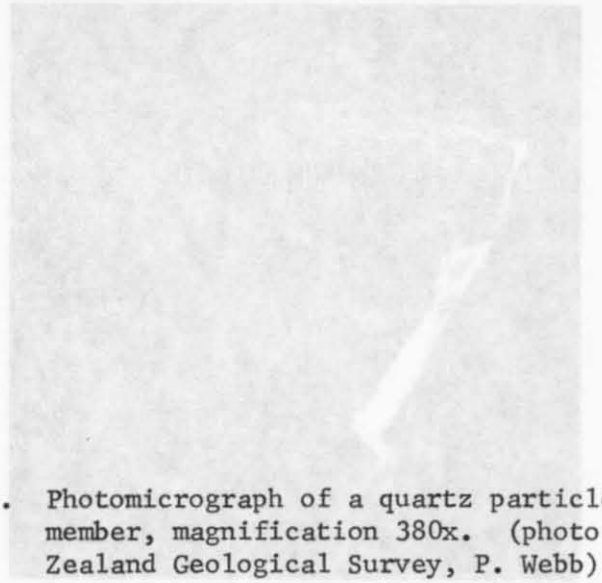

Figure 24. Photomicrograph of a quartz particle from the till member, magnification 380x. (photo courtesy of New Zealand Geological Survey, P. Webb)

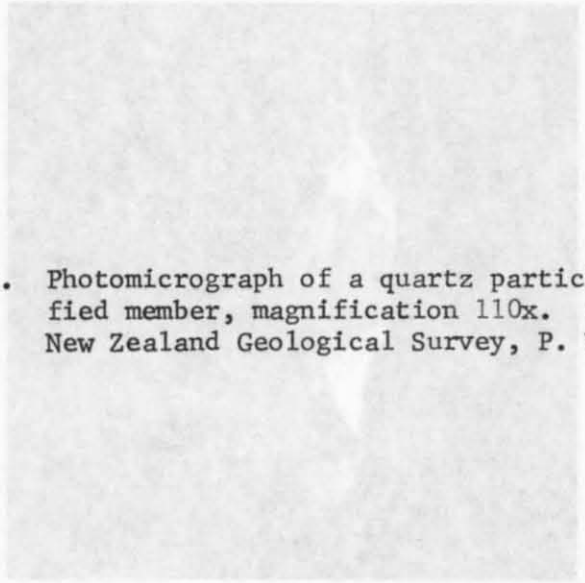

Figure 25. Photomicrograph of a quartz particle from the stratified member, magnification 110x. (photo courtesy of New Zealand Geological Survey, P. Webb)

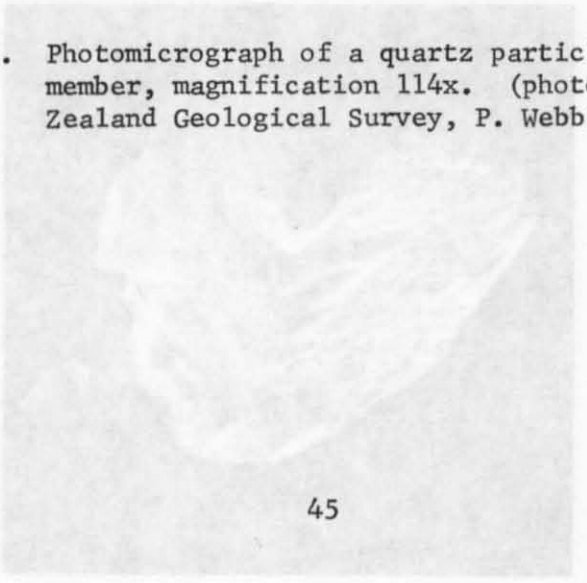

Figure 26. Photomicrograph of a quartz particle from the till member, magnification 114x. (photo courtesy of New Zealand Geological Survey, P. Webb)

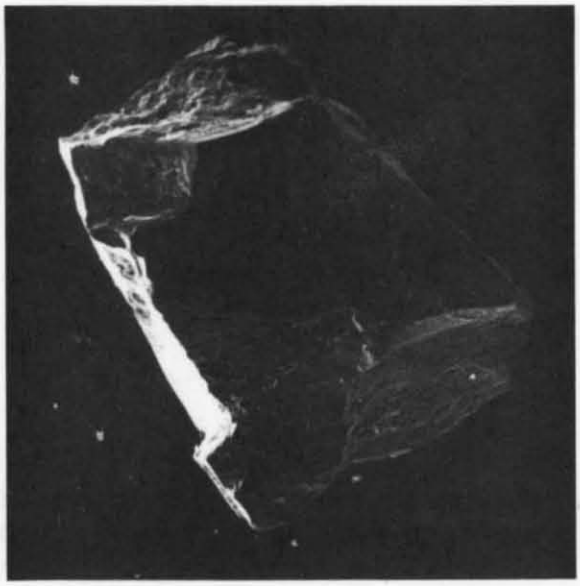

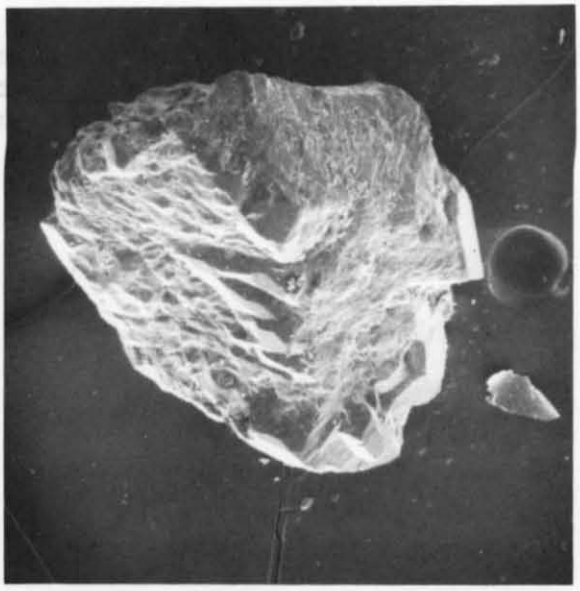

result of the addition of reworked Beacon Supergroup sediments, as noted for other Antarctic samples by Webb. Slight rounding of some of the grains (Figure 25) from the stratified member may be a function of fluvial action and partially aids in the differentiation of the till and stratified members.

In addition to the microscopic glacial imprints noted above, faceted and striated clasts were commonly found in the Sirius Formation. Examples of these clasts appear in Figure 27, from Queen Maud Mountains samples, and in Figure 28, from southern Victoria Land samples.

Directional Indicators

Evidence regarding the direction of ice flow during the deposition of the Sirius Formation is the most important single point in favor of a thick continental ice sheet versus the local temperate glacier hypothesis. Three types of evidence are used to determine the direction of the ice which deposited the till member (Figure 29):

(1) fabric measurement of elongate clasts within the till member,

(2) orientation of grooves on bedrock surfaces, and (3) orientation of striations on bedrock surfaces.

Till fabric

Fabric data at each locality measured included the measurement of 50 strikes and dips (Pessl, 1971) on clasts within the till member. These clasts met the following minimum standards: (1) length to width ratio equal to at least 2.5 to 1, and (2) clast long axis of 5-15 cm. Fine- to medium-grained dolerites and siltstones were the two most favorable lithologies for these measurements. Strikes of the 50 clasts at each location are plotted as mean values (Figure 29) in order to indicate only primary flow orientation of the depositing ice. Non-horizontal dips measured on clasts are used to determine the direction of former glacier movement assuming that the clasts dip upstream in the direction of former glacier flow (Harrison, 1957).

Grooves

Directional information was also determined from a study of grooved bedrock surfaces. A grooved bedrock surface overlain by the till member of the Sirius Formation was noted at Roberts Massif. At this site the fabric of the till and the groove directions coincide. Ridges between these grooves, when viewed in long section (Figures 5 and 6), are smoothed on their up-glacier side and are jagged on their down-glacier side, and thus indicate the direction of ice flow.

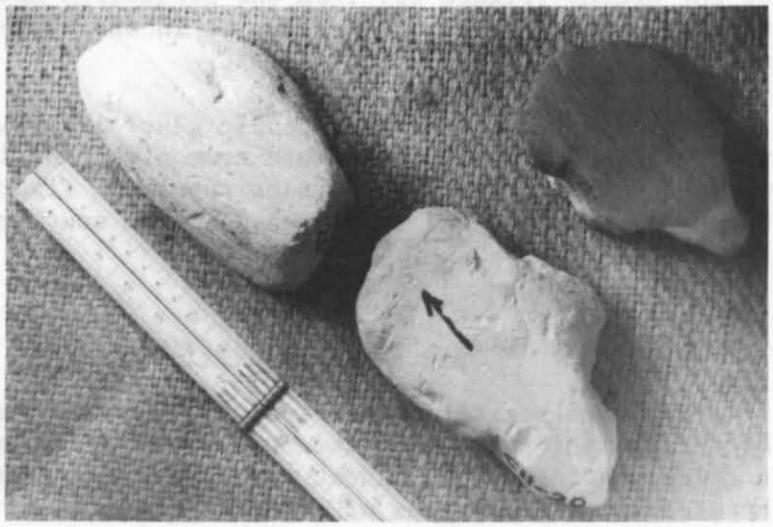

Figure 27. Examples of striated and faceted clasts from the till member, Queen Maud Mountains. (photo by R. Wilkinson)

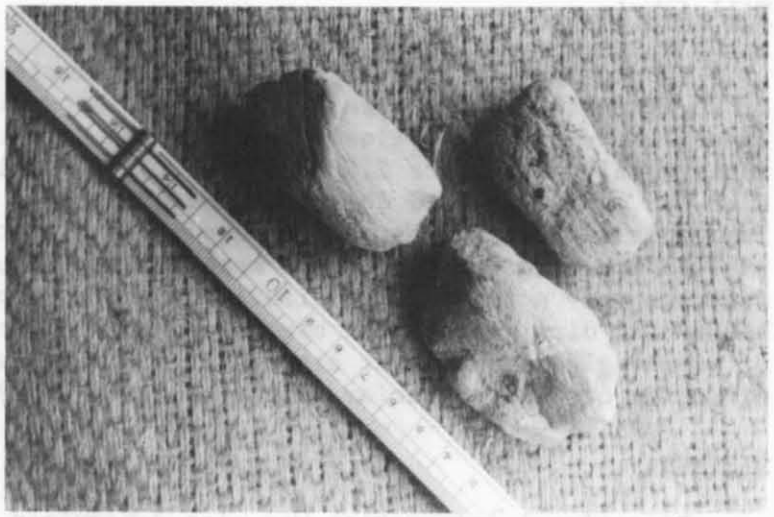

Figure 28. Examples of striated and faceted clasts from till member, southern Victoria Land. (photo by R. Wilkinson)

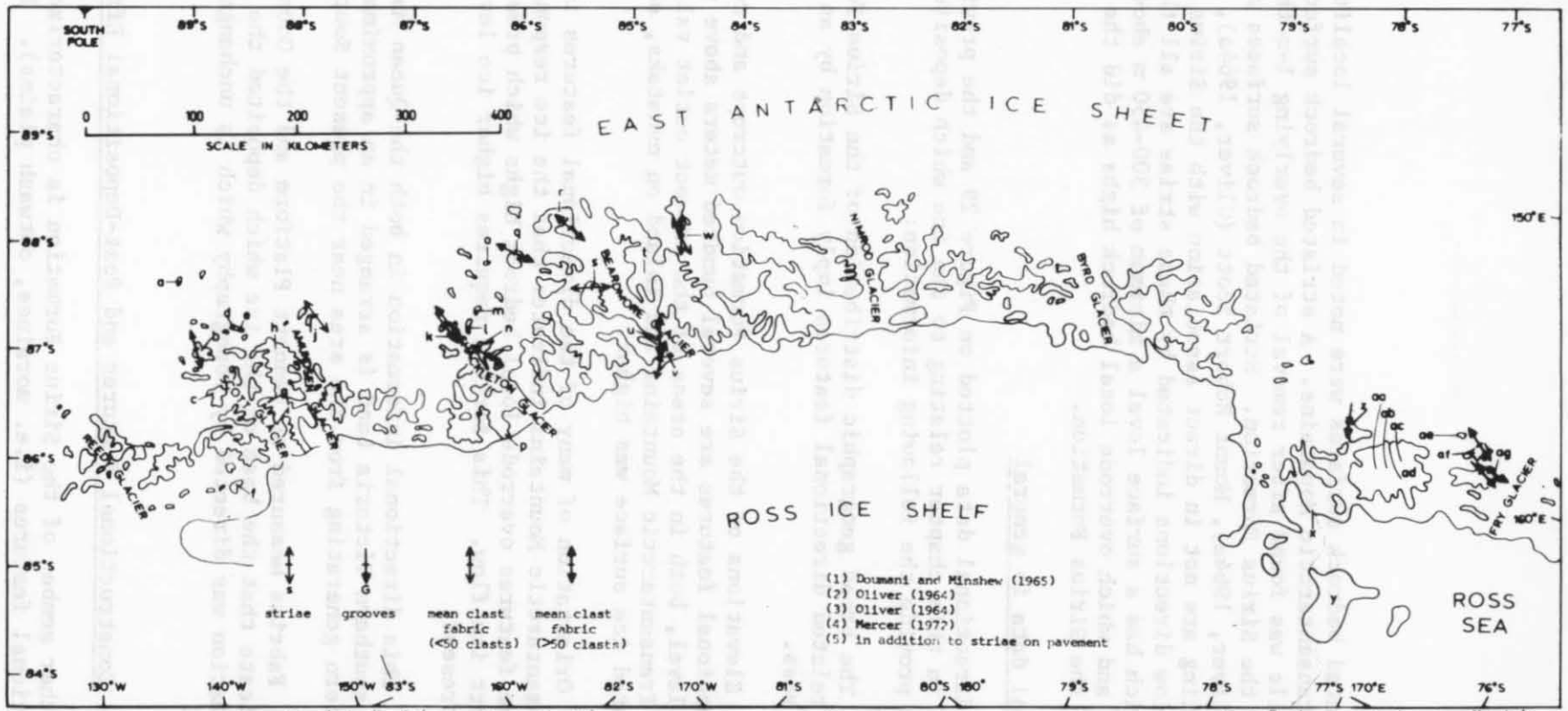

a: Mount Howe
b: La Gorce Mountains
c: Mount Blackburn
d: Mount Saltonstall
e: Mount Innes-Taylor
f: Supporting Party Mountain
g: Mount Crockett
h: Nilsen Plateau
i: Mount Pulitzer
j: Mount Wisting
k: Roberts Massif
l: Dismal Buttress
m: Half Century Nunatak
n: Bennett Platform
o: Mount Block
p: Mount Roth
q: Otway Massif
r: Dominion Range
s: Mount Deaken
t: Mount Kirkpatrick
u: Mount Kyffin
v: Mount Robert Scott
w: Mount Sirius
x: Cape Chocolate
y: Ross Island
z: Mount Feather
aa: Taylor Valley
ab: Wright Valley
ac: Victoria Valley
ad: Shapeless Mountain
ae: Carapace Nunatak
af: Allan Nunatak
ag: Coombs Hills

Striae

Striated bedrock surfaces were noted in several localities throughout the Transantarctic Mountains. A striated bedrock surface in the Coombs Hills was found after removal of the overlying 1-m-thick till member of the Sirius Formation. Striated bedrock surfaces at Mount Kyffin (Oliver, 1964a), Mount Robert Scott (Oliver, 1964a), and near Mount Wisting are not in direct association with the Sirius Formation. The ice flow directions indicated by these striae are all the result of ice which had a surface level a minimum of 300-450 m above present ice level and which overrode local bedrock highs as did the ice which deposited the Sirius Formation.

Directional data in general

The directional data plotted on Figure 29 and the previous evidence developed in this chapter relating to the ice which deposited the Sirius Formation provide the following information:

(1) The broad geographic distribution of the Sirius Formation and related directional features imply formation by an extensive ice mass.

(2) Elevations of the Sirius Formation outcrops and related directional features are several hundred meters above present ice level, both in the areas of the present outlet valleys of the Transantarctic Mountains and inland on nunataks, so the related ice surface was higher.

(3) Orientation of many of the directional features in the Transantarctic Mountains indicates that the ice responsible for these features overrode local bedrock highs which presently divert ice flow. This further requires higher ice levels than at present.

(4) This directional information in both the Queen Maud Mountains and southern Victoria Land is arranged in an approximately radial pattern generating from the area near the present South Pole.

(5) Fabrics measured at Bennett Platform and the Coombs Hills indicate that the base of the ice which deposited the Sirius Formation was directed by topography which is unchanged to this day.

Constructional Features and Post-Depositional Effects

Neither member of the Sirius Formation is characterized by any constructional features (i.e. moraines, outwash plains). The Sirius

Formation must have been more extensive formerly, but it has been reduced to its present patchy geographic distribution and subdued morphology by a complex of post-depositional processes.

Evidence of fluvial action, far in excess of that today, following the deposition of the Sirius Formation can be noted in places throughout the Transantarctic Mountains and provides evidence of an ameliorated climate following deposition and, therefore, an "interglacial". The following information applies to this hypothesis:

(1) A deep gully (Figure 30) is incised into the upper portion of the Sirius Formation at Bennett Platform marking the extensive fluvial action which followed the deposition of the Sirius Formation at some time.

(2) Drainageways exist stranded above post-Sirius Formation glacial deposits at Matador Mountain. These drainageways extend to the top of Matador Mountain and are evidence of the water which flowed off the thick deteriorating ice which had deposited the Sirius Formation.

(3) Potholes up to 1 m in diameter adjacent to the Sirius Formation outcrop and within the Lashly Formation on Mount Feather are further evidence of the fluvial action occurring after the deposition of the Sirius Formation. Mirsky and others (1965, p. 173), working in the Alatna Valley of the Convoy Range, noted "..an intricate system of giant plungepools and spillways, some more than 100 feet in diameter and in depth, which occur in the quartzose sandstone of the Razorback Formation at the Battleship Promontory." They consider these high level features as effects which post-date the retreat of the ice which sculptured Alatna Valley. Thus, these features post-date the Sirius Formation.

(4) Large slumped and fractured blocks of the stratified member of the Sirius Formation are found at Bennett Platform. They result from water percolation into the stratified member during the post Sirius Formation wet period and consequent slippage along planes of weakness.

In order for these large scale fluvial features to exist:

(1) considerable portions of the ice which deposited the Sirius Formation must have disappeared and (2) a water source must have been present either due to increased precipitation in the area or the partial deterioration of the ice which deposited the Sirius Formation. In any case, the climate must have become less conducive to the

Figure 30. Gully formed in upper portion of stratified member, Bennett Platform.

continuation of a full-bodied ice sheet. Therefore, these fluvial features mark an interglacial period occurring between the deposition of the Sirius Formation and the deposition of the younger glacial deposits which overlap these features.

More minor post-depositional features which are found associated with the Sirius Formation can also be noted:

(1) On a very minor scale water erosion in the form of rills on the outer surface of the Sirius Formation has resulted in the excavation of material surrounding large boulders. The removal of this material eventually results in the isolation of boulders on columns of fine-grained compact debris. Pedestals capped by these boulders are characteristic of the Sirius Formation (Figure 31).

(2) Rill erosion in the form of alternating channels between surficial silt-clay accumulations has aided the deterioration of the outer surface of the Sirius Formation.

(3) Fracture systems and small scale platy sheets of silt and clay (average 5-10 cm) result from alternate drying and wetting by snow on the surface of the Sirius Formation.

(4) Minor evidence of iron staining is found surrounding and within coarse-grained dolerite clasts on the surface of the Sirius Formation. Oxidation of the outer surface of the deposit (1-3 cm) has resulted in a characteristic light gray color (i.e. 7.5YR 7/0 to 8.0) which has been extremely useful in identifying the Sirius Formation from the air. Beneath the light gray weathered surface is the gray (i.e. 7.5YR 6/0) to dark gray (i.e. 7.5YR 5/0) unweathered deposit.

Interpretative Review of Characteristics

The following conclusions can be drawn from the characteristics of the Sirius Formation:

(1) The deposit post-dates the deep exposed glacial sculpturing of the Transantarctic Mountains because: (a) it lies within the valleys of these mountains, (b) directional data conform to the present bedrock topography, and (c) the lack of organic remains in the deposit requires prior erosion of the underlying bedrock.

(2) It is a widespread deposit found in 24 localities throughout the Transantarctic Mountains. All of the characteristics investigated at these localities imply a similar environment of deposition. Anomalous differences in these characteristics are a

Figure 31. Example of boulder balanced on column of fine-grained compact debris, till member, Dominion Range.

function of the amount of glacial transport and the types of parent material.

(3) Two members make up this deposit: (a) a till member at the base interpreted as a lodgement till overlain by (b) a stratified member interpreted as an ice-contact deposit. These members are differentiated by their contrasting structure, particle size distribution, lithologic and mineralogic components and the roundness of their included clasts.

(4) The till member comprises the major portion of all outcrops of the Sirius Formation. The high elevation at which this member is usually noted, i.e. in excess of 1750 m above sea level, and the orientation of directional indicators which record the ice movement during deposition of this member imply that this member is the result of an ice mass: (a) of continental scale that (b) exceeded the elevation of the present Antarctic ice sheet, and (c) had a flow pattern which radiated from an area close to the present South Pole. Therefore, this deposit is not the result of deposition by localized temperate ice located high in the Transantarctic Mountains.

(5) The deposits of the stratified member mark the declining stages of the ice sheet which deposited the till member. Deformed and fractured portions of the stratified member and dip of included lenses substantiate an ice-contact association for this deposit. A boulder pavement overlying a thin till layer within this member attests to at least one minor readvance of ice.

(6) Prominent fluvial features are found cut into the Sirius Formation and at elevations above or close to the level of this deposit. These mark a period of milder climate during which the ice surface in the Transantarctic Mountains was lower than at the time of Sirius Formation deposition. This milder climate is considered to be an "interglacial" following the deposition of the Sirius Formation. Glacial deposits younger than the Sirius Formation overlap these fluvial features.

Relative Position in the Glacial Record and Age

The name Queen Maud Glaciation is proposed here for the glacial event during which a thick ice sheet inundated the Queen Maud Mountains. This ice sheet resembled an enlarged version of the present Antarctic ice sheet. An ice sheet of this dimension may have existed as early as 5 to 10 million years ago based on the evidence noted by Rutford (1972), Hamilton (1969) and Doumani (1963). Glacial erosion by cirque glaciers and valley glaciers prior to the formation of this ice sheet

may have been vastly modified by erosion at the base of this ice sheet. As a result, a complex interrelation of glacially eroded features underlies the present Antarctic ice sheet. Overlying these glacially eroded features and post-dating this major period of erosion which sculptured the Queen Maud Mountains and the Transantarctic Mountains as a whole is the Sirius Formation. This deposit was formed in the latter stages of glaciation as are most tills (Goldthwait, 1971).

In southern Victoria Land the glacial event during which the area was inundated by ice and glacially eroded is named the McMurdo Glaciation (Péwé, 1961) and the Taylor V Glaciation (Denton and others, 1971) in Taylor Valley, the Vanda glacial episode (Nichols, 1971) and the First Glaciation (Bull and others, 1962) in Wright Valley, and the Insel Glaciation (Calkin, 1971) in Victoria Valley. Directly inland from each of these outlet valleys in southern Victoria Land, deposits of the Sirius Formation have been investigated (Mayewski, 1972). It is proposed that each of these glaciations include in time both the glacial sculpturing of southern Victoria Land and the deposition of the Sirius Formation in southern Victoria Land and that they are equivalent to the Queen Maud Glaciation.

The Horlick drift sequence reported by Mercer (1968) from the Reedy Glacier area is reinterpreted here as an equivalent to the Sirius Formation. This 40 m thick sequence is considered by Mercer to represent from bottom to top:

(1) a frost shattered bedrock or C horizon of a former soil (unit 1),

(2) a wet-based till derived from a local temperate glacier (unit 2),

(3) deposits derived from subaerial deposition (unit 3),

(4) a disconformity,

(5) a lodgement till (units 4 and 5) deposited by more extensive ice than that responsible for the deposition of unit 2,

(6) a disconformity

(7) ablation deposits (unit 6) of the Reedy Glacier (Reedy I).

In light of the new information derived from the study of the Sirius Formation throughout the Transantarctic Mountains, units (1) to (5) are reinterpreted as equivalents of the till member of the Sirius Formation. Unit (6) is maintained as an ablation deposit of

the Reedy Glacier equivalent to ablation deposits throughout the Transantarctic Mountains which overlie deposits of the Sirius Formation. More specifically, unit (3) is equivalent to the stratified lenses which are found within the till member. The transition from the shattered bedrock, unit (1), to the slightly less localized unit (2) deposit to the further travelled units (4) and (5) deposits is considered to be a function of continued deposition within a shallow bedrock depression. After the locally derived source material was deposited, it was overlain by new source material scoured from further inland. The disconformity between units (3) and (4) may represent a readvance or a slump plane. The Horlick drift sequence seems to fit perfectly as a Reedy Glacier area example of deposition beneath the ice sheet that deposited the Sirius Formation and not a transition from localized temperate glaciers to cold glaciers as suggested by Mercer. Therefore, the Horlick Glaciation is considered to be an equivalent of the Queen Maud Glaciation.

Throughout the remainder of this text the Queen Maud Glaciation will be considered the glaciation during which the Transantarctic Mountains were most deeply sculptured and during which the Sirius Formation was deposited in the Transantarctic Mountains.

Approximate minimum dates can be assigned to the Queen Maud Glaciation by its association with: (1) interglacial features in Wright Valley and (2) basalt cones post-dating the glacial sculpturing of Wright Valley.

Fluvial channels and potholes throughout the Transantarctic Mountains mark the interglacial period which separates the Queen Maud Glaciation from younger glacial maxima. In Wright Valley the stratigraphic position of this interglacial period is marked by the Pecten glacial episode (Nichols, 1971). This episode post-dates the glacial sculpturing of Wright Valley (Vanda glacial episode of First Glaciation) and the deposition of moraines marking a renewal of glaciation in Wright Valley. The terminal position of the Pecten glacial episode is marked by the Pecten moraine. Investigation of this moraine by Webb (1972) and McSaveney and McSaveney (1972) has revealed that this deposit is not really a moraine. Webb (1972, p. 229) has examined the taxa within this deposit and has noted similarities between these taxa and those found in "....fjords, channels, and in-shore glacio marine environments in Alaska and British Columbia." A Pliocene date has been temporarily assigned to this assemblage by Webb. He proposes that this deposit marks a period during which a fjord with a calving glacier tongue occupied Wright Valley. Nichols (1971) suggested as an alternate proposal to his Pecten glacial episode that the Pecten deposits resulted from marine invasion of the valley immediately following the retreat of a thick ice mass capable of isostatically

depressing the valley floor below sea level. The ice mass is believed by this author to be the same one which deposited the Sirius Formation, and thus, yields a minimum Pliocene date to the Sirius Formation. This relationship is discussed in more detail in Chapter IV of this report.

The Queen Maud Glaciation is the last glaciation during which ice completely filled Wright Valley, and thus was the last glaciation which could have substantially glacially sculptured the valley. Basalt cones believed to post-date the glacial sculpturing of Wright Valley have been potassium-argon dated at 3.7 and 3.9 million years (Denton and others, 1970) and 4.2 million years (Fleck and others, 1972). To have remained, these cones must post-date the ice which filled Wright Valley and thus post-date the Queen Maud Glaciation.

LATERAL MORAINES

Throughout the Transantarctic Mountains lateral moraines record the position of former, more extensive glacier margins. These moraines lie stratigraphically above and most commonly at lower elevations than deposits of the Sirius Formation. They provide the primary geologic evidence for the Transantarctic Mountains glacial record after the Queen Maud Glaciation and the "interglacial" that followed it.

In southern Victoria Land a detailed glacial chronology has been developed through the investigation of these moraines primarily by Nichols (1961, 1971), Péwé (1961), Bull and others (1962), Calkin (1964, 1971), Everett and Behling (1968), Denton and others (1970, 1971), and Behling (1971, 1972). Dates have been assigned to the southern Victoria Land glacial sequence by potassium-argon (Denton and others, 1970; Fleck and others, 1972) and reaction-rate kinetics (Behling, 1972).

The methods of moraine differentiation employed by workers in southern Victoria Land are used in this chapter to characterize and differentiate moraines in the Queen Maud Mountains. The use of these characteristics in both areas allows a correlation of these moraines in both areas, and therefore, a correlation of the glacial chronologies of the Queen Maud Mountains and southern Victoria Land. This provides a glacial record for the Transantarctic Mountains which includes all of the major glacial responses recorded in these mountains since the formation of the Antarctic ice sheet during the Queen Maud Glaciation. Obviously it does not, and never can, designate lesser overridden stages if any occurred.

Characteristics of Lateral Moraines in the Queen Maud Mountains

Moraines in the Queen Maud Mountains are primarily composed of thin, rubbly till containing angular clasts, lacking a fabric, and they are either ice-cored or ice-cemented at depth. Geomorphically the moraines in these mountains may be described as lateral moraines or perched moraines (German, 1968). They flank glacier margins and range morphologically from fairly prominent hummocks to prominent ridges to subdued hummocks (Fig. 32, right to left). These moraines are best preserved where the Beacon Supergroup and Ferrar Dolerite crop (Fig. 2) because of the structural platforms and moderately gentle slopes developed on these lithologies. The area of basement outcrop, in contrast, is composed of slopes which are too steep to retain the unconsolidated drift which makes up these moraines.

Figure 32. Moraines formed by a tributary glacier of the Shackleton Glacier, Bennett Platform. High Moraine (H), Middle Moraine (M) and Low Moraine (L).

Figure 33. Englacial debris in terminus of Gallup Glacier, adjacent to Bennett Platform. S. Etter in foreground.

The ablation till composing these moraines is transported both englacially and superglacially. Englacially transported debris (Fig. 33) can be commonly noted downglacier from nunataks. It is either ablated from ice edges or mores toward the glacier surface in thin, highly disseminated dirt bands by upward diffusion (Goldthwait 1971). Some debris is added to the glacier surface by mass-movement of material from adjacent talus slopes. Once on the glacier this material travels superglacially (Fig. 34). The transfer of this mass-movement material onto glacier surfaces is a slow process yielding only thin (maximum 20 cm thick) accumulations in localized areas. In general, the superglacial till is concentrated almost entirely within the immediate periphery of ice-free areas. The localization of these accumulations suggests that this debris is picked up, transported and deposited within the area peripheral to an individual ice-free area. The combination of englacial and superglacial debris becoming entrapped between valley walls and ice edges marks the peripheral position of an ice edge. Repeated oscillations of ice margins produce an offlap series of lateral moraines marking successively lower and lower maximum ice edge positions.

In the Queen Maud Mountains three systems of lateral moraines have been differentiated. From oldest to youngest these moraines are named the High, the Middle, and the Low Moraine, and each is prefaced by the geographic area in which it is found, i.e. Scott High Moraine, Scott Middle Moraine, and Scott Low Moraine. Four such geographic areas have been investigated in the Queen Maud Mountains corresponding to the major outlet glaciers in this region: the Scott, the Amundsen, the Shackleton, and the Beardmore Glaciers. Reconnaissance glacial geologic maps of the key areas used for study appear in Figures 35 to 41. The information on these maps will eventually be combined with the bedrock geology and will appear as part of a map series (i.e. Barrett and others, 1970; Elliot and others, 1974).

Each of the three lateral moraine systems in the Queen Maud Mountains is characterized and differentiated by the evaluation of eight properties: (1) elevation and continuity relative to present ice surface, (2) morphologic features including thickness of drift and presence of an ice-core, (3) weathering of surficial clasts, (4) particle size distribution of the soils developed on these moraines, (5) color of moraine surfaces and soils developed at depth within the moraines, (6) secondary salt content on the surface and at depth within the soils, (7) acidity-alkalinity from surface to depth within the soils, and (8) clay minerals developed within the soils. These eight criteria do not always agree but a clear majority do in each case.

Elevation and Continuity Relative to Present Ice Surfaces

The elevations of the tops of the Low, Middle, and High Moraines were measured at 24 localities throughout the Queen Maud Mountains

Figure 34. Superglacial debris derived from adjacent ice-free slope by mass-movement, Mount Dort.

Table 8. Legene for Glacial Maps (Figures 35 to 41)

Low Moraine

Glacial deposits, undivided

Middle Moraine

High Moraine

High and/or Middle Moraine, undivided

Sirius Formation

Glacial grooves

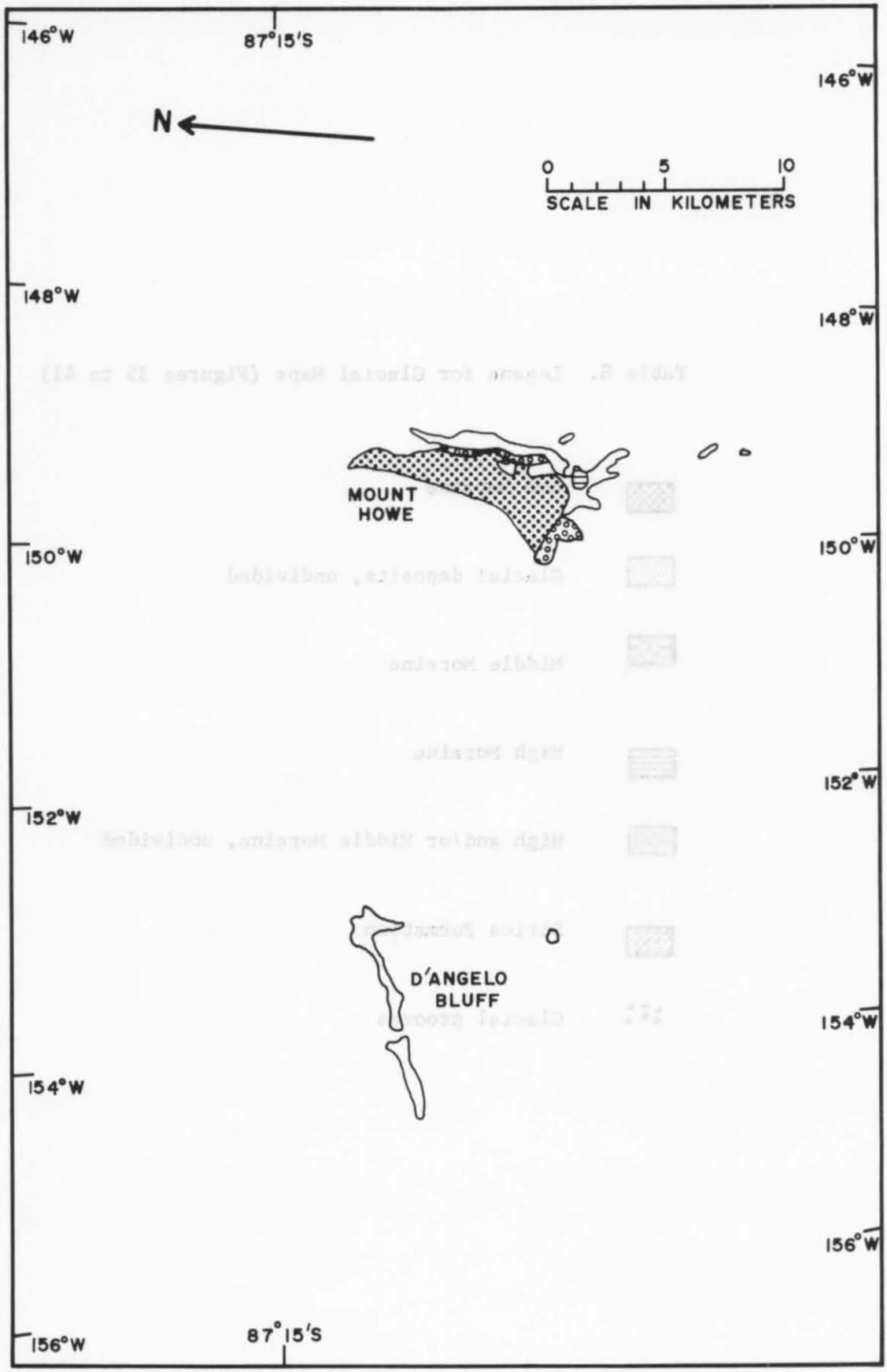

Figure 35. Glacial map of the Mount Howe area. (see Legend, Table 8)

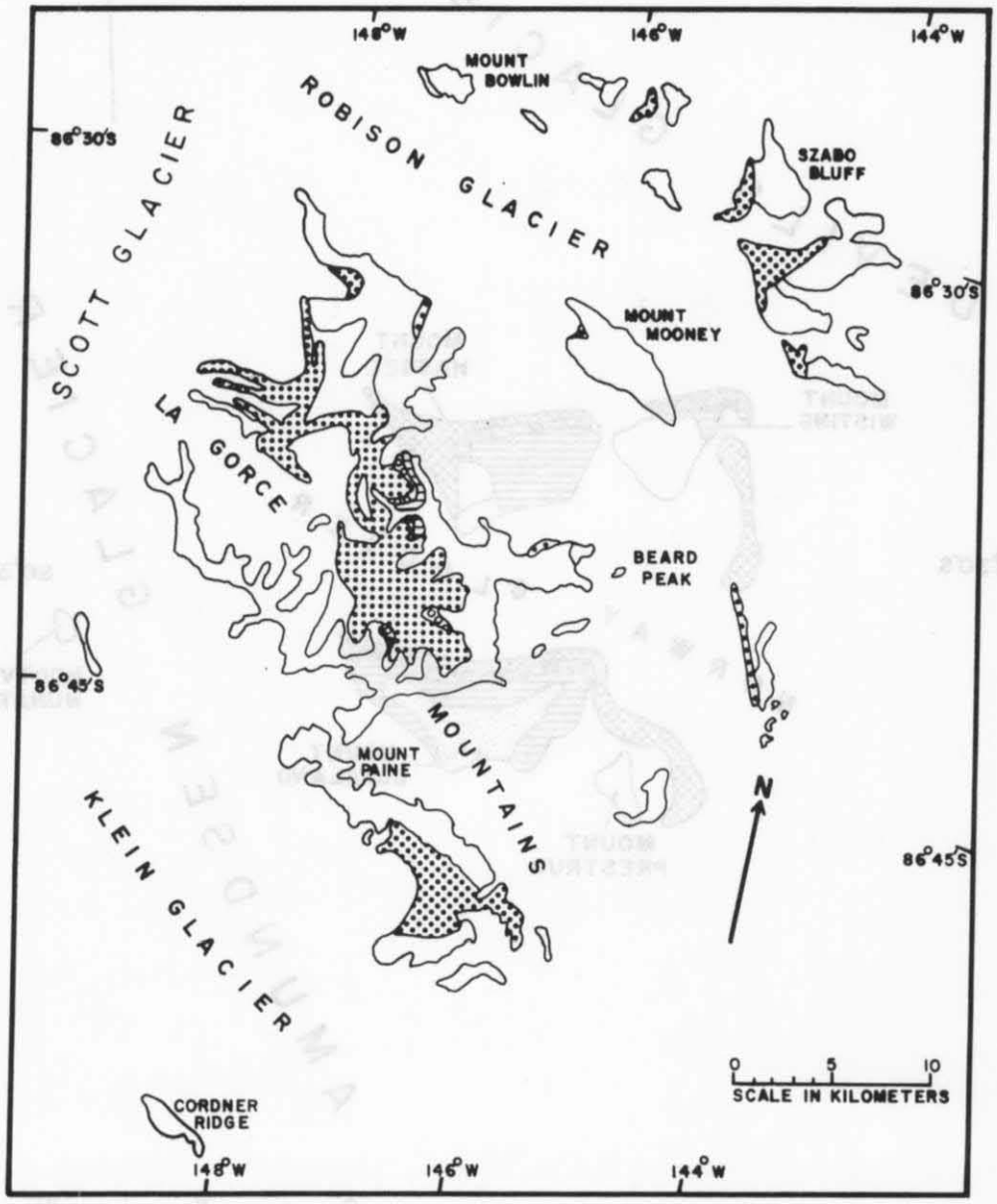

Figure 36. Glacial map of the La Gorce Mountains area. (see Legend, Table 8)

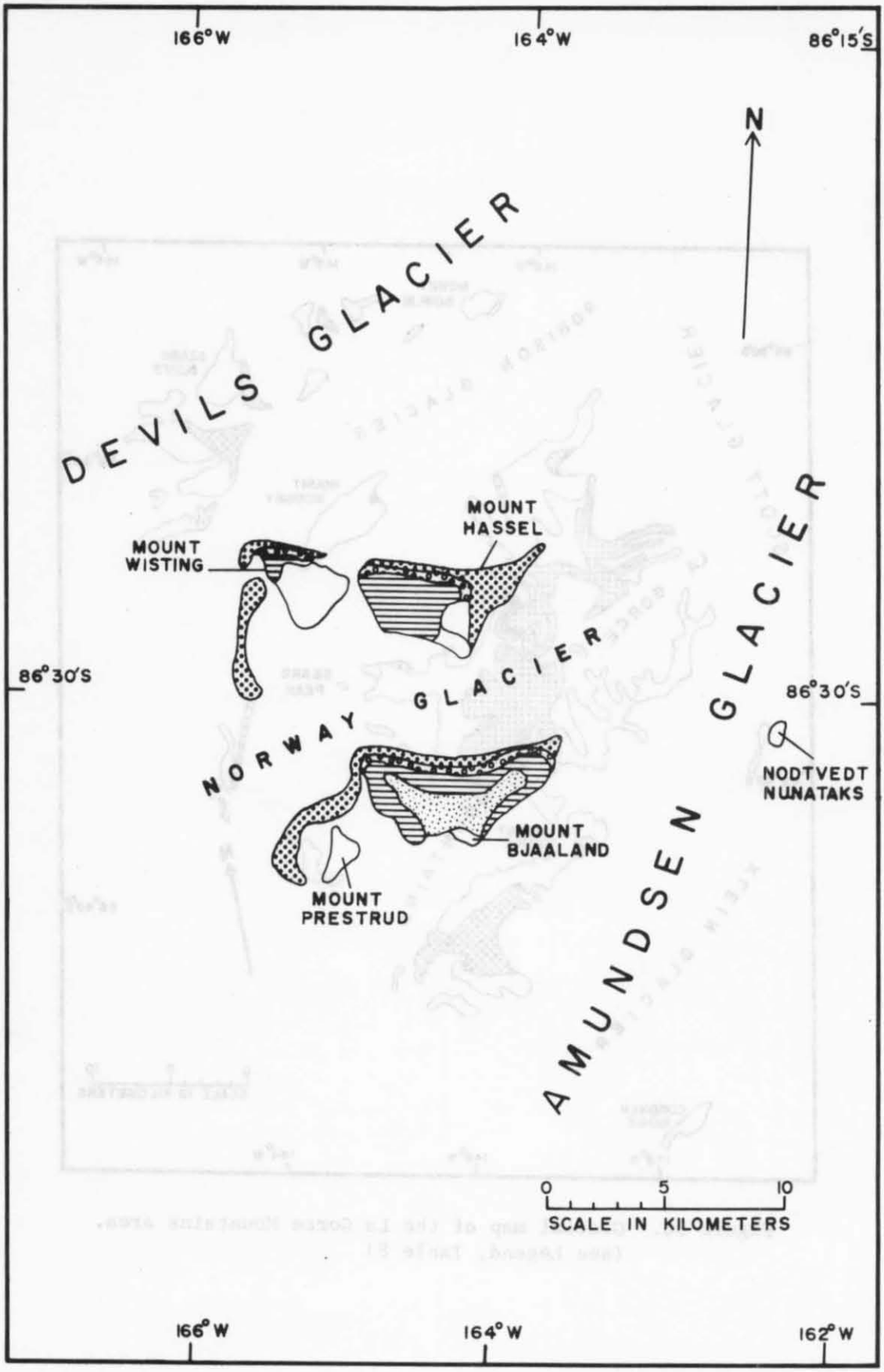

Figure 37. Glacial map of the Norway Glacier area. (see Legend, Table 8)

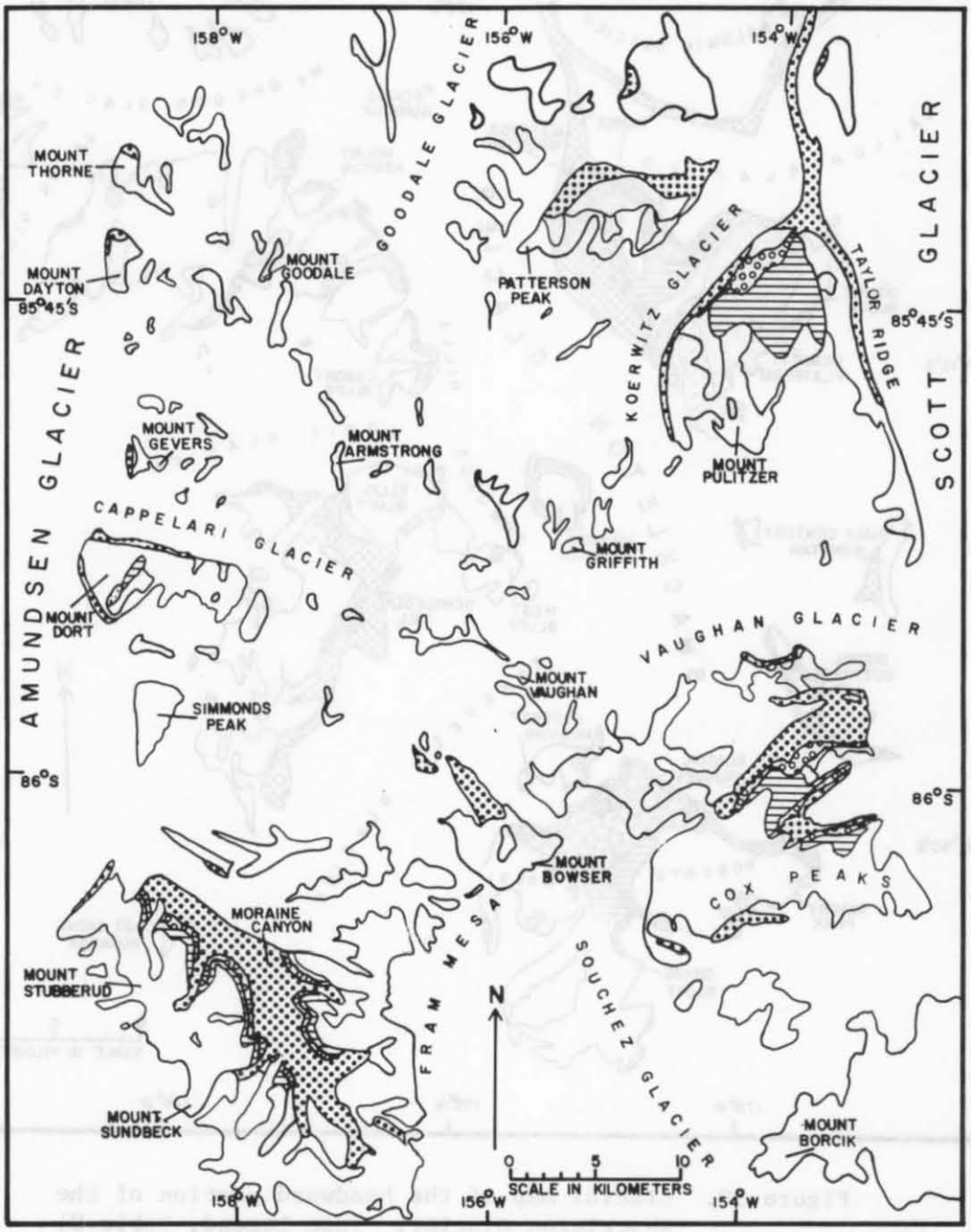

Figure 38. Glacial map of the area between the headward portion of the Scott Glacier and the headward portion of the Amundsen Glacier. (see Legend, Table 8)

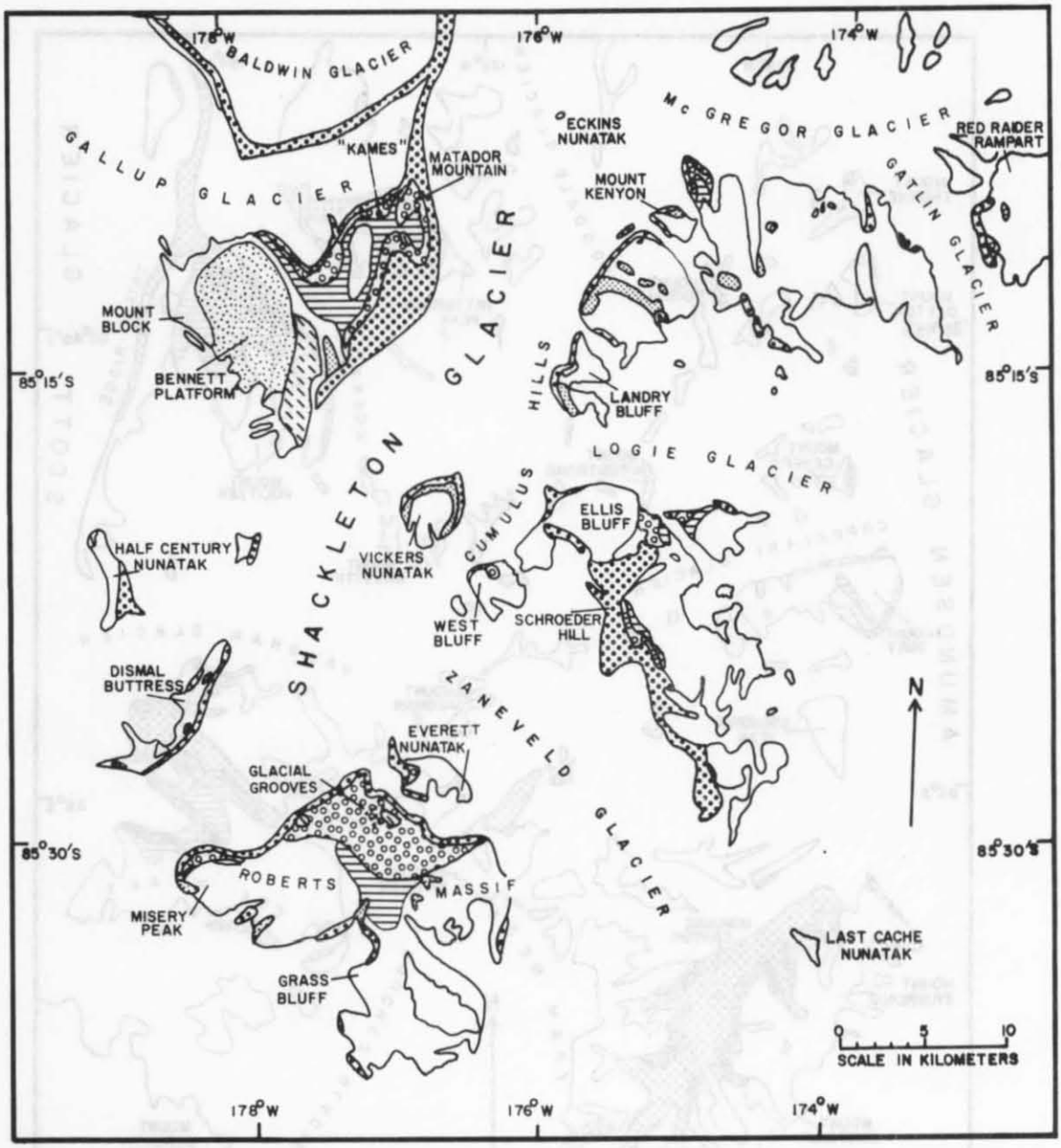

Figure 39. Glacial map of the headward portion of the Shackleton Glacier. (see Legend, Table 8)

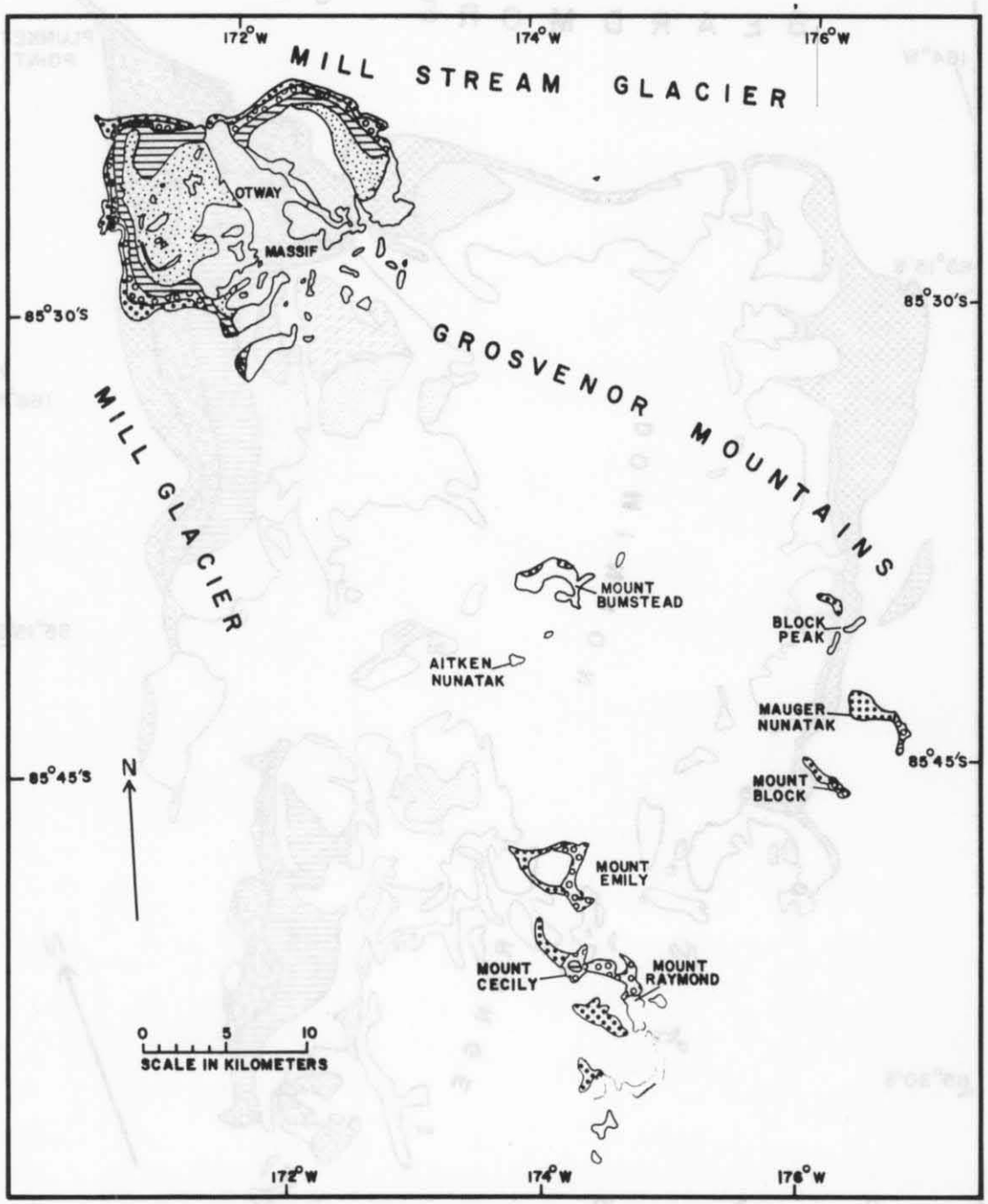

Figure 40. Glacial map of the Grosvenor Mountains area. (see Legend, Table 8)

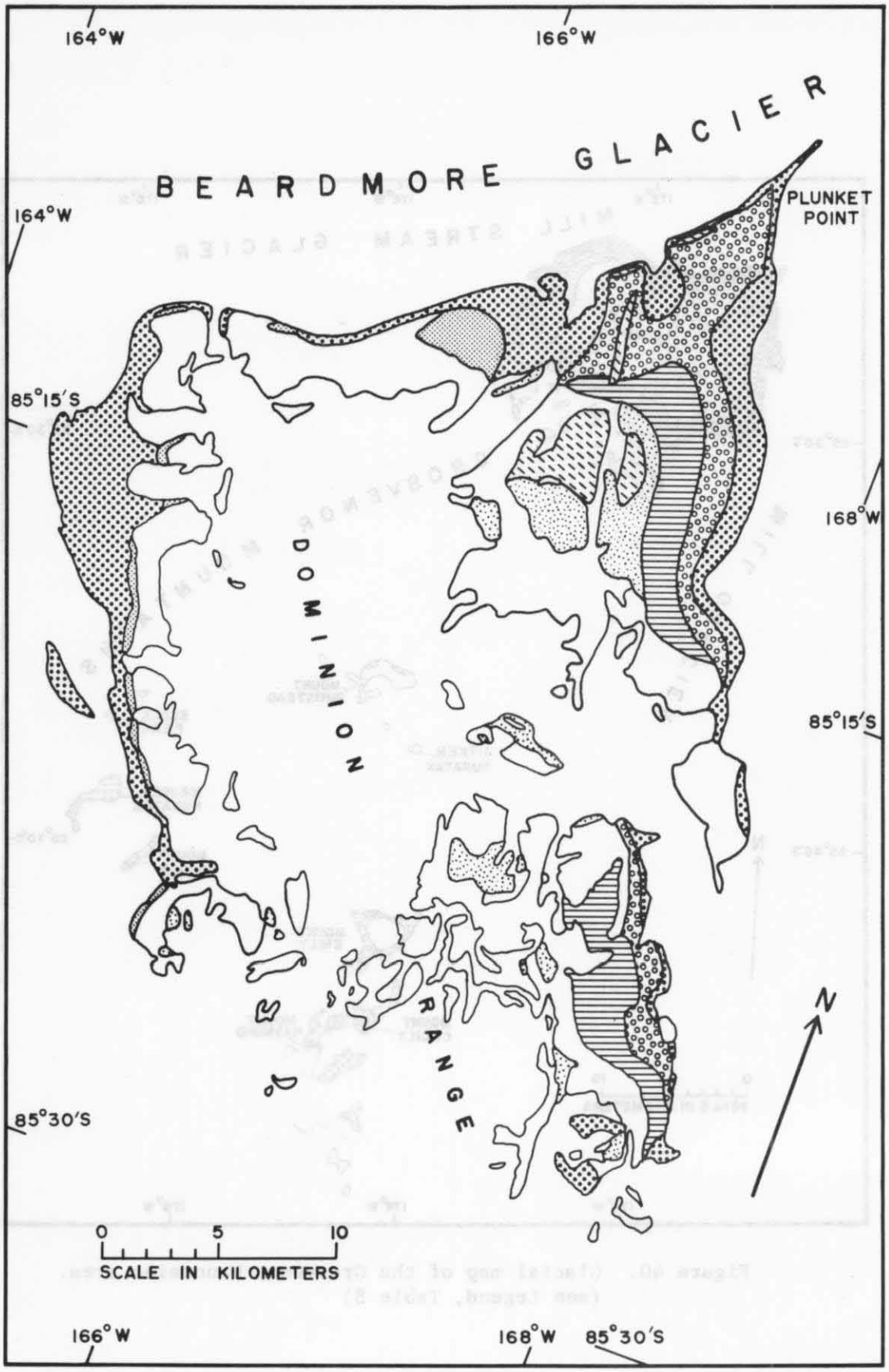

Figure 41. Glacial map of the Dominion Range.
(see Legend, Table 8)

(Table 9, Fig. 42). These moraines are found to be differentiable by analysis of elevation relative to the present ice surface. The highest portion of the Low Moraine rarely exceeds 20 m elevation above the present ice surface; therefore, it effectively parallels the present ice surface. Because of the small difference in elevation between the highest extent of the Low Moraine and the present ice surface they are considered nearly equivalent. The Middle Moraine does not parallel the present ice surface, its highest extent ranging from a minimum of 90 m above the present ice surface at the La Gorce Mountains to a maximum of 310 m above it at Mount Pulitzer. Similarly, the High Moraine does not parallel the present ice surface, its highest extent ranging from a minimum of 180 m above the present ice surface at the La Gorce Mountains to a maximum of 670 m above it at Mount Pulitzer. Both the Middle and High Moraines, therefore, increase in elevation relative to the present ice surface if these moraines are traced from the southwest inland side of the Queen Maud Mountains to the northeast or coastal portion of these mountains.

Morphology, Thickness of Drift and Presence of an Ice-Core

Field differentiation of the lateral moraines in the Queen Maud Mountains can usually be made by examining the morphology, drift thickness, and presence or lack of an underlying ice-core. In a generalized traverse from the High to the Middle to the Low Moraine (Fig. 32) the following differences are noted:

High Moraine

Morphologically the High Moraine grades with decreasing age, i.e. from top to bottom in cross-section, from a cover of sparse erratics and/or thin patches of drift overlying bedrock to a subdued series of ridge segments. In general, this moraine is fairly nondescript morphologically. Drift comprising this moraine grades from a few centimeters to at least 2 m in depth and overlies bedrock in the former case and ice-cemented bedrock and/or drift in the latter.

Middle Moraine

The Middle Moraine marks a readvance overlapping the lower portion of the High Moraine. At the contact between the High and Middle Moraines there are a series of hummocks. These hummocks contain crudely stratified sands and gravels and are classified here as kames. These kames are found at Roberts Massif, the southern Cumulus Hills, and Bennett Platform. They record a "moist period" of fluvioglacial local runoff immediately prior to the retreat of the ice which deposited the Middle Moraine. They do not necessarily imply excessive fluvial action and/or

Table 9 Elevation of Tops of Former Moraines in the Queen Maud Mountains

Location	Elevation at top of moraine		
	Low Moraine (meters) (≅present ice surface)	Middle Moraine (meters)	High Moraine (meters)
(Scott Glacier area)			
Mount Howe	2600	≅2700	>2930
LaGorce Mountains	1800	1890	1980
Mount Crockett	910	1130	>1280
Mount Pulitzer	630	940	1300
(Amundsen Glacier area)			
Mount Wisting	2000	2300	2500
Norway Glacier	2000	2400	2500
Mount Hassel	1910	2180	>2390
Roaring Valley	1980	2100	>2250
Moraine Canyon (B)	1161	1390	1548
Moraine Canyon (A)	1210	1345	1495
Mount Dort	900	-	>1500
(Shackleton Glacier area)			
Roberts Massif	2150	2320	2420
Southern Cumulus Hills	1900	2150	>2230
Landry Bluff	1650	-	1900
Bennett Plafform	1560	1700	1840
Mount Kenyon	1430	1630	1820
Red Raider Rampart	2100	2250	-
Mount Rosenwald	1800	-	2100
(Beardmore Glacier area)			
Otway Massif	2150	2230	2380
Dominion Range (A)	2270	2400	2600
Dominion Range (B)	1900	1990	2200
Buckley Island[1]	1750	-	2000
The Cloudmaker[1]	850	-	1420
Mount Kyffin[2]	500	-	1150

[1] Mercer (1972)

[2] Oliver (1964a)

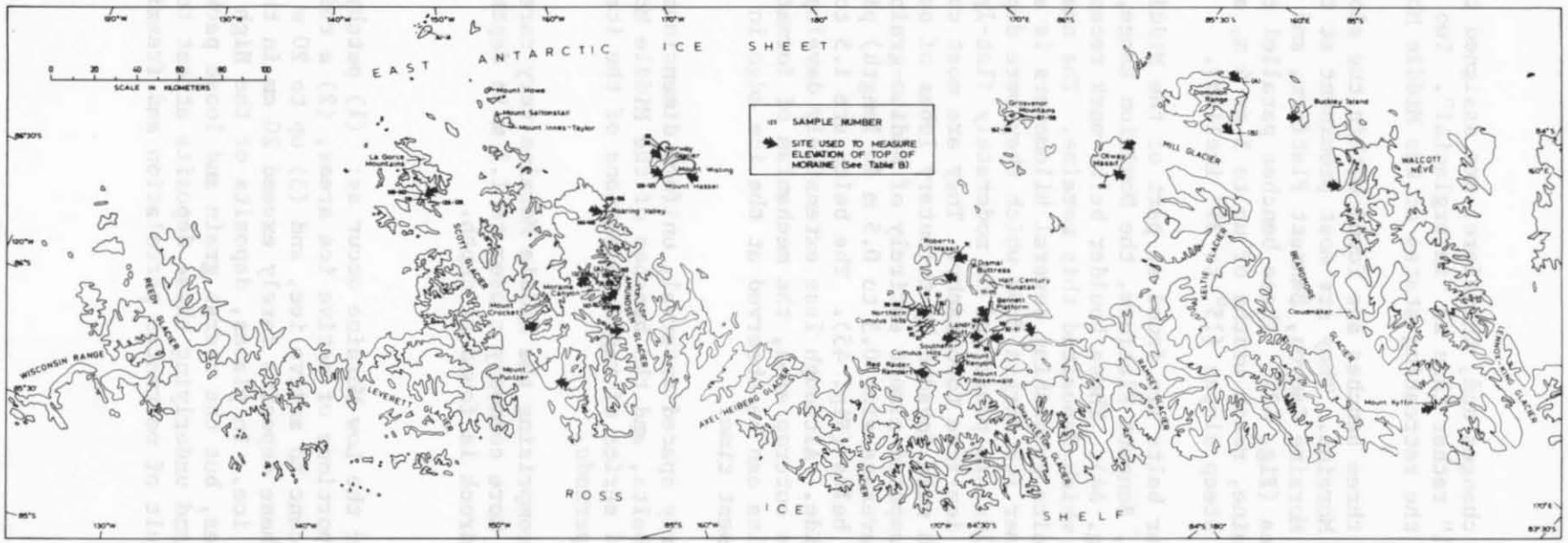
EAST ANTARCTIC ICE SHEET
ROSS ICE SHELF
SCALE IN KILOMETERS
SAMPLE NUMBER
SITE USED TO MEASURE ELEVATION OF TOP OF MORAINE (See Table 8)
WISCONSIN RANGE
REEDY GLACIER
SCOTT GLACIER
LEVERETT GLACIER
AXEL HEIBERG GLACIER
HERBERT RANGE
HILL GLACIER
KEITH GLACIER
WALCOTT NÉVE
BUCKEY ISLAND
MOUNT HOWE
MOUNT SALTONSTALL
MOUNT INNES-TAYLOR
MOUNT HASSEL
MOUNT CROCKER
MOUNT PULLEN
MOUNT ROSENFIELD
MOUNT KYLIN

marked climatic changes and, therefore, are assigned to a "moist period" or "interstadial" rather than an "interglacial". Two morphologic features record the retreating states of the Middle Moraine:

(1) Up to three benches are found within the slope exposure of the Middle Moraine. They are most prominent at the La Gorce Mountains, Moraine Canyon, Bennett Platform, and the Norway Glacier area (Fig. 43). These benches parallel the long profile of the moraine, reach widths of up to 5 or 6 m, and occur on moderately steep slopes (15° to 31° incline).

(2) Boulder belts are found as part of the Middle Moraine at Mount Dort, Bennett Platform, the Dominion Range, and Roberts Massif (Fig. 44). These boulder belts mark recessional halts of the ice which deposited this moraine. The amazing continuity of these belts stretching several kilometers is a clear indicator of the former ice margin from which they were deposited. These boulder belts are preserved on moderately flat-lying to gently undulating ice-free topography. They are most common in embayed areas which were invaded by tributary lobes of outlet glaciers. They are composed almost entirely of medium-grained dolerite boulders (average size 0.3 to 0.5 m in length) piled into continuous belts (Fig. 45). The belts are 1.5 to 2 m high and 2 to 4 m wide. Although less extensively developed within the Low Moraine outcrop area, the mechanism of formation of these boulder belts can be observed at the ice edge in some places at the present time.

The regularly spaced interval, uniform dimensions and continuity of the boulder belts, and the benches of the Middle Moraine require a regularly spaced series of rapid recessions of the ice edge separated by long stable periods.

The drift comprising the Middle Moraine very rarely exceeds 2 m in depth and is more commonly closer to 1.5 m in depth. Ice-cemented drift and/or bedrock is found at depth.

Low Moraine

Deposits of the Low Moraine occur as: (1) patchy coverings on the peripheral portions of active ice areas, (2) a thin cover on ice-free areas adjacent to active ice, and (3) up to 20 m above the level of this ice. These deposits rarely exceed 20 cm in thickness and always overlie glacial ice. In places, deposits of the High and Middle Moraine overlie ice-cores, but the coarse grain and loose packing of the ice crystal within and underlying these deposits attest to their secondary origin as a result of meltwater percolation and freezing. The thin

Figure 43. Benches in Middle Moraine near Mount Wisting.

Figure 44. Arrows point to boulder belts, Middle Moraine, Roberts Massif.

Figure 45. Close-up of boulder belt, Roberts Massif. S. Etter perched on boulder.

debris cover of the Low Moraine results in uneven ablation of the underlying glacial ice. Localized drift accumulations coalesce and in places protect the underlying ice from ablation producing extremely hummocky topography such as ice hillocks (Fig. 46).

The highest portion of the Low Moraine is marked by a push moraine in areas such as the southern Cumulus Hills (Fig. 47) and Mount Howe. This push moraine contains large shoved boulders and laps over older deposits. It marks a readvance which occurred within the time period during which the Low Moraine was deposited. A general recession of the ice associated with the Low Moraine has occurred since the formation of this push moraine.

Associated deposits

The High, Middle and Low Moraines are all related to fluctuations in the level of outlet and tributary glaciers within the outlet valleys of the Queen Maud Mountains. Similar drift sequences also mark fluctuations in the extent of: (a) localized ice masses (i.e. the Dominion Range), (b) tongues of plateau ice (i.e. the Grosvenor Mountains), and (c) alpine glaciers (i.e. Roberts Massif). These drift sequences were investigated in several areas and were found equivalent to the High, Middle, and Low Moraines. This equivalence suggests a general in-phase response of all bodies of ice within the Queen Maud Mountains.

Weathering of Surficial Clasts

Weathering studies by Behling (1971) and Calkin (1971) in southern Victoria Land have indicated the importance of the examination of the relative weathering of clasts on moraines of differing ages. Similar weathering studies were performed on clasts covering moraines in the Queen Maud Mountains in order to differentiate these moraines and provide a relative time scale. Abrupt changes in the weathering characteristics between clasts covering the High, Middle, and Low Moraines were one of the most useful criteria for field differentiation of these moraines. Although some gradations in clast weathering occurred from the oldest to the youngest exposed portions of the High, Middle, and Low Moraines, the abrupt changes at the contacts between these moraines were marked enough to allow differentiation. These abrupt changes in weathering characteristics record the readvance of each successively younger moraine over the lower portions of the previous moraine. The gradations in weathering characteristics mark the gradual lowering or retreat of the glaciers which deposited these moraines.

In the Queen Maud Mountains a weathering classification was employed which allowed the differentiation of clasts (15 to 60 cm in length) into four categories (Table 10). This weathering classification was used on a 50 X 1 m traverse area. Wherever possible the traverse area was chosen on flat ground in order to avoid mass-movement contamination. All clasts meeting the size specifications, within the

Figure 46. Example of an ice hillock capped by drift of the Low Moraine near Mount Wisting. P. Colbert standing on the hillock.

Figure 47. Push moraine developed in the upper portion of the Lor Moraine, southern Cumulus Hills.

Table 10. Weathering Classification

Category	Subcategory	Description
Fresh	A	Fresh (unweathered) and very angular
	B	Moderate faceting (smooth edge and roughly developed facets)
Faceted	C	Well developed faceting (smoother edge than B or flat facet
	D_1	Very well faceted (smooth edge and flatter facet than C)
	D_2	Very well faceted (sharp edge and flatter facet than C)
	E	Hollows 5 centimeters or less in depth
Cavernously hollowed	F	Hollows 5-10 centimeters or less in depth
	G	Hollows 15-30 centimeters or less in depth
	H	Hollows 30 or more centimeters or less in depth
Dinintegrated	K	Disintegrating
	I	Weathered to the ground

traverse area, were recorded by lithology and weathering subcategory. If a clast displayed more than one weathering feature, more than one weathering subcategory was assigned. The less dominant weathering subcategory, if differentiable, was recorded with lower case letters, i.e. medium-grained dolerite - Be. A sample of several of these weathering study traverses appears in Table 11. The results of the weathering studies conducted in the Queen Maud Mountains are summarized in Table 12. In this summary, a general field description of the weathering characteristics of surficial clasts can be viewed by lithology or by moraine, including the relative proportion of that lithology per moraine. For example, fine-grained dolerite clasts increase in relative proportion with increasing moraine age and progress from faceted and fresh to predominantly faceted with age. This summary provides a working method for the field differentiation of the weathering characteristics of clasts on the surface of the High, Middle, and Low Moraines in the Queen Maud Mountains.

Particle Size Distribution

The investigation of particle size distribution in soils developed within moraines in the Transantarctic Mountains has been used by several previous workers: Claridge and Campbell (1968), Everett and Behling (1968), Ugolini (1970), Behling (1971), Everett (1971) and Linkletter (1972) to mention only a few. Analysis of the particle size distribution of the drift comprising the Low Moraine and of soils developed in the Middle and High Moraine in the Queen Maud Mountains provides a reasonably reliable lab method of differentiating these moraines. Data from these analyses listed by parent material assemblage and by moraine appear in Appendix A. Sample locations are recorded in Figure 42.

The only detailed study of the particle size distribution in morainic soils undertaken in the Queen Maud Mountains prior to this study was made by Claridge and Campbell (1968) at Roberts Massif. They stressed the importance of examining the relationship between particle size distribution and parent material. Particle size analysis of samples from the Low Moraine drift are chosen for this study because they have undergone the least amount of particle size redistribution of any of the morainic material in this area owing to their age. Average values of gravel (percent total sample) and of sand, silt, and clay (percent of less than 2 mm fraction) of Low Moraine samples (Fig. 48) indicate the following relation between parent material and size distribution:

(1) Beacon sediments and Ferrar Dolerite and metasediment with granite and Ferrar Dolerite parent material assemblages contain roughly 40 to 50 percent gravel-sized particles.

Table 11. Sample of Weathering Studies

Lithology	% of Total Lithology	Percent of Total Weathering Characteristics Per Location																	
		A	b	c	B	c	D_1	D_2	e	f	g	h	E	F	G	H	I	J	k	K
(Moraine Canyon - Low Moraine; Site 185)																				
Med.-Gr. Doler.	48.0		3.0	3.0	23.0	17.0													1.0	
Co.-Gr. Doler.	2.0		1.0		1.0	1.0														
Metasediment	50.0			2.0	31.0	14.0													3.0	
(Moraine Canyon - Middle Moraine; Site 190)																				
Med.-Gr. Doler.	13.0				7.0	6.0														
Sandstone	3.0				2.0	1.0														
Metasediment	61.0		1.0		29.0	29.0													1.0	
Granite	24.0			1.0	4.0	18.0													1.0	
(Moraine Canyon - Middle Moraine; Site 188)																				
Fine-Gr. Doler.	10.0				6.0	3.0	1.0													
Med.-Gr. Doler.	22.0		1.0	1.0	8.0	11.0													2.0	
Sandstone	1.0				1.0															
Metasediment	51.0		4.0	3.0	17.0	23.0	1.0		3.0										1.0	1.0
Granite	17.0				1.0	6.0			1.0				1.0						5.0	2.0
(Moraine Canyon - High Moraine; Site 186)																				
Fine-Gr. Doler.	9.0					5.0	4.0													
Med.-Gr. Doler.	47.0				15.0	20.0							12.0							
Metasediment	20.0				5.0	7.0							8.0							
Granite	24.0					10.0								14.0						

Table 12. Summary of Weathering Characteristics

Lithology	Relative Proportion of Lithology by Moraine	Descriptive Weathering Characteristics of Lithology by Moraine		
		Low Moraine	Middle Moraine	High Moraine
fine-grained dolerite	L $\ll$ M $\leq$ H	faceted & fresh	faceted	faceted
medium-grained dolerite	L < M < H	faceted & fresh	faceted, disintegrated & hollowed	faceted, disintegrated & hollowed
coarse-grained dolerite	L $\cong$ M > H	fresh, faceted & disintegrated	faceted, disintegrated & hollowed	faceted, disintegrated & hollowed
shale	only L	fresh, faceted & disintegrated	not present	not present
siltstone	L $\gg$ M; no H	fresh, faceted & disintegrated	faceted, hollowed & disintegrated	not present
sandstone	L $\gg$ M; no H	fresh, faceted & disintegrated	faceted, hollowed & disintegrated	not present
metasediment	L $\geq$ M $\ll$ H	fresh, faceted & disintegrated	faceted & disintegrated	faceted, hollowed & disintegrated
granite	L = M = H	fresh, faceted & disintegrated	faceted & disintegrated	faceted, hollowed & disintegrated
granodionite	L = M = H	fresh, faceted & disintegrated	faceted & disintegrated	faceted, hollowed & disintegrated

Legend

L = Low Moraine
M = Middle Moraine
H = High Moraine

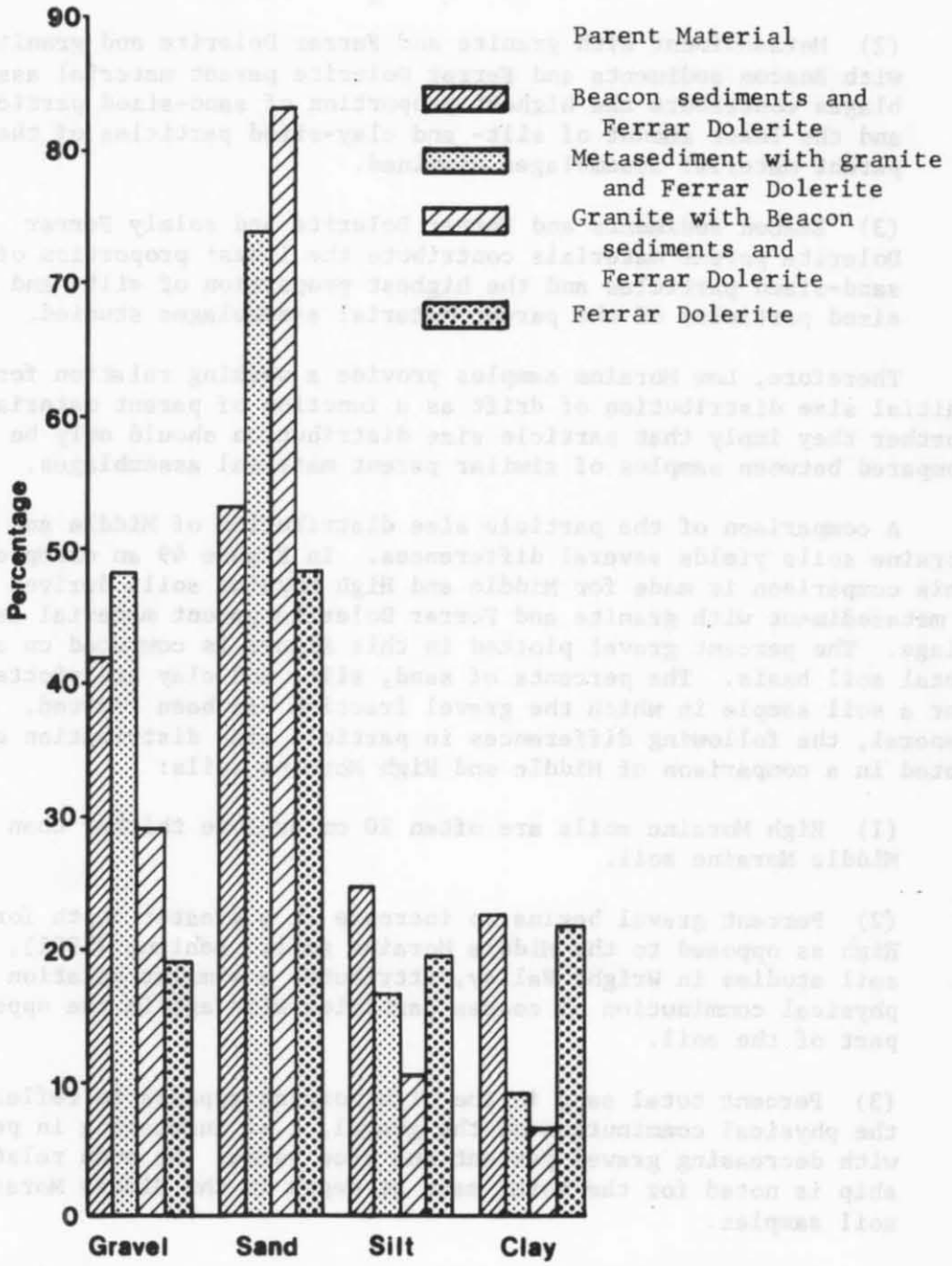

Figure 48. Relation between parent material and particle size distribution, Low Moraine.

(2) Metasediment with granite and Ferrar Dolerite and granite with Beacon sediments and Ferrar Dolerite parent material assemblages contribute the highest proportion of sand-sized particles and the least amount of silt- and clay-sized particles of the parent material assemblages examined.

(3) Beacon sediments and Ferrar Dolerite and solely Ferrar Dolerite parent materials contribute the lowest proportion of sand-sized particles and the highest proportion of silt- and clay-sized particles of the parent material assemblages studied.

Therefore, Low Moraine samples provide a working relation for the initial size distribution of drift as a function of parent material. Further they imply that particle size distribution should only be compared between samples of similar parent material assemblages.

A comparison of the particle size distribution of Middle and High Moraine soils yields several differences. In Figure 49 an example of this comparison is made for Middle and High Moraine soils derived from a metasediment with granite and Ferrar Dolerite parent material assemblage. The percent gravel plotted in this figure is computed on a total soil basis. The percents of sand, silt, and clay are plotted for a soil sample in which the gravel fraction has been removed. In general, the following differences in particle size distribution can be noted in a comparison of Middle and High Moraine soils:

(1) High Moraine soils are often 20 cm or more thicker than the Middle Moraine soil.

(2) Percent gravel begins to increase at a greater depth for the High as opposed to the Middle Moraine soil. Behling (1971), in soil studies in Wright Valley, attributes a similar relation to physical comminution of coarse particles with age in the upper part of the soil.

(3) Percent total sand in the High Moraine appears to reflect the physical comminution of the gravel, i.e. increasing in percent with decreasing gravel percent and vice versa. No such relationship is noted for the total sand at depth in the Middle Moraine soil samples.

(4) Percent total silt appears to increase and decrease in direct relation to the percent gravel in the upper 40 cm of the High Moraine soil and remains fairly uniform in distribution below this level. The comminution of gravel to sand may effectively dilute the small percentages of silt in the High Moraine soil. The Middle Moraine soil contains a marked increase in total silt at the surface which appears to disappear with age in the High Moraine soil.

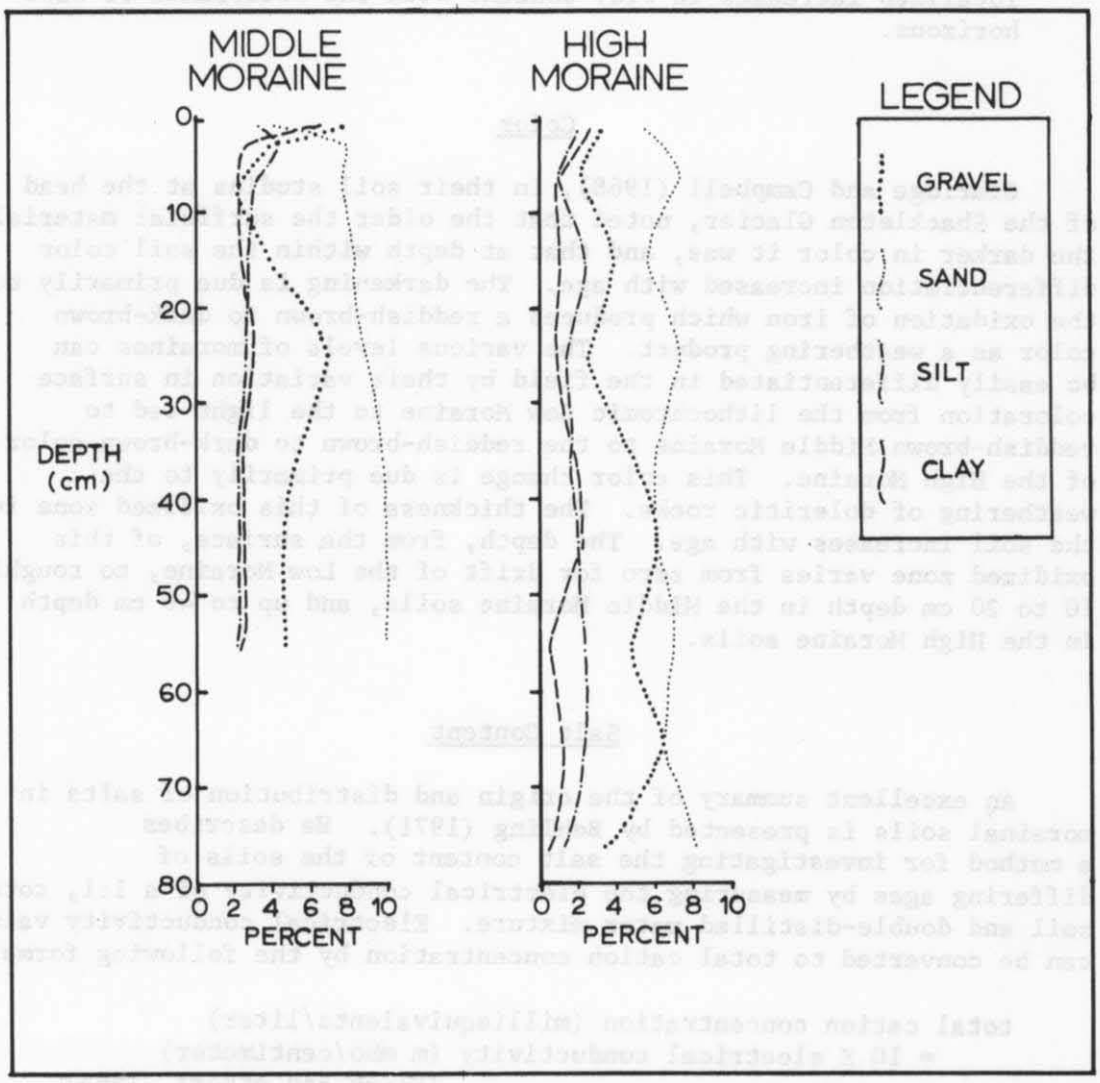

Figure 49. Particle size distribution of High and Middle Moraine soils at depth.

(5) Total clay percents increase irregularly from the Middle to the High Moraine soil with depth. Everett (1971) correlates the localized increases in clay content with the occurrence of salt horizons.

Color

Claridge and Campbell (1968), in their soil studies at the head of the Shackleton Glacier, noted that the older the surficial material, the darker in color it was, and that at depth within the soil color differentiation increased with age. The darkening is due primarily to the oxidation of iron which produces a reddish-brown to dark-brown color as a weathering product. The various levels of moraines can be easily differentiated in the field by their variation in surface coloration from the lithochromic Low Moraine to the light-red to reddish-brown Middle Moraine to the reddish-brown to dark-brown color of the High Moraine. This color change is due primarily to the weathering of doleritic rocks. The thickness of this oxidized zone in the soil increases with age. The depth, from the surface, of this oxidized zone varies from zero for drift of the Low Moraine, to roughly 10 to 20 cm depth in the Middle Moraine soils, and up to 40 cm depth in the High Moraine soils.

Salt Content

An excellent summary of the origin and distribution of salts in morainal soils is presented by Behling (1971). He describes a method for investigating the salt content of the soils of differing ages by measuring the electrical conductivity of a 1:1, total soil and double-distilled water mixture. Electrical conductivity values can be converted to total cation concentration by the following formula:

total cation concentration (milliequivalents/liter)
= 10 X electrical conductivity (m mho/centimeter)
(Black and others, 1965)

Behling finds that the total cation concentrations of soils measured in Wright Valley closely parallel values of total salt content derived by acid digestion. Thus, by expressing the electrical conductivity of a soil sample as a function of total cation concentration a good estimate can be made of the total salt content of this sample.

Near-surface samples

In Figure 50 values of total cation concentration of near-surface samples (0 to 5 cm depth) are plotted. These total cation concentration values decrease slightly from the Beardmore to the Scott Glaciers.

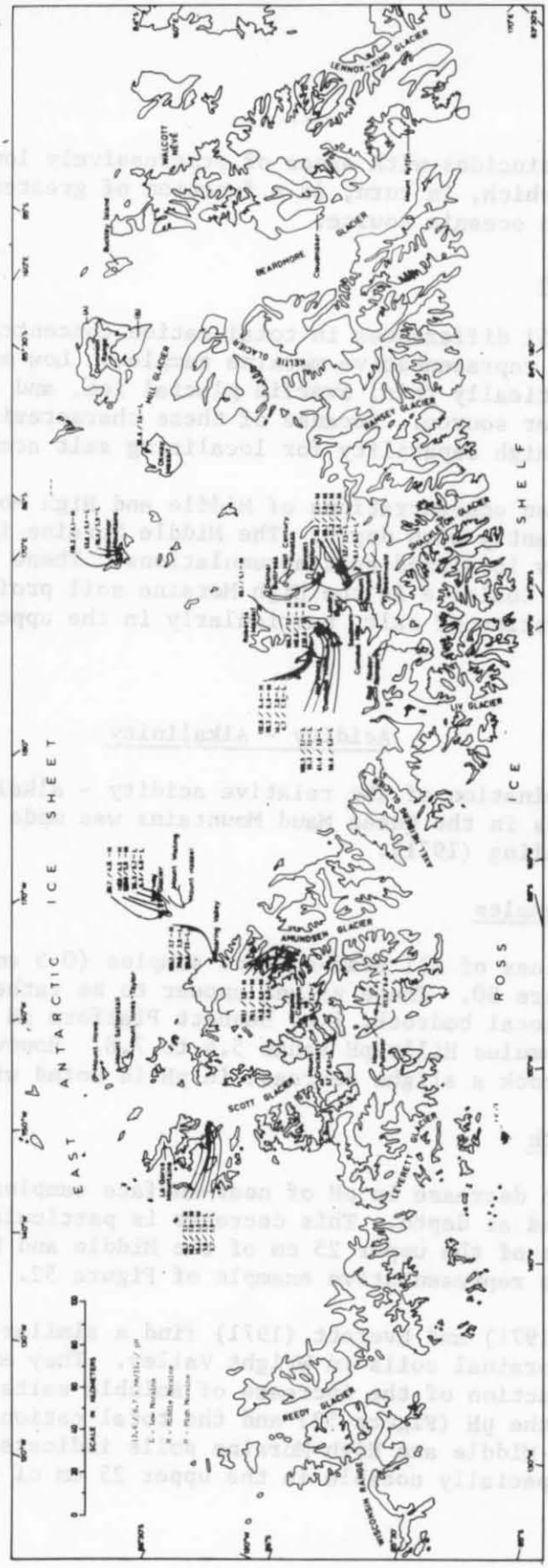
EAST ANTARCTIC ICE SHEET
ROSS ICE SHELF
LENNOX-KING GLACIER
WALCOTT NEVE
MARSHALL GLACIER
KELTIE GLACIER
MILL GLACIER
BYRD GLACIER
SHACKLETON GLACIER
LIV GLACIER
AMUNDSEN GLACIER
SCOTT GLACIER
REEDY GLACIER
SCALE IN KILOMETERS

This decrease coincides with areas of progressively lower and lower precipitation, which, in turn, is a function of greater and greater distance from an oceanic source.

Samples at depth

In Figure 51 differences in total cation concentrations at depth are plotted for representative moraine samples. Low moraine samples are characteristically thin, overlie glacial ice, and are often found near a melt-water source. Because of these characteristics, these samples have a high capability for localizing salt accumulations.

Total cation concentrations of Middle and High Moraine soil samples differ significantly with depth. The Middle Moraine is often characterized at depth by localized salt accumulations. These localized accumulations tend to coalesce in the High Moraine soil profile, producing a high concentration of salt, particularly in the upper 25 cm of the profile.

Acidity - Alkalinity

The determination of the relative acidity - alkalinity or pH of morainal samples in the Queen Maud Mountains was made using the method employed by Behling (1971).

Near-surface samples

The pH values of all near-surface samples (0-5 cm depth) are plotted on Figure 50. These values appear to be rather sensitive indicators of local bedrock, i.e. Bennett Platform pH range 7.7 to 8.5 and southern Cumulus Hills pH range 5.4 to 7.8. However, within areas of similar bedrock a slight decrease in pH is noted with age.

Samples at depth

The slight decrease in pH of near-surface samples with age appears to be maintained at depth. This decrease is particularly prevalent in a comparison of the upper 25 cm of the Middle and High Moraine soils, as noted in the representative example of Figure 52.

Behling (1971) and Everett (1971) find a similar decrease in pH with age for morainal soils in Wright Valley. They explain this decrease as a function of the increase of soluble salts with age. A comparison of the pH (Figure 52) and the total cation concentration (Figure 51) of Middle and High Moraine soils indicates this inverse relation is especially notable in the upper 25 cm of these profiles.

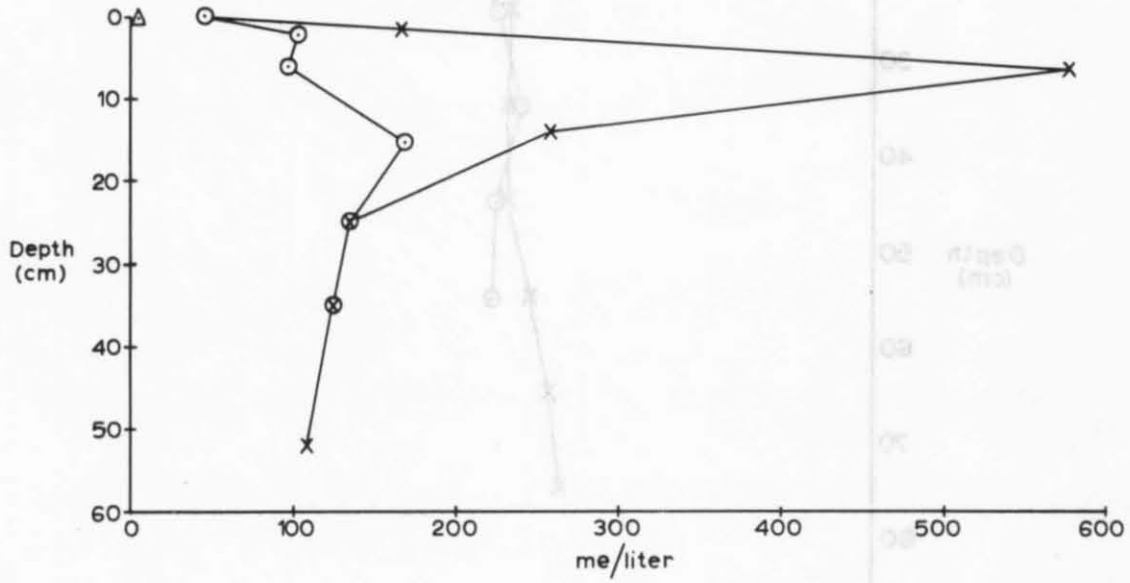

Figure 51. Variation in total cation concentration with depth. Low Moraine (triangle), Middle Moraine (circle) and High Moraine (cross).

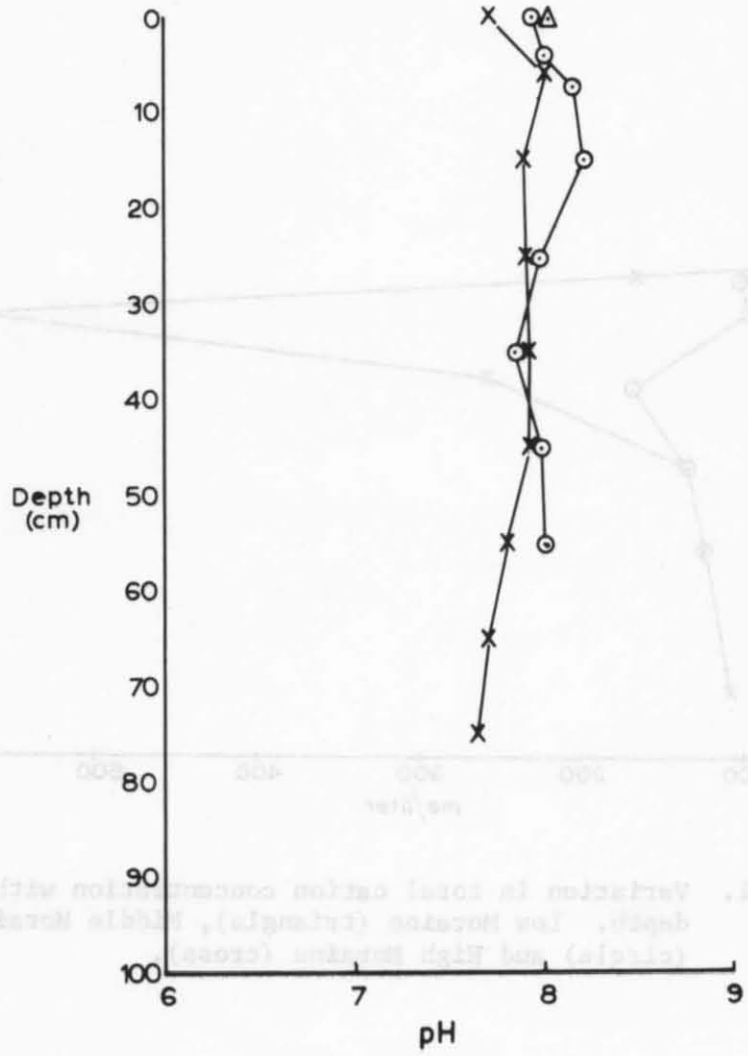

Figure 52. Variation in pH with depth. Low Moraine (triangle), Middle Moraine (circle), and High Moraine (cross).

Clay Minerals

The less than 2μ fractions of 18 soil samples of different parent material assemblages, relative ages and depths were examined for their clay mineral content. Each sample was plated onto four ceramic plates and each of these plates was subjected to a separate treatment:

(1) air drying, (2) ethylene-glycolating, (3) heating to 400°C for two hours, and (4) heating to 550°C for two hours. The treated samples were analyzed by x-ray diffraction. Relative clay mineral abundances were estimated by measurement of peak areas using the method presented by Johns and others (1954) modified by Wilding and Drees (1966, unpublished paper). Percent clay minerals and quartz are listed by parent material assemblage, moraine and depth in Table 13. Variations in these percentages as a function of these parameters produced little in the form of a discernible trend. Similar studies conducted by Claridge and Campbell (1968) and Everett (1971) have noted the same lack of trend.

Review of Moraine Characteristics and Correlation of Transantarctic Mountains Glacial Chronologies

The characteristics used to differentiate the Low, Middle, and High Moraines in the Queen Maud Mountains are presented in Table 14, with the exclusion of relative elevation above the present ice surface which is discussed in detail in the following section. The characteristics developed in this section indicate that the Low, Middle, and High Moraines were deposited during marked and separate glacial events. Each of these moraines records a major advance of the outlet glaciers in the Queen Maud Mountains and a subsequent retreat of these glaciers. The major portion of the glacial drift composing these moraines was deposited during this subsequent retreat. The continuity of these moraines throughout the Transantarctic Mountains and their distinct differentiation reflect the response of glaciers in the Queen Maud Mountains to broad-scale and very probably long-term events. Therefore, the Low, Middle, and High Moraines are assigned to separate glaciations here named the Amundsen, Shackleton, and Scott Glaciations, respectively.

Included in the Queen Maud Mountains section of Table 14 are the moraines described by Mercer (1968) from the Reedy Glacier area. The notable difference between the number of moraines in the Reedy Glacier area compared to the Scott, Amundsen, Shackleton, and Beardmore Glacier areas remains undecided. Lacking a complete set of moraine characteristics for the Reedy Glacier area, the Reedy II and III moraines are lumped together under the Middle Moraine. The lumping is effectively the result of default since the Reedy I moraine is comparable to the

Table 13. Percent Distribution of Clay Minerals

Sample Number	Depth (cm)	% Illite	% Vermiculite	% Montmorillonite	% Interstratified	% Kaolinite	% Chlorite	% Quartz
Parent Material:	Beacon Sediment and Dolerite - Low Moraine							
80	0-4	62.0	9.0	13.0	5.0	1.0	6.0	4.0
Parent Material:	Beacon Sediment and Dolerite - Middle Moraine							
92	0-1	31.0	N.D.	13.0	14.0	3.0	21.0	18.0
93	3-10	46.0	6.0	11.0	19.0	N.D.	15.0	3.0
95	10-20	36.0	N.D.	11.0	25.0	1.0	22.0	6.0
97	30-41	46.0	N.D.	15.0	5.0	N.D.	18.0	16.0
Parent Material:	Beacon Sediment and Dolerite - High Moraine							
102	0-2	48.0	8.0	14.0	10.0	3.0	7.0	11.0
106	20-30	71.0	4.0	9.0	1.0	N.D.	5.0	10.0
110	60-70	81.0	N.D.	13.0	6.0	N.D.	N.D.	N.D.
Parent Material:	Metasediment with Granite and Dolerite - Low Moraine							
129	0-5	56.0	6.0	7.0	11.0	5.0	13.0	2.0
Parent Material:	Metasediment with Granite and Dolerite - Middle Moraine							
132	0-2	49.0	2.0	12.0	20.0	3.0	9.0	5.0
136	20-30	44.0	N.D.	12.0	20.0	3.0	21.0	N.D.
139	50-60	50.0	12.0	12.0	15.0	4.0	6.0	1.0
Parent Material:	Metasediment with Granite and Dolerite - High Moraine							
143	0-5	49.0	N.D.	9.0	19.0	3.0	17.0	3.0
Parent Material:	Granite with Dolerite and Beacon Sediment - Low Moraine							
144	0-5	30.0	11.0	19.0	17.0	1.0	10.0	12.0
145	5-15	47.0	15.0	11.0	16.0	2.0	9.0	N.D.
Parent Material:	Granite with Dolerite and Beacon Sediments - High Moraine							
148	0-2	51.0	N.D.	14.0	13.0	N.D.	14.0	8.0
152	30.40	46.0	N.D.	13.0	12.0	3.0	16.0	9.0
156	70-80	51.0	7.0	9.0	18.0	1.0	4.0	10.0

N.D. = Not Determined

Characteristics	QUEEN MAUD MOUNTAINS Including: Reedy, Scott, Amundson, Shackleton and Beardmore Glacier Areas based on information from: (1) Mayewski (this report) and (2) Mercer (1968)		
	Scott, Amundson, Shackleton, Beardmore (Reedy IV Drift)(2) Low Moraine Drift(1)	Scott, Amundson, Shackleton, Beardmore (Reedy III & II Drift)(2) Middle Moraine Drift(1)	Scott, Amundson, Shackleton, Beardmore (Reedy I Drift)(2) High Moraine Drift(1)
Morphology including drift thickness and presence of an ice core	(a)ice-cored (1) (b)up to 20 cm. thick (1) (c)polygonal features in moist areas (1) (d)extremely hummocky (1) (e)limited extent (1) (f)contains a push-moraine (1) marking a readvance (1)	(a)ice-cemented at depth (1) (b)up to 2 m. thick (1) (c)contains a series of recessional boulder moraines and prominent lateral moraines (1) (d)kames in terminal area (1)	(a)ice-cemented or bedrock at depth (1) (b)up to > 2 m thick or occurring as lone erratics (1) (c)no morainal form (1) (d)overlies fluvial channels (1)
Weathering of surficial clasts	(a)all clasts unweathered except some slightly disintegrated sandstone and siltstone (1)	(a)very few or no boulders weathered to the ground except ss., silt. and shale (1) (b)upstanding boulders faceted and mildly cavernous (1)	(a)in oldest portion boulders weathered to ground (1) (b)boulders in younger portions are cavernously hollowed and faceted (1)
Particle size distribution and compaction	(a)predominantly in coarse grades (1) (b)directly related to parent material (1) (c)loose rubbly structure and poorly sorted (1)	(a)slight increase in total silt and total clay in upper part of soil (1) (b)fairly compact structure (1)	(a)total sand and total silt > Middle Moraine in upper part of soil (1) (b)gravel increases at depth which total sand & total silt decrease (1) (c)irregular increase of total clay with depth (1) (d)very compact (1)
Color differentiation (Surface and at depth)	(a)lithochromic (1)	(a)oxidized zone 10-20 cm. depth yielding light-brown to reddish or yellowish colors (1)	(a)oxidized zone to 40 cm. depth yielding brownish-yellow to brownish-red (1)
Salt Content	(a)concentrated in moist patches (1)	(a)some salt at near-surface depth and beneath clasts at depth (1)	(a)greater salt concentration throughout soil than in Middle Moraine (1)
Acidity-Alkalinity	(a)dependent on parent material (1)	(a)see High Moraine	(a)lower than Middle Moraine throughout soil profile (1)
Clay Minerals	(not a conclusive index of relative age) (1)		

SOUTHERN VICTORIA LAND									
Taylor Valley based on information from: (3) Denton and others (1970), (4) Pewe (1961)			Wright Valley based on information from: (5) Behling (1971), (6) Everett (1971), (7) Nichols (1971) *see Table 14 (Alpine Glaciations slightly older than corresponding Axial Glaciations)			Victoria Valley based on information from: (8) Calkin (1964)		
(Taylor I Drift)(3) (Koettlitz Drift)(4)	Taylor II and III Drift(3) (Fryxell Drift)(4)	Taylor IV Drift (3) (Taylor Drift)(4)	*Alpine I Drift Wright Upper I & II Drift (5) Wright Lower Drift	*Alpine II Drift Wright Upper III Drift (5) Trilogy Drift	*Alpine III Drift Wright Upper IV Drift (5) Loop Drift	Packard Drift	Vida Drift	Bull Drift
(a)ice-cored (4) (b)limited extent (3)	(a)well-preserved moraines both loops and lateral (4)	(a)occurs as patches of till or as erratics (4)	(a)ice-cored (5) (b)10-50 cm. thick (5) (c)hummocky (5) (d)polygons in moist areas (5) (e)limited extent (1) (f)evidence of readvance (7)	(a)ice-cemented at 1 m. depth (5) (b)> 1.5 m. thick (5) (c)contains a series of recessional moraines & indistinct lateral moraines (7) (d)prominent end moraine with associated kames (7) (e)overlaps fluvial features	(a)no ice-cemented zone within 2 m. depth (5) (b)one prominent end moraine (c)sometimes thin, multiple moraines (5) (d)glacio-fluvial sands against proximal slope (5)	(a)ice-cored (8) (b)hummocky (8) (c)associated washed and sorted drift (8) (d)limited extent (1)	(a)moderately preserved moraines (8) (b)associated extensive outwash (8)	(a)isolated areas of erratic boulders (8) (b)no morainal topographic except marked end moraine (8) (c)local lake deposits (8) (d)indistinct meltwater channels (8)
	(a)granites cavernously hollowed and weathered to ground (3) (b)a few cobbles of sandstone (4)	(a)wind-abraded clasts (4)	(a)all clasts unweathered except some iron-stained (5)	(a)no boulders weathered to the ground (7) (b)very minor or no cavernous hollowing (7) (c)a few faceted clasts (7)	(a)very few upstanding boulders (5) (b)upstanding boulders are cavernously hollowed or faceted (7)			(a)extreme cavernous weathering of boulders and bedrock (8)
			(a)poorly sorted (5) (b)no concentration of fines (5)	(a)increase in total silt and total clay in upper 20 cm. associated with salt horizon (5) (b)looser structure than Alpine III (5)	(a)increase in total silt and total clay more than Alpine II (5) (b)firmly interlocked and compact (5) (c)boulders disintegrated to 30 cm. depth (5)	(a)sandy and bouldery (8)	(a)sandy (8)	(a)very silty (8) (b)boulders disintegrated to 40 cm. depth (8)
			(a)soil color pale brown with little or no differentiation (5)	(a)color like Alpine III with thinner yellow-brown layer (5)	(a)upper few cm. yellow-brown and lower part pale brown (5)			
			(a)thin salts in patches (5)	(a)indurated and massive to 15 cm. depth (5)	(a)increase in depth and degree of salt concentration compared to Middle Moraine (5)			
					(a)decrease in pH at 10-40 cm. depth corresponding to salt horizon (5)			
			(not a conclusive index of relative age) (6)		(a)increase in montmorillonite in salt horizons compared to Alpine II (5)			

High Moraine and the Reedy IV moraine is comparable to the Low Moraine, based on Mercer's description of the Reedy moraines. A summary of the number of moraines differentiated in each specific area throughout the Transantarctic Mountains indicates a general agreement with the three reported in this study.

Since the characteristics used for moraine differentiation in the Queen Maud Mountains were chosen on the basis of work done by investigators in southern Victoria Land, comparison of the moraines in these two areas can be made. Southern Victoria Land moraine characteristics are summarized in Table 14. A close correlation is noted between the characteristics of the moraines in these two areas. This correlation is used to determine the correlation table of glacial events from the Queen Maud Mountains to southern Victoria Land (Table 15). Included in this correlation are the Queen Maud Glaciation equivalents determined in the preceding section. The dates assigned to glacial events in southern Victoria Land are applied to equivalent glacial events in the Queen Maud Mountains. Throughout the remainder of this text the Queen Maud Mountains glacial terminology will be used as synonymous with the overall glacial chronology of the Transantarctic Mountains:

Amundsen Glaciation	< 9490 years
Shackleton Glaciation (moist period)	49,000 to 1.6 million years
Scott Glaciation "Interglacial"	2.1 to 2.4 million years
Queen Maud Glaciation	> 4.2 million years

Reedy Glacier (Mercer, 1968)	Scott Glacier	Amundsen Glacier	Shackleton Glacier	Beardmore Glacier	Taylor Valley (Péwé, 1961)	Taylor Valley (Denton and Others, 1970) Axial Glaciations from West	Taylor Valley (Denton and Others, 1970) Axial Glaciations from East	Wright Valley (Bull and others, 1962)	Wright Valley (Nichols, 1971 and Behling, 1971) Axial Glaciations from West	Wright Valley (Nichols, 1971 and Behling, 1971) Alpine Glaciations	Wright Valley (Nichols, 1971 and Behling, 1971) Axial Glaciations from East	Victoria Valley (Calkin, 1971) Axial Glaciation from West	Victoria Valley (Calkin, 1971) Local Glaciation	Mount Gran (Treves, Mirsky & Calkin, 1965) Axial Glaciation from West	Mount Gran (Treves, Mirsky & Calkin, 1965) Axial Glaciation from East	Mount Gran (Treves, Mirsky & Calkin, 1965) Local Glaciation
Reedy I	Amundsen Glaciation	Amundsen Glaciation	Amundsen Glaciation	Amundsen Glaciation	Koettlitz Glaciation	Taylor I Glaciation	[4450-9490 yr][3] (Ross I) (Ross II)	Fourth Glaciation	Wright Upper I & II Glaciations	Alpine I Glaciation [4400-6000 yrs][5]	Wright Lower Glaciation		Packard Drift Episode			Episode[3]
(Reedy II (moist period?)[S] (Reedy III)	Shackleton Glaciation	Shackleton Glaciation	Shackleton Glaciation	Shackleton Glaciation	Fryxell Glaciation	Taylor II & Taylor III Glaciations [1.6-2.1 m.y.]	(Ross III) (Ross IV)	Third Glaciation	Wright Upper III Glaciation	Alpine II Glaciation [.24-.32 m.y.][6] (moist period)[M]	Trilogy (moist period)[M,K]		Vida Drift Episode		Episode[2]	
(moist period)[S]			(moist period)[K]	(moist period)[K]									(moist period)[F]			
Reedy IV	Scott Glaciation	Scott Glaciation	Scott Glaciation	Scott Glaciation	Taylor Glaciation	Taylor IV Glaciation [2.7-3.5 m.y.][2]		Second Glaciation	Wright Upper IV Glaciation	Alpine III Glaciation [2.4-3.4 m.y.][7]	Loop (moist period)[F]	Bull Drift Episode			Episode[1]	
	"Interglacial"	"Interglacial"	"Interglacial"[F]	"Interglacial"[F]					[3.7-3.9 & 4.2 m.y.][4]		Pecten Marine Invasion[8]				(moist period)[F]	
Horlick Glaciation	Queen Maud Glaciation	Queen Maud Glaciation	Queen Maud Glaciation	Queen Maud Glaciation	McMurdo Glaciation	Taylor V Glaciation		First Glaciation	Vanda Glacial Episode			Insel Glaciation		A Glaciation		

Examples of Evidence

S = Solifluction
K = Kames
F = Fluvial Channels
M = Mudflows and Fans
P = Potholes

1 Denton and Others, 1970 (potassium-argon dating method)
2 Denton and Others, 1970 (potassium-argon dating method)
3 Olson and Broecker, 1961, Nichols, 1968; Denton and Others, 1970 (carbon-14 dating method)
4 Denton and Others, 1970, Fleck and Others, 1972 (potassium-argon dating method)
5 Behling, 1972
6 Behling, 1972
7 Behling, 1972
(salt concentration and reaction rate kinetics dating method)
8 Webb, 1972

GLACIOLOGICAL RECONSTRUCTIONS OF FORMER GLACIATIONS

The glacial deposits in the Transantarctic Mountains record four glaciations, including the present one. However, there is no evidence of complete deglaciation in interglacial time as occurred in North America and Europe. The vertical separation of the deposits corresponding to each of these glaciations is large enough to invoke markedly distinct ice surfaces to each of these glaciations. In this section reconstructions are derived for the ice surface configurations corresponding to the Queen Maud, Scott, and Shackleton Glaciations, and several comparisons are made with the present Amundsen Glaciation ice surface configuration. These reconstructions are projected in detail for the area of the Queen Maud Mountains. Ice surface reconstructions determined for southern Victoria Land are used primarily as a northwestern extension of the Queen Maud Mountains reconstructions.

The method of ice surface reconstruction employed involves analysis of the three-part continuum: (1) outlet glaciers and their basins of exudation, (2) ice shelf, and (3) interior high ice sheet. Detailed computer simulations of ice surface - bedrock topography are made for the area of outlet glaciers and their basins of exudation. This area is simulated in detail because it contains the outcrop area of the glacial deposits which define the glaciations. Former ice surfaces which are represented in this area are a key to corresponding former ice shelf and ice sheet surfaces. Theoretical equations are employed in the extension of the former ice shelf and ice sheet surfaces from their connection with the outlet glaciers and basins of exudation.

The resultant ice surfaces provide a fairly comprehensive coverage of the Queen Maud Mountain area, the western portion of the Ross Ice Shelf, the East Antarctic portion of the Ross Ice Shelf drainage system, and the extension of all of these into southern Victoria Land. An analysis of the profiles of these ice surfaces is made to determine the degree of influence which glacio-isostasy, tectonism, subglacial erosion, and eustasy may have on these profiles.

The reconstruction of these ice surfaces yields a model of the: (1) former grounding lines, (2) burial by ice of many of the lower mountains in the Transantarctic Ranges, and (3) surface level of the East Antarctic ice sheet during former glaciations. Extrapolation of these surfaces over the entire area of present grounded ice and ice shelves for Antarctica provides values for ice volumes related to these former glaciations. These ice volumes are converted into sea level equivalents to determine the effect which Antarctic glaciation has had on world-wide sea level.

Determination of Ice Surface Profiles Related to Former Glaciations

The concept of the continuum ice sheet-outlet glacier-ice shelf, similar to that proposed by Weertman (1964), allows a working hypothesis for the investigation of fluctuations of ice surfaces, assuming a knowledge of these ice surfaces in at least one of the segments of the continuum. The most productive segment, in terms of its connection with the other two segments is the outlet glacier which ideally marks ice sheet and ice shelf surface level fluctuations at its proximal and distal ends. This system applied to the study areas in this text allows the recreation of ice surfaces for the Ross Ice Shelf drainage system and the Ross Ice Shelf from a study of the former ice surfaces marked by glacial deposits in the outlet glaciers and basins of exudation of the Transantarctic Mountain sector of the Ross Ice Shelf drainage system.

To represent the former ice surfaces related to the Shackleton, Scott, and Queen Maud Glaciations in the ice sheet-outlet glacier-ice shelf continuum the following maps were constructed: (1) an overall base map of the Ross Ice Shelf drainage system and the Ross Ice Shelf (Fig. 53), (2) cross-sections of the Scott, Amundsen, Shackleton, and Beardmore Glacier areas and the former ice surfaces in these areas (Fig. 54-57, respectively), (3) cross-sections of Taylor, Wright and Victoria Valleys and the former ice surfaces in these areas (Figs. 58-60, respectively), and (4) an idealized cross-section (Fig. 61) through a portion of the East Antarctic ice sheet, an outlet glacier and part of the Ross Ice Shelf.

In the area encompassed by Figure 53, ice surface reconstructions are based on the division of this area into four parts, labeled 1-4 in Figure 53 and listed below:

(1) the central portion of the outlet glaciers extending into their respective basins of exudation,

(2) the coastal portions of the outlet glaciers and their extension into the area of the present Ross Ice Shelf,

(3) the peripheral portion of an ice sheet which has totally inundated any coastal outlet valleys, and

(4) an ice sheet on the inland side of a mountain range.

The central portion of the outlet glaciers extending into their respective basins of exudation

Examples of the ice surface reconstructions developed for this area are the former ice surfaces related to the Shackleton and Scott Glaciations which were confined within the valleys of the present Scott, Amundsen, Shackleton, and Beardmore Glaciers (Figs. 54-57), respectively). These former ice surfaces are determined by lines connecting

Table 16. Legend for Figures 54 to 61.

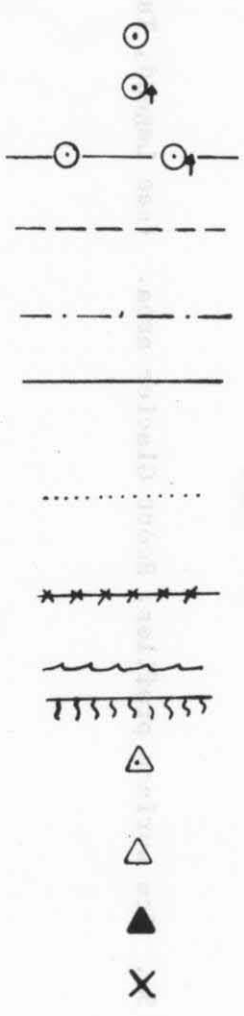

Upper surface of moraine (field observation)

Minimum upper surface of moraine (field observation)

Former ice surface extrapolated between field observations

Theoretical ice surface profile (non-isostatically corrected)

Theoretical ice surface profiles (isostatically-corrected)

Present ice surface and bottom of Ross Ice Shelf (after USGS topographic maps; Crary and others, 1962)

Theoretical simulation of the terminal portions of current outlet glaciers

Upper surface of deposits of the Pecten Marine Invasion (after Calkin and others, 1970)

Ocean surface

Ocean Floor (after Crary and others, 1962)

Depth of bedrock beneath the terminal portions of current outlet glaciers (after Giovinetto and others, 1966)

Non-isostatically corrected grounding point

Isostatically corrected grounding point

Depth of the floor of Wright Valley during the Queen Maud Glaciation

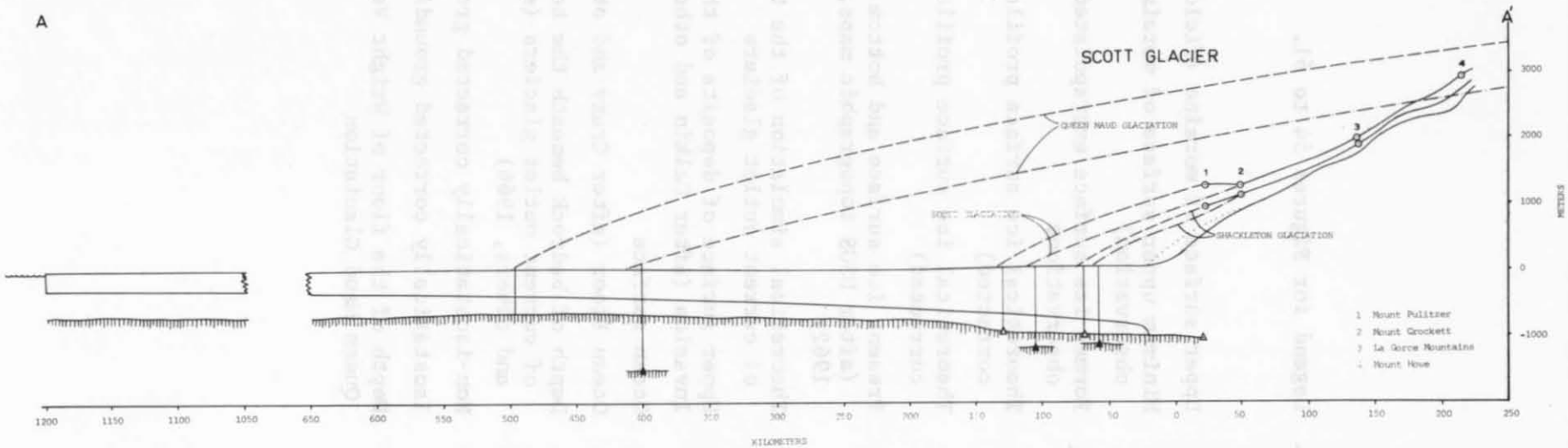

100

Figure 54. Ice surface profiles, Scott Glacier area. (see Legend, Table 16)

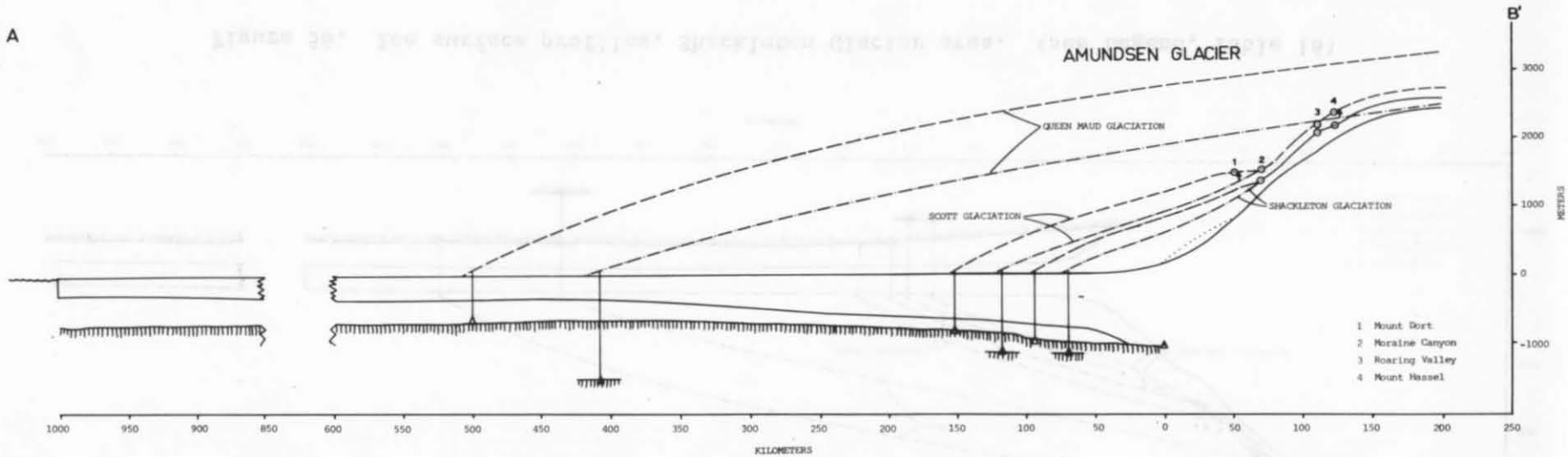

Figure 55. Ice surface profiles, Amundsen Glacier area (see Legend, Table 16)

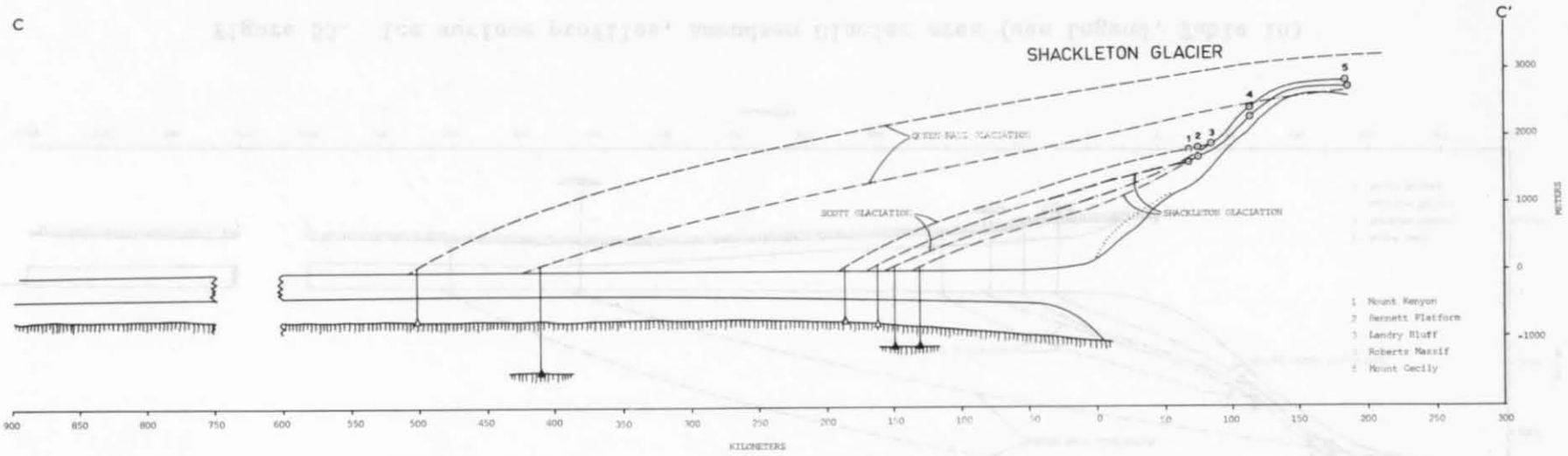

Figure 56. Ice surface profiles, Shackleton Glacier area. (see Legend, Table 16)

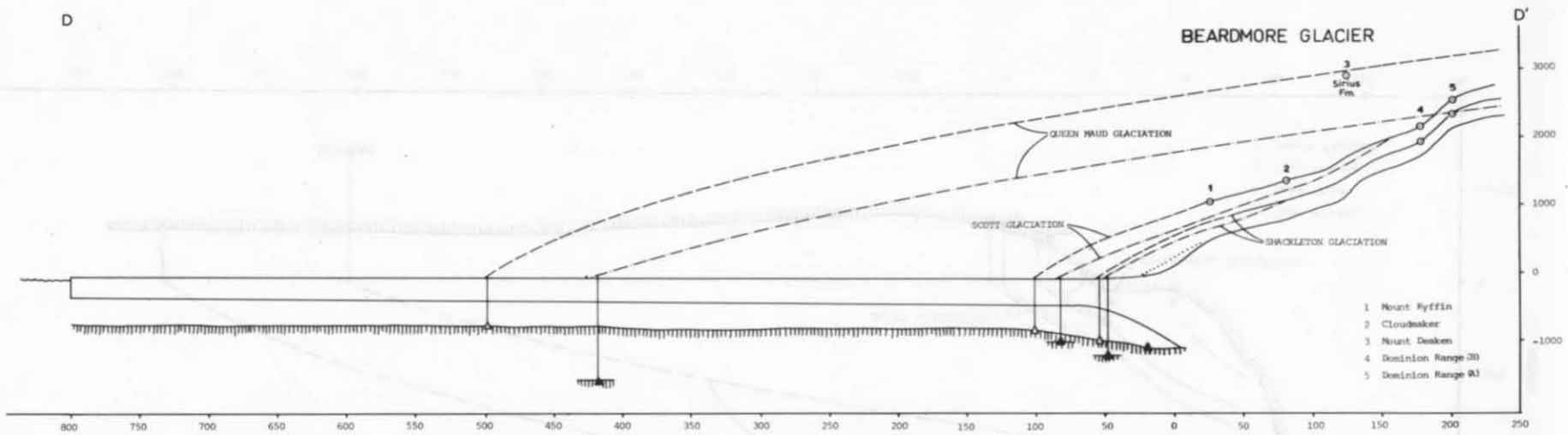

Figure 57. Ice surface profiles, Beardmore Glacier area. (see Legend, Table 16)

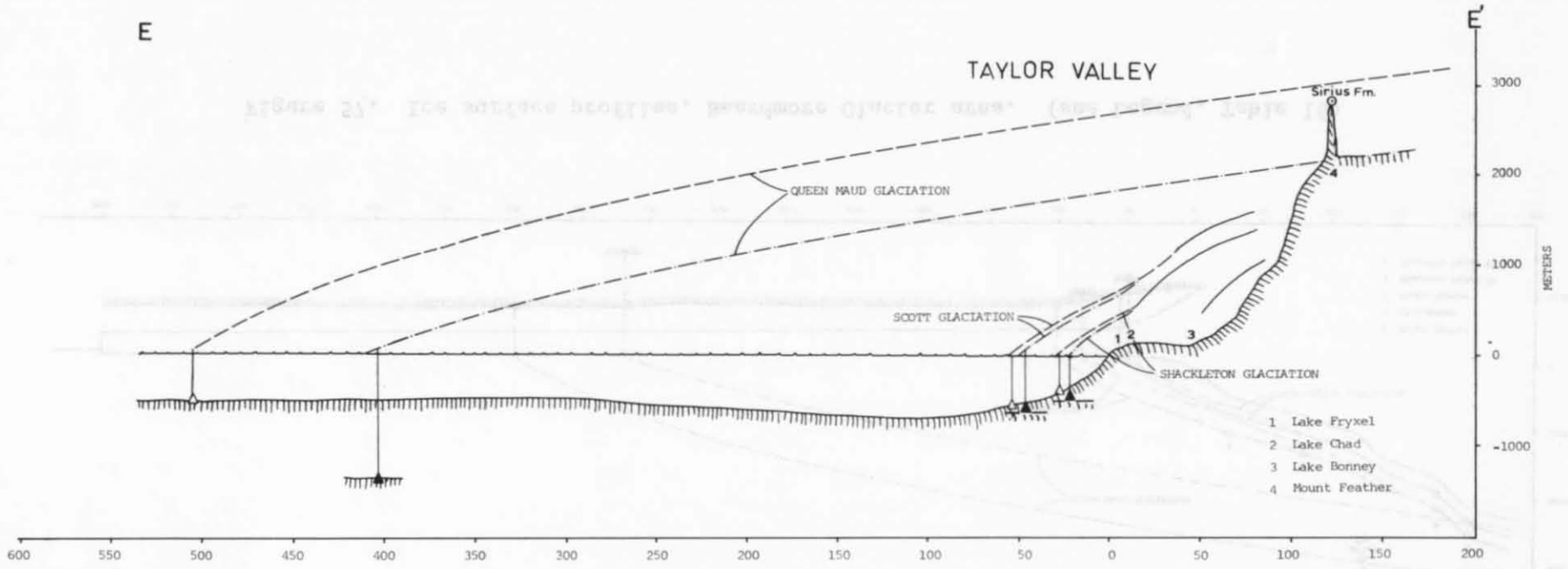

Figure 58. Ice surface profiles, Taylor Valley area. (see Legend, Table 16)

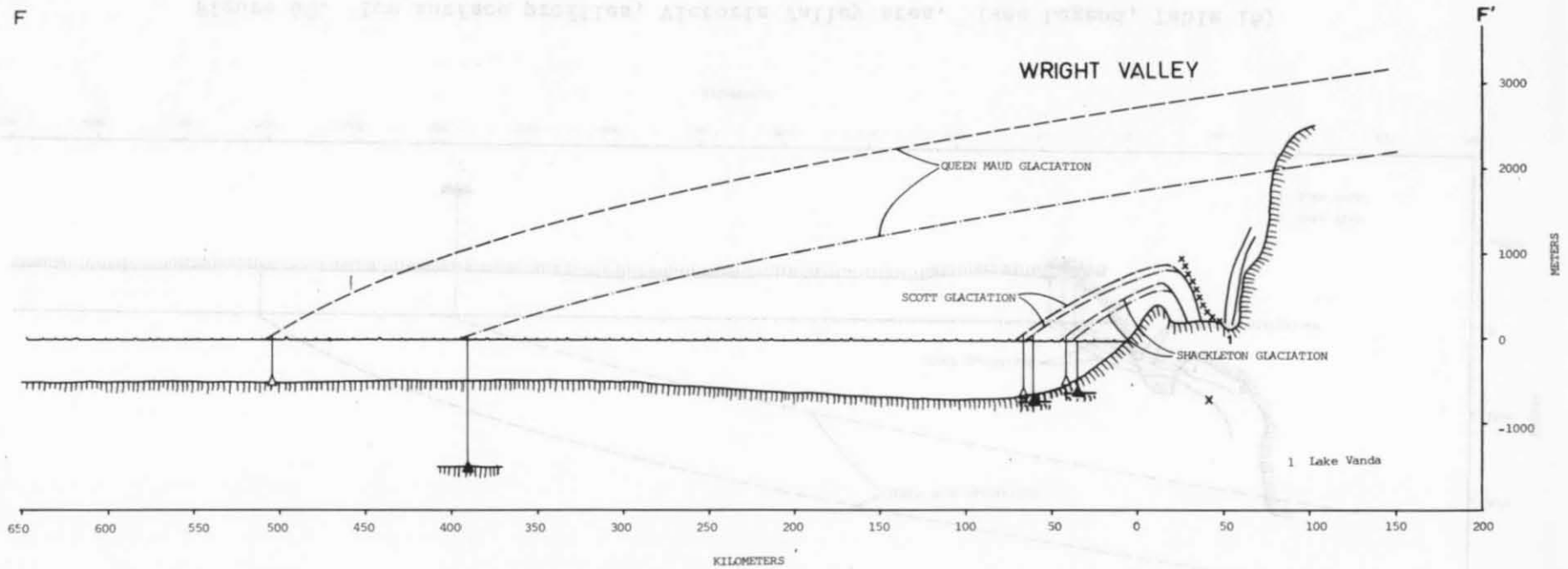

Figure 59. Ice surface profiles, Wright Valley area. (see Legend, Table 16)

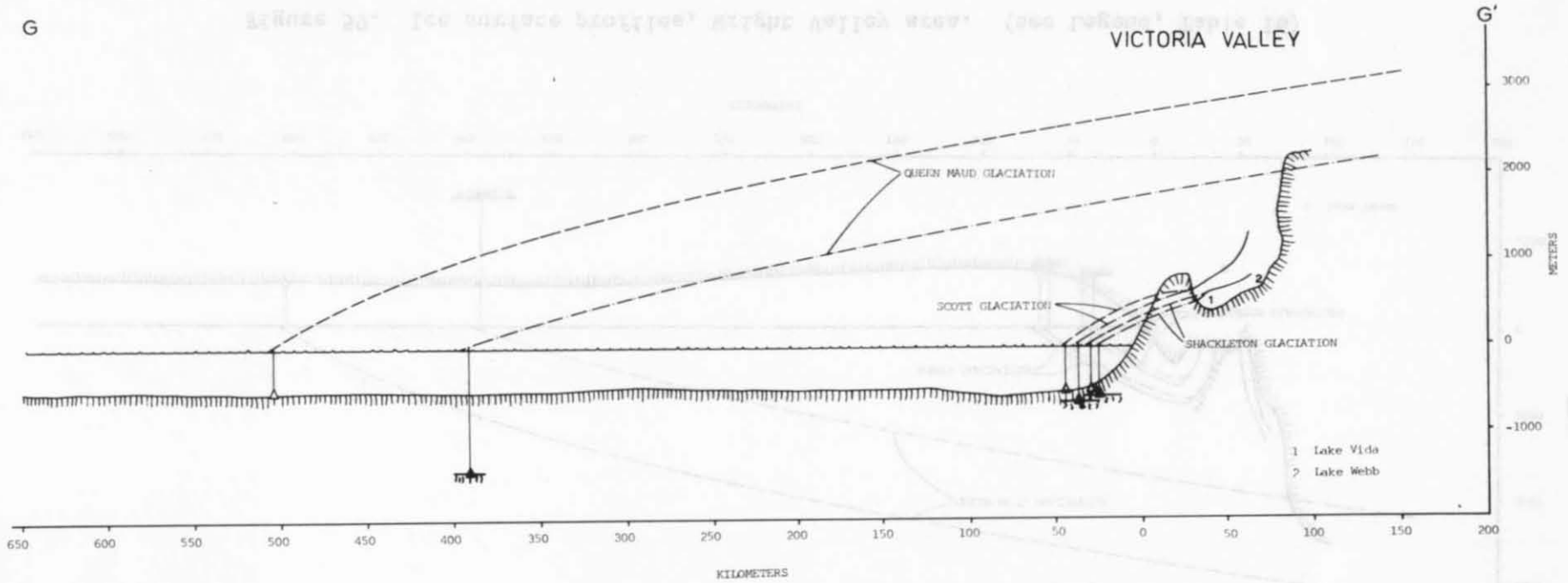

Figure 60. Ice surface profiles, Victoria Valley area. (see Legend, Table 16)

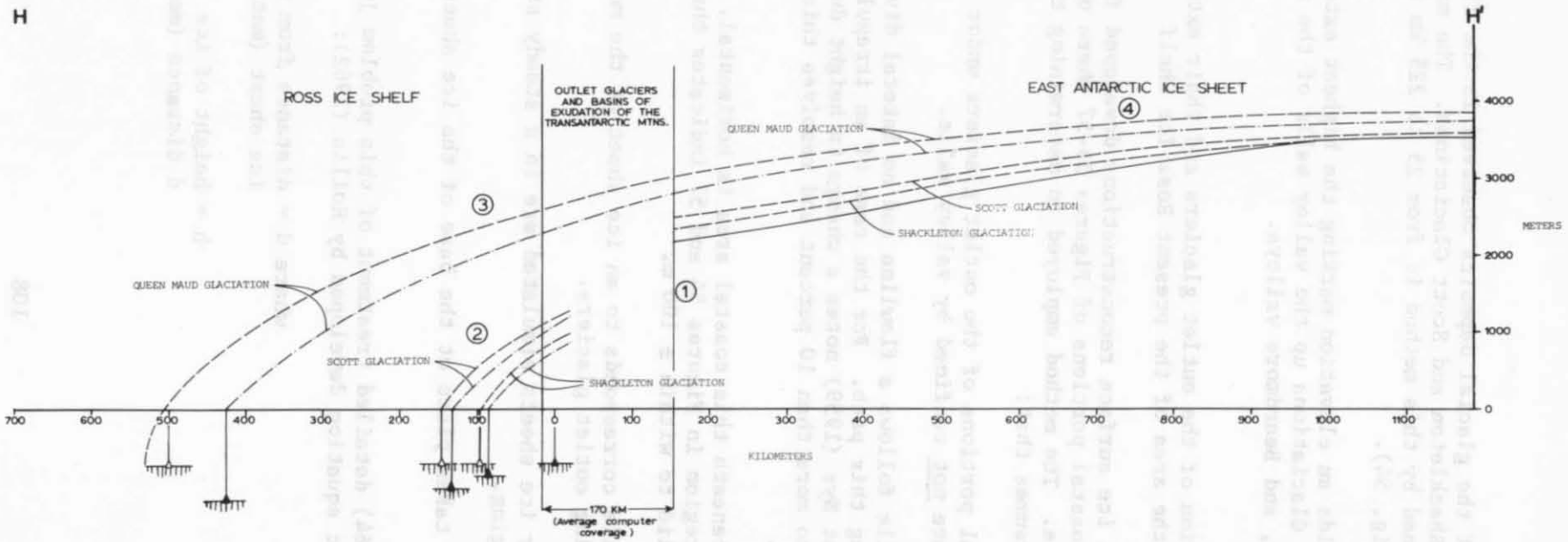

Figure 61. Idealized cross-section through Ross Ice Shelf, outlet glaciers of the Transantarctic Mountains and the East Antarctic ice sheet. (see Legend, Table 16)

the upper portions of the glacial deposits observed in the field which were related to the Shackleton and Scott Glaciations. The maximum long profile extent attained by this method is from 25 to 225 km inland along the Scott Glacier (Fig. 54).

This method yields an elevation marking the highest extent of the Shackleton and Scott Glaciations up the valley walls of the Scott, Amundsen, Shackleton, and Beardmore valleys.

The coastal portion of the outlet glaciers and their extension into the area of the present Ross Ice Shelf

Examples of the ice surface reconstructions developed for this area are taken from the coastal portions of Figures 54-57 where observed field data is not available. The method employed in determining this portion of these profiles assumes that:

(1) The coastal portions of the outlet glaciers under study (Figs. 54-57) are not confined by valley walls.

(2) This profile follows a flowline and no lateral divergence is assumed along this path. For the case of an irregularly shaped ice sheet Nye (1959) notes a change in height due to divergence of no more than 10 percent and resolves this as a minimal effect.

(3) The base beneath this coastal area is horizontal. Review of this basal region in Figures 54 and 57 indicates that this is essentially valid to within ± 100 m.

(4) Each profile corresponds to an ice sheet at the mouth of the corresponding outlet glaciers.

(5) The former ice sheets simulated are in a steady state, i.e. slow changing.

(6) All shear takes place at the base of the ice sheet (Nye, 1959).

Weertman's (1964) detailed treatment of this problem justifies using this parabolic equation developed by Hollin (1962):

$$h = 4.7\sqrt{d}$$

where d = distance from edge of ice sheet (meters)

h = height of ice sheet at d distance (meters)

This parabola fits observed profiles of the peripheral portions of the East Antarctic ice sheet, i.e. inland from Mirny (Hollin, 1962). At approximately 375 km inland the parabola departs at a steep angle from the observed profile as noted by Hollin (1962), rendering it ineffective in the simulation of the interior portion of the ice sheet.

The grounding point related to the Ross Ice Shelf terminating point of this parabola can be computed by fitting the equation for floating ice in sea water used by Crary and others (1962):

$$\frac{H}{e} = \frac{\rho H_2O}{\rho H_2O - \rho \text{ ice}} = \frac{10}{1}$$

where: H = total ice thickness
e = surface elevations
ρ = density (gm/cm^3)

Both isostatically and non-isostatically corrected grounding points are plotted on Figure 61 based on the average values of the grounding points in Figures 54 to 57 of the Queen Maud Mountain outlet glaciers. Isostatically corrected grounding lines are plotted on Figure 53 based on the grounding points in Figures 54 to 57 of the Queen Maud Mountains and Figures 58 to 60 of southern Victoria Land with extrapolations made in the adjoining areas.

The peripheral portion of an ice sheet which has totally inundated any coastal valleys

Examples for this case are taken from the ice surface corresponding to the Queen Maud Glaciation in the Scott, Amundsen, Shackleton, and Beardmore Glacier areas (Figs. 54 to 57, respectively). The assumptions employed in generating this ice surface are:

(1) The mountain ranges have only a small effect on the overall profile of the ice sheet (Weertman, 1964) when as in this case:

(a) R>3D where: R = radius of the ice sheet from its grounding line to its inland ice divide (Fig. 61)

D = width of the coastal mountain range

(b) the spacing between outlet glaciers is small compared to the overall dimensions of the ice sheet, i.e. Figure 53.

(2) The ice which deposited the Sirius Formation during the latter stages of the Queen Maud Glaciation was a thick, polar ice sheet with a basal melt-freeze zone in the vicinity of the Sirius Formation.

The ice thickness (h_o) required to have pressure melting at each locality of the Sirius Formation can be found by Weertman's (1962) equation:

$$h_o = k \frac{\Delta T}{Qg+Qs}$$

where: ΔT = difference between pressure melting point of ice and upper surface temperature

k = coefficient of thermal conductivity (1.75×10^5 cal/cm-yr-°C)

Qg = geothermal heat (cal/cm^2/yr)

Qs = heat of sliding (cal/cm^2/yr)

This thickness (h_o), added to the elevation of the highest outcrop of the Sirius Formation (h_r), yields a minimum value for the surface elevation (non-isostatically corrected) required to deposit the Sirius Formation at this site. The site at Mount Deacon (2800 m above sea level) is used for the Queen Maud Mountains, and Mount Feather (2800 m above sea level) is used for southern Victoria Land.

A minimum value of h_o of 300 m is employed based on the following values for Q_g, Q_s and ΔT which are chosen as:

Q_g = 39 cal/cm^2/yr (after Weertman, 1962)

Q_s = 190 cal/cm^2/yr (after Weertman, 1962), and where Q_s is considered to be the average velocity of basal ice over the region of the Sirius Formation

ΔT = (basal pressure melting point of -3°C after Hughes, 1971) minus (a surface temperature of -45°C after Bentley and others, 1964; after adjusting for a rise in ice surface level)

The parabola $h = 4.7\sqrt{d}$ (Hollin, 1962) is used for the portion of this ice sheet less than 375 km inland with the assumptions previously developed for this parabolic equation and with $h = h_o + h_r$.

The basal shear stress (τ) of the ice surface profile developed in this portion of the ice sheet for the Queen Maud Glaciation is computed by the equation:

where: ρ = density of ice (.92 kg(m^3))

g = gravitational constant ($.98 \times 10^{-4}$ m/sec^2)

$\tau + \rho\ gh \sin \alpha$

h = ice thickness (2400 meters)

α = ice surface slope (.02°)
(Paterson, 1969)

This yields a basal shear stress of .126 bars. This extremely low value compared to typical values of basal shear stress of 0.4 to 1.0 bars (after Weertman, 1962) indicates that the h_o employed in the development of this profile is, in fact, close to a minimum value as intended. This low value also indicates that the ice may have been moving fairly rapidly as a result of a basal melt layer.

The grounding line formed at the terminus of the ice surface of the Queen Maud Glaciation is developed in the manner previously discussed (Crary and others, 1962).

Ice sheet on the inland side of the Transantarctic Mountains

The example for this case is taken from the idealized profiles related to the Shackleton, Scott, and Queen Maud Glaciations in Figure 61. The parabola introduced by Hollin (1962) departs from the present inland ice surface profile in this area too drastically to be considered for the simulation of former ice surface profiles in this area.

Robin (1964) provides a simple equation for an ellipse:

$$\left(\frac{h_x}{H}\right)^2 + \left(\frac{x}{L}\right)^2 + 1$$

where H is the height (kilometers) of an ice sheet 2L (kilometers) wide and h_x is the height (kilometers) at x (kilometers) distance from the center of this ice sheet. Surface heights to within ± 100 m of observed heights have been computed for various portions of the Antarctic and Greenland ice sheets employing this equation (Robin, 1964).

In Figure 61 this ellipse has been generated for a section of the Ross Ice Shelf drainage system along profile H-H' chosen for its moderately flat ice surface. The ellipse approximates the present ice surface to within ± 100 m from the ice divide at H' to approximately 350 km inland from the present coast.

Values used in determining the dimensions of this ellipse for the former glaciations in this area are:

(1) Average, non-isostatically corrected grounding lines at 90, 140, and 500 km seaward off the coast line of the Queen Maud Mountains are added to the value of L for the Shackleton, Scott, and Queen Maud Glaciations, respectively.

(2) Average values for h_x of 2650, 2800, and 3350 m are used for the ice surfaces related to the Shackleton, Scott, and Queen Maud Glaciations, respectively. These values are derived by an extrapolation of the field data from the zone 25 to 225 km inland from the present coast into the zone from 225 to 350 km from the present coast (Fig. 61).

Ice Volume Changes Determined From Former Ice Surface Profiles

Factors affecting former ice surface profiles

Prior to any consideration of the ice volume changes which correspond to the former ice surface profiles previously determined, the following factors should be considered: (1) glacio-isostasy, (2) tectonism, (3) subglacial erosion, and (4) eustasy. Each of these factors might complicate the interpretation of ice volume changes.

Glacio-isostasy

Former ice surface profiles in the area of Figure 53 have been isostatically adjusted (Figs. 54 to 60) assuming:

(1) Glaciations affecting this area were all separated by long enough time periods to allow isostatic equilibrium prior to the next glaciation. Farrand (1968) assumes a 10,000 year time period to be sufficient for the majority of isostatic compensation. This time period represents only a fraction of the interval between the glaciations in question if weathering phenomena are judged correctly.

(2) The present area covered by Figure 53 is in isostatic compensation with respect to ice loading. Although negative gravity anomalies attributed to partial isostatic rebound have been encountered in Antarctica (Kaula, 1969), studies in Marie Byrd Land (Bentley and Chang, 1971) and in Queen Maud Land (Beitzel, 1971) have postulated that these areas are isostatically compensated to within 500 m.

(3) An isostatic depression due to former ice loading is used for correcting former ice surface profiles (Figs. 54 to 60), based on the ratio of the density of ice (.91 gm/cm^3). An approximate ratio of 1:3 is resolved from these density differences and is considered to be reasonable in light of the scale of the area involved.

(4) Considering the scale of the representations of the former ice profiles, only former ice thicknesses in excess of 600 m are isostatically corrected.

(5) No buoyancy effects are assumed at the ice edge as a result of the termination of this ice edge into the Ross Sea. This assumption tends to yield steeper terminal profiles for former ice surfaces than those presently observed.

(6) No eustatic effects are calculated in the isostatic adjustments. Even a maximum sea level lowering of 150 m (Ewing and others, 1960) during a maximum glacial period yields only a 50 m change in the isostatic depression of the area. This latter figure falls well within the error limit introduced by the scale of the ice surface profiles.

Isostatically corrected former ice surface profiles related to the Shackleton and Scott Glaciations parallel quite closely present ice surface profiles, except in the extreme terminal portions of these profiles. Thus, factors determining the shape of present ice surface profiles in these areas have been similar since the deposition of the High Moraine during the Scott Glaciation.

Using the isostatically corrected ice surface related to the Queen Maud Glaciation, calculation yields only a 210 m increase in elevation in the area of the present ice sheet divide (H' in Fig. 61). A 2550 m thickness of ice is estimated to have overlain the locale of the deposits of the Pecten Marine Invasion in Wright Valley (Fig. 59) prior to their deposition during the Queen Maud Glaciation. Assuming an isostatic depression of this area by approximately one-third of the thickness of the ice load, places this area 850 m below present sea level. McSaveney and McSaveney (1972) estimate the highest occurrence of the Pecten deposits in Wright Valley at 600 m above sea level, which if isostatically depressed by a 2550 m ice load would place the highest outcrop of these deposits 250 m below present sea level.

The only problem presented by the coincidence of the isostatic depression and the highest recorded outcrop of the Pecten deposits after completion of isostatic rebound results from the fact that ice cannot be grounded in the valley during a marine invasion and yet any depletion of ice load will be followed by at least partial isostatic rebound. This discrepancy can be explained by several mechanisms:

(1) The rapid removal or surging of ice in the coastal portions of Antarctica (Wilson, 1966) has the potential of yielding a lag time between unloading of ice and isostatic compensation. This lag period may be of a sufficient duration to allow marine invasion of a gradually rising area. This is well demonstrated in other areas, such as Hudson's Bay.

(2) Removal of a 500 m thickness of ice at 100 km inland over the Wright Valley bedrock threshold (Fig. 59) either by a surge mechanism, diverted ice flow, or ablation accompanied by partial isostatic rebound of this threshold will cut off the source of ice filling the valley. Once ice no longer enters the valley the coastal climate and calving of ice into the Ross Sea will cause a rapid depletion of the ice in the valley. A fjord as proposed by Webb (1972) and McSaveney and McSaveney (1972) would then replace the grounded ice in Wright Valley and allow a marine invasion.

Tectonism

Although evidence exists for Cenozoic tectonic activity in the Transantarctic Mountains (Nichols, 1966), the absolute age and rate of this tectonic movement are still unknown. The glaciations represented by the preceding ice surface profiles may extend back to more than 4.2 million years, thus allowing plenty of time for tectonic interaction in the development of various moraine levels. Because of this potential for tectonic interaction either causing or affecting these ice surface profiles, consideration is made to separate or eliminate tectonic interference during these glaciations.

Grindley (1967) estimates a regional elevation of the Transantarctic Mountains accompanying depression of basins inland from the Transantarctic Mountains. Assuming such a model, the portion of the ice surface profiles furthest inland from the coast in the Transantarctic Mountains should converge toward a common point. The moraine levels investigated in this inland region and the ice surface profiles developed from these moraine levels show only slight convergence inland.

Furthermore, a relative rise of the Transantarctic Mountains would produce a relative subsidence of the Ross Sea basin adjacent to the Transantarctic Mountains. Were this differential action recorded in the moraine levels in the Queen Maud Mountains, it would result in the steepening of the coastal portions of the ice surface profiles developed from these moraines. This differential movement does not appear to be apparent in the coastal portion of the isostatically corrected profiles.

In the evidence reviewed by Nichols (1966), numerous examples of block-faulting are noted to have affected moderately small areas (i.e. opposite sides of valleys, ridges, etc.). These tectonic elements must have occurred prior to glaciation in the Transantarctic Mountains because present and former ice surface profiles show moderately uniform slopes and elevations from glacial valley to glacial valley. These profiles are not steplike, suggestive of block-faulting. The only discrepancies noted in comparing ice surface profiles throughout the Queen Maud Mountains per glaciation result from the dimensions of the outlet glacier and its valley, i.e. the smaller the valley, the steeper the ice surface profile.

Unless extensive subglacial erosion has occurred along with tectonic uplift of the Transantarctic Mountains, the progression of younger glacial deposits at lower and lower elevations along the valley wall might not occur. Rather, tectonic uplift with limited subglacial erosion may result in the total overlap of older moraines by younger ones, if the rate of draining of the inland ice sheet remained constant.

Therefore, the majority of the Tertiary tectonic disturbances affecting the Transantarctic Mountains very possibly occurred prior to the formation of the glacial deposits used to determine the four former ice surface profiles. Thus, tectonic activity in the Transantarctic Mountains may have been confined to the early or possibly middle Tertiary.

Subglacial erosion

Another unknown factor related to the interpretation of former ice surface profiles in the Transantarctic Mountains is the amount and rate of subglacial erosion. It has been implied that the predominant glacial sculpturing of the Transantarctic Mountains occurred prior to the deposition of the Sirius Formation. If erosion is effectively downcutting outlet valleys, the moraine levels in these valleys do not appear to reflect these changes. This is indicated by observing that: (a) the present mass balance of the Antarctic ice mass is positive (Bull, 1971) and (b) the area of the outlet valleys is disproportionately small compared to the area of their source, the East Antarctic portion of the Ross Ice Shelf drainage system. Thus, Weertman (1964) notes that the outlet glacier surfaces will always be graded to the surface level of the ice sheet feeding them and that base level fluctuations, i.e. subglacial erosion, in these valleys will be readjusted and will not affect outlet glacier ice surface profiles.

In addition to the above, differential downcutting is not implied by an examination of the isostatically corrected former ice surface profiles. These profiles closely parallel present ice surface profiles and thus imply a constant rate of downcutting. However, the structure

of the sediments cropping out in the Queen Maud Mountains indicates a very gentle inland dip, and the varying resistances to abrasion of each of these sedimentary layers would not tend to result in uniform downcutting rates as a function of time and location. In addition, the bedrock map of the Queen Maud Mountains (Fig. 2) indicates that the Shackleton Glacier valley is composed of an inland half of Beacon sediments and a coastal half of basement rocks and that the Amundsen Glacier valley is composed almost entirely of basement rocks. Comparison of the ice surface profiles (Figs. 55 and 56) for these two areas demonstrates that they contain similarly shaped surface profiles regardless of this subglacial lithologic difference.

If subglacial erosion had caused the differences in level noted between the ice surface profiles of the glaciations in the Transantarctic Mountains, the surficial weathering features used to characterize the moraines related to these glaciations should be gradational. On the contrary, although gradations in surficial weathering of moraines occur within moraines of a single glaciation, rather abrupt changes occur at the contact between moraines of differing glaciations. Such contacts imply a periodic erosion, or more than likely a renewed rise in ice surface level following every major decline in ice surface level of the previous glaciation.

Eustasy

Hollin (1962) attributes the size of the Antarctic ice sheet to the elevation of the grounding line surrounding the continent. He notes that sea level depressions on the order of 150 m (Ewing and others, 1960) and thickening of the ice shelf as a function of increased freezing beneath the ice shelf might be capable of extending the grounding line and thus affect the ice surface profile inland. Although sea level fluctuations may have affected the grounding line of outlet glaciers draining through the Transantarctic Mountains, these effects are shown not to have been the major cause of ice level fluctuations.

Grounding points (Figs. 54 to 60) plotted for the former glaciations in the Queen Maud Mountains indicate that a sea level decrease in excess of the 150 m estimated by Hollin (1962) would be necessary to ground areas of presently floating ice. Furthermore, sea level depressions capable of grounding ice to form the ice surface related to the Scott Glaciation are equivalent to those which are required to form the ice surface related to the Queen Maud Glaciation according to Figures 54 to 60. In addition, as pointed out by Hollin (1962), isostatic depression resulting from grounding ice tends to counteract lowered sea level effects. Isostatic depression of the ocean bottom within a few kilometers of the computed grounding points exceeds the 150 m maximum sea level depression (Figs. 54 to 57).

If sea level fluctuations were so effective in causing the different ice surface levels recorded in the Transantarctic Mountains, then there should be a complete late Quaternary record of glaciations in this area exactly equal to Quaternary sea level fluctuations. Such a record is not apparent in the Transantarctic Mountains.

Computation of Ice Volume Changes

Ice volumes of former glaciations relative to present ice volumes are computed for the area of the whole Ross Ice Shelf drainage system and the Ross Ice Shelf. These volumes are computed by comparing former ice surface profiles to present ice surface profiles and determining the difference. Two simplifying assumptions are invoked, both based on the previous section of this text:

(1) Differences in elevation between present and former ice surface profiles are assumed to be a function of actual ice volume changes and not of the redistribution of a static ice volume by tectonic, erosional, and/or eustatic changes.

(2) Non-isostatically corrected ice surface profiles are employed in these computations to avoid errors in the interpretation of values for isostatic adjustment and the configuration of subglacial topography.

The computation of ice volume changes for the whole Ross Ice Shelf drainage system is based on a division of this area into three regions (Figs. 53 and 61): (1) outlet glaciers and their basins of exudation, (2) the Ross Ice Shelf, and (3) an inland ice sheet region. From the Queen Maud Glaciation to the present this area has been marked by a gradually declining ice surface separated by lesser rises in the ice surface, defining the initiation of new "glaciations". Obviously, in this pole-centered continent these are not complete advances and retreats of continental ice sheets as is the usual "glaciation" at lower latitudes.

Ice volume changes in the region of outlet glaciers and their basins of exudation

In this region ice volume change computations for a lowering ice surface are complicated by the uncovering of irregular bedrock topography of the Transantarctic Mountains. Computer simulation of this relationship allows for the topographic correction required in these ice volume computations. The computer programs (Appendix B) employed in this simulation yield: (1) non-isostatically corrected maps displaying the ice surface - bedrock topography relation for each

glaciation and (2) frequency tables listing the percent area of each map within specific contour intervals. These frequency tables are used to determine the total ice surface to bedrock topography "map volume" for each map. The volume in each case is that added to present ice to achieve each past "higher" condition.

The Scott, Amundsen, and Shackleton Glacier areas were chosen for computer simulation in order to determine the ice volume increases of the Queen Maud, Scott, and Shackleton Glaciations and to compare them to the present total map volume. These areas were chosen because they contain quite complete evidence for the long profiles (Figs. 54 to 56) of former ice surfaces. Base maps of the present ice surface and bedrock topography were reproduced on an IBM 1620 plotter system using data derived from the United States Geological Survey topographic maps covering the Scott, Amundsen, and Shackleton Glacier areas. To these base maps thicknesses of ice determined from the former ice surface profiles of each of the former glaciations are added. Thus, for each area a map is produced corresponding to the Amundsen, the Shackleton, the Scott, and the Queen Maud Glaciations. These maps are designated respectively by glaciation: Figures 62 to 65 for glaciations of the Scott Glacier area, Figures 66 to 69 for glaciations of the Amundsen Glacier area, and Figures 70 to 73 for glaciations of the Shackleton Glacier area. Map volumes (Table 17), including the total ice and bedrock volumes computed from frequency table listings, are computed for each of these maps. Subtraction of the Amundsen Glaciation map volume from older glaciations yields the ice volume of that glaciation.

Extrapolation of these resulting ice volumes over the area of the outlet glaciers and their basins of exudation (194,830 km^3) yields the ice volumes for the former glaciations in this area (Table 18).

Ross Ice Shelf ice volume changes

Ice volumes are determined also for the Ross Ice Shelf itself (Table 19) during former glaciations from average grounding lines. These grounding lines are determined from the grounding points of the former ice surface profiles of the Scott to Beardmore Glacier areas (Figs. 54 to 57). These grounding lines are then extrapolated into portions of the Ross Ice Shelf area not yet investigated (Fig. 53). Extrapolation of these values northwestward along the western side of the Ross Ice Shelf is substantiated by their fit with grounding lines computed for former glaciations related to the Taylor, Wright, and Victoria Valleys (Figs. 58 to 60). Application of these extrapolated values to the former grounding lines on the eastern side of the Ross Ice Shelf, the Marie Byrd Land drainage area, is fairly subjective. The lack of bedrock outcrops and evidence of former glaciations along the coast of Marie Byrd Land prevents any further sophistication of the placement of these grounding lines by the methods employed in this text.

Figure 62. Scott Glacier area during Amundsen Glaciation.

Outline of present ice-free areas.

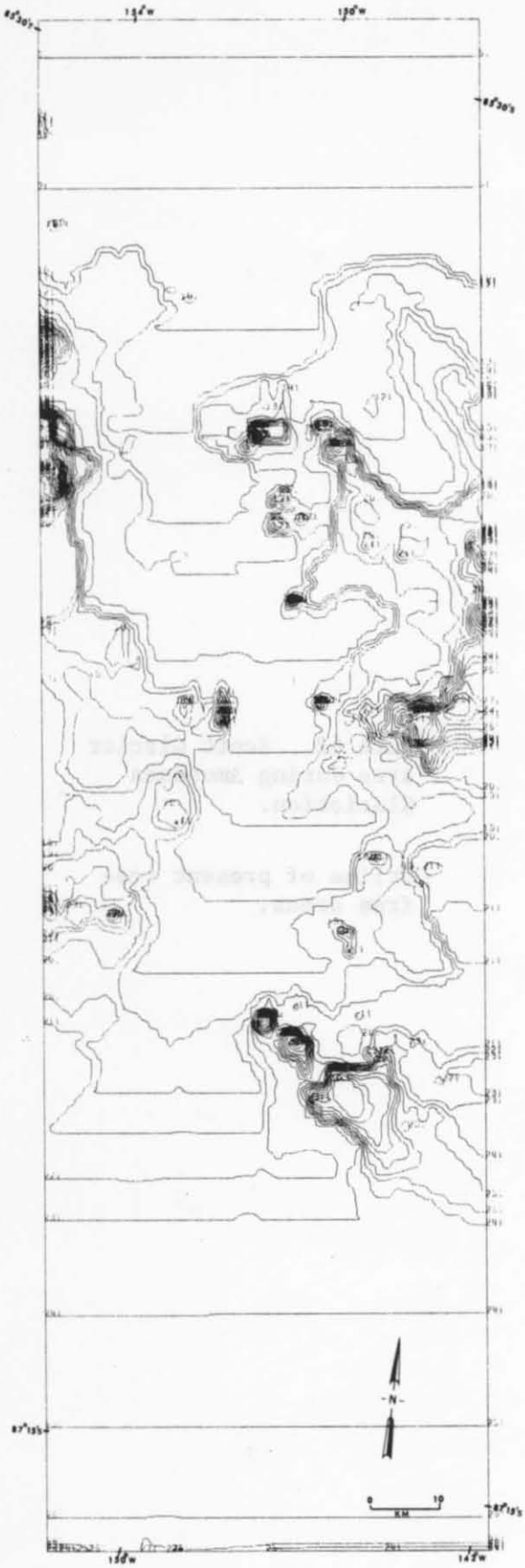

Figure 63. Scott Glacier area during Shackleton Glaciation.

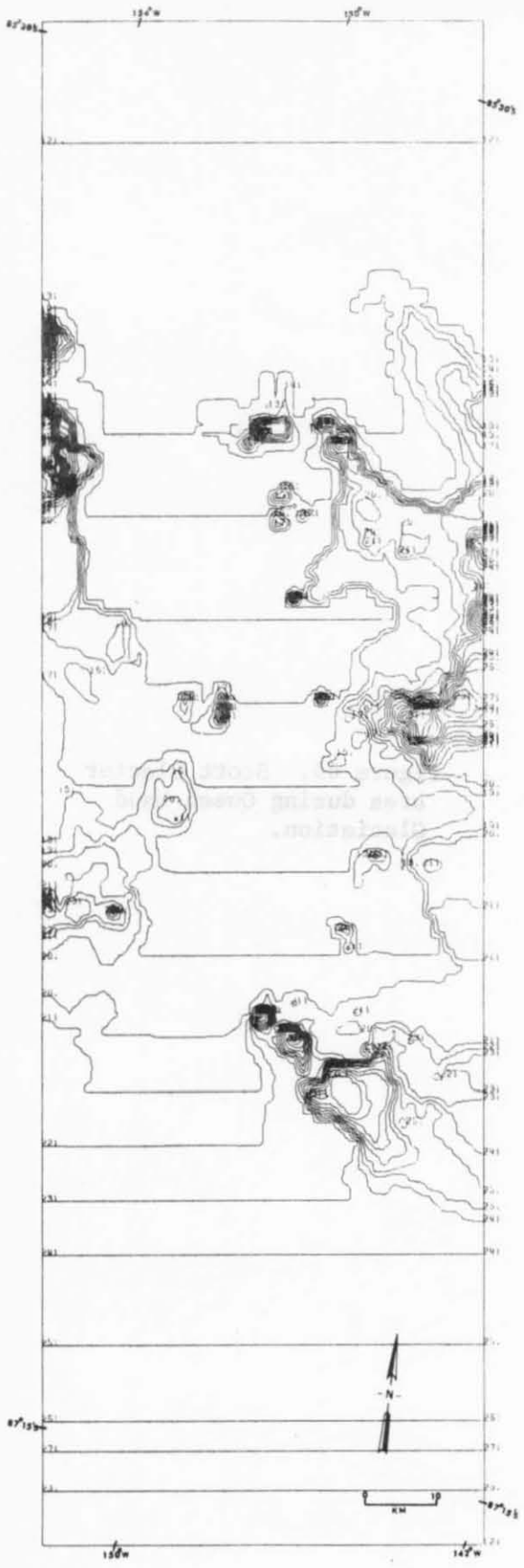

Figure 64. Scott Glacier area during Scott Glaciation.

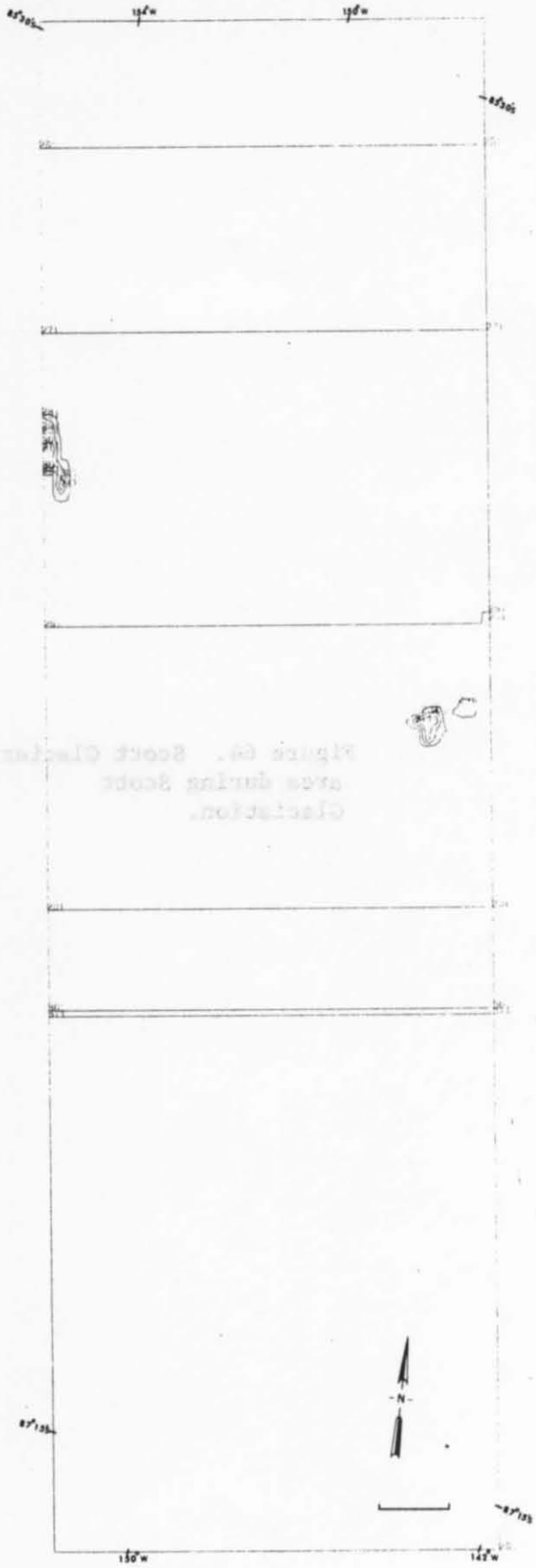

Figure 65. Scott Glacier area during Queen Maud Glaciation.

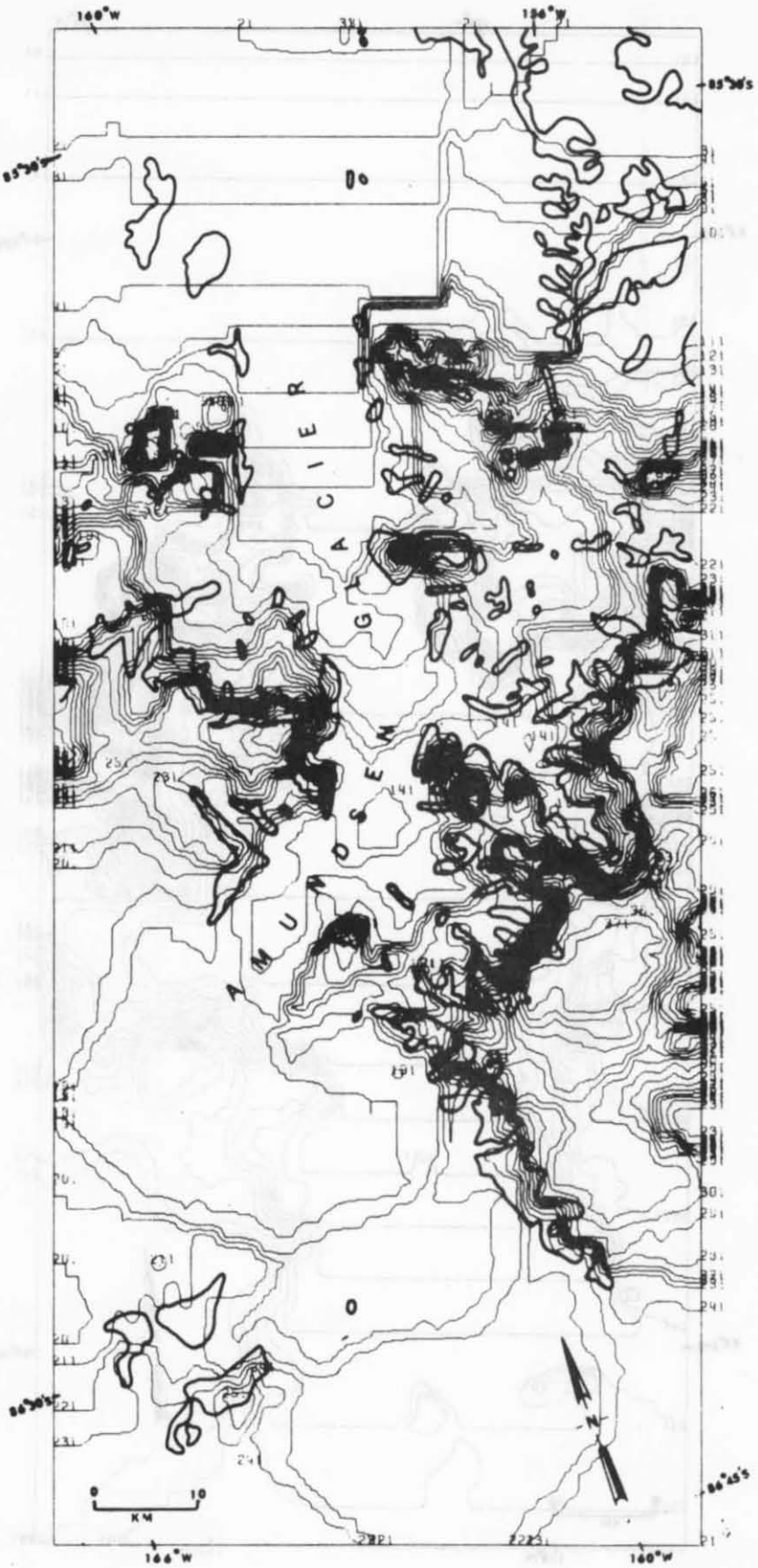

Figure 66. Amundsen Glacier area during Amundsen Glaciation.

Outline of present ice-free areas.

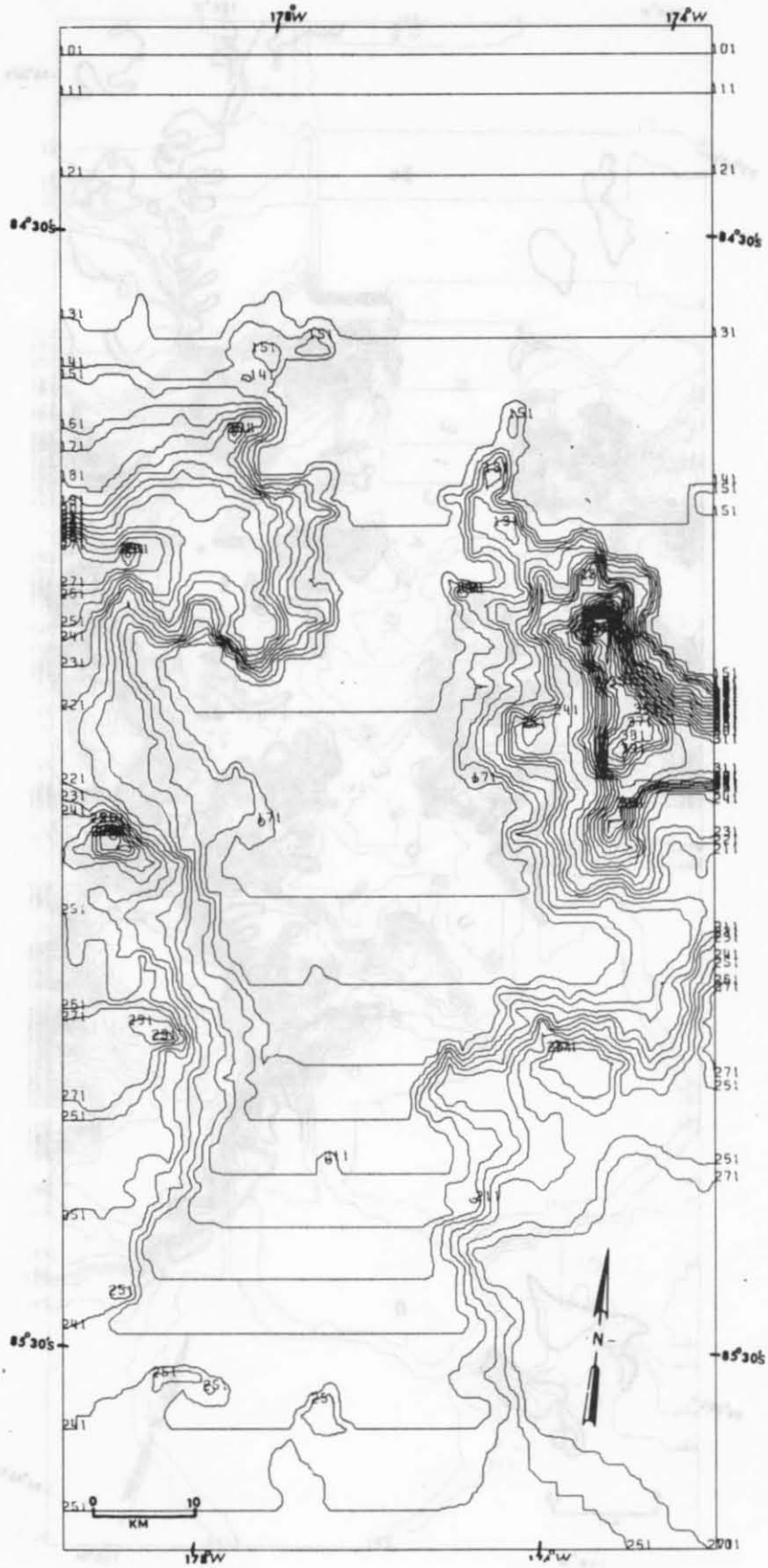

Figure 67. Amundsen Glacier area during Shackleton Glaciation.

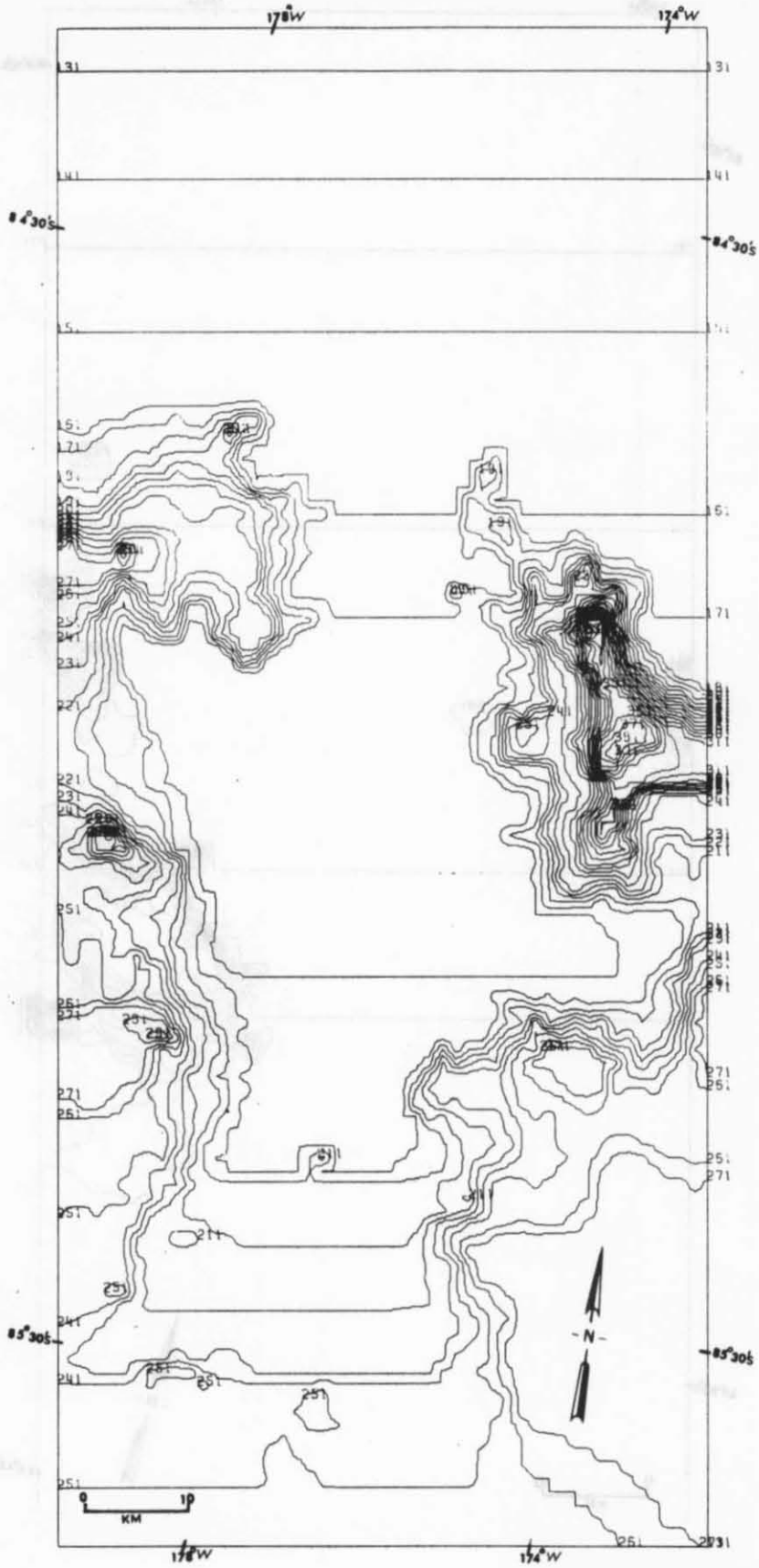

Figure 68. Amundsen Glacier area during Scott Glaciation.

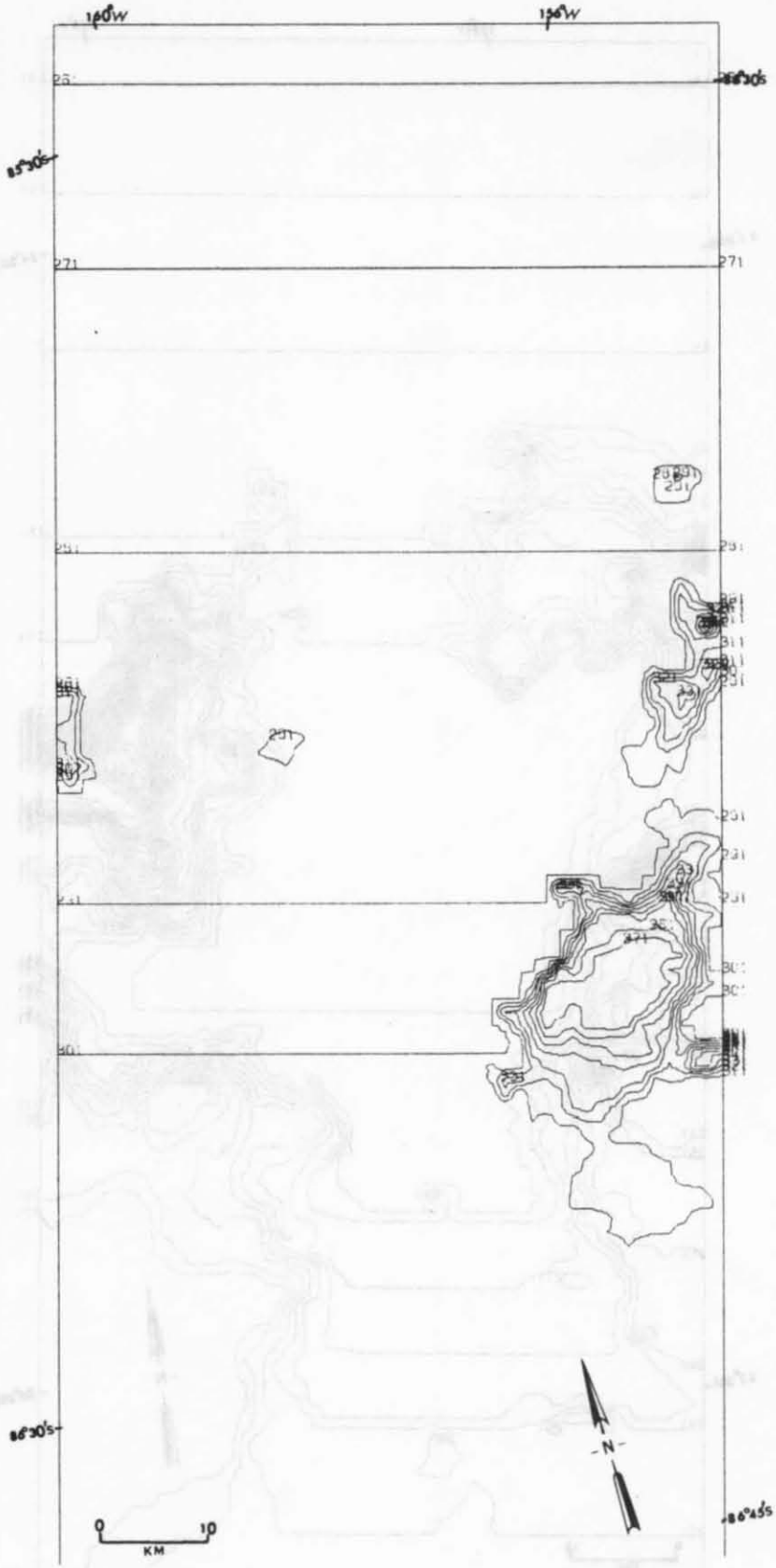

Figure 69. Amundsen Glacier area during Queen Maud Glaciation.

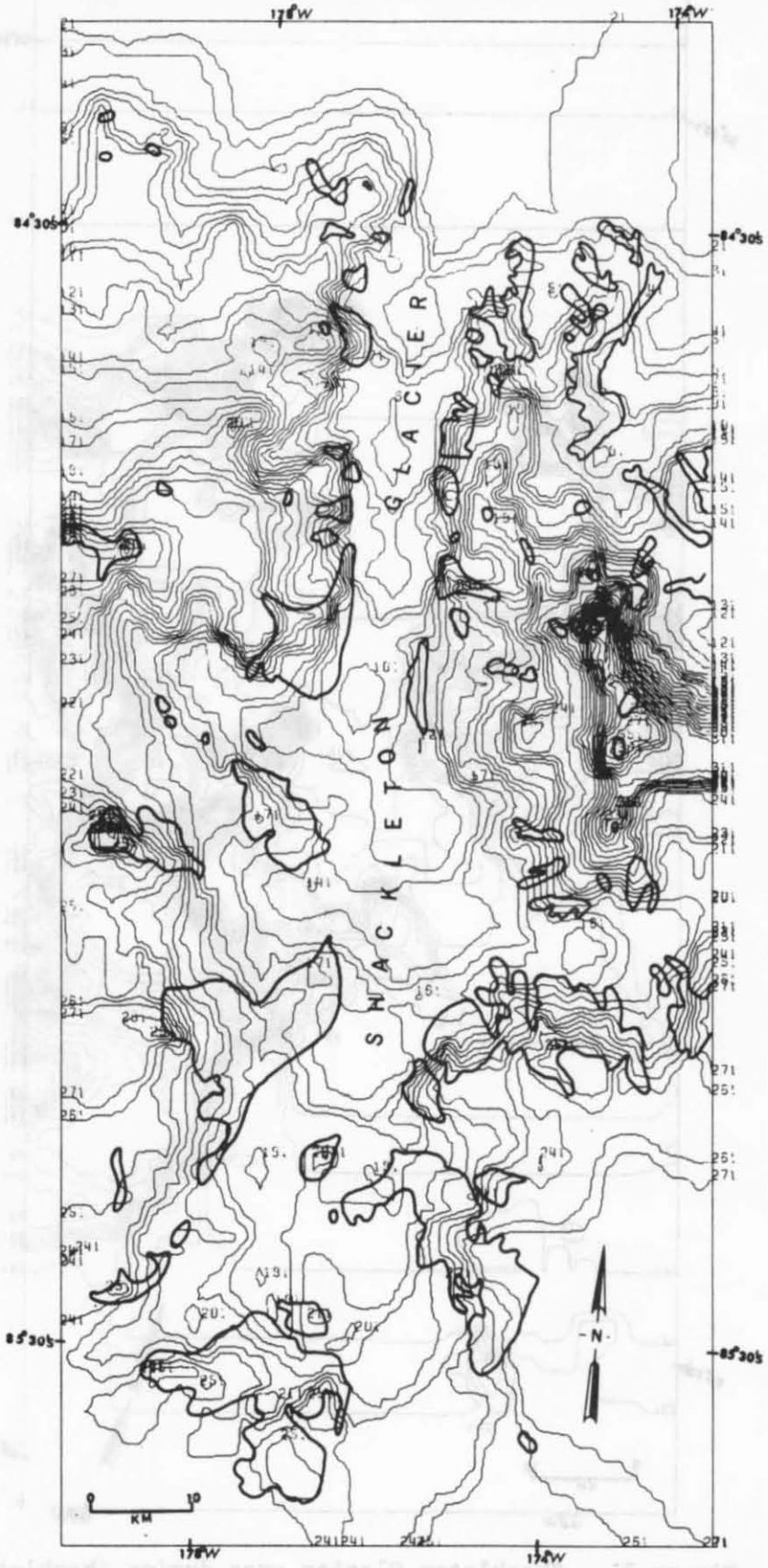

Figure 70. Shackleton Glacier area during Amundsen Glaciation.

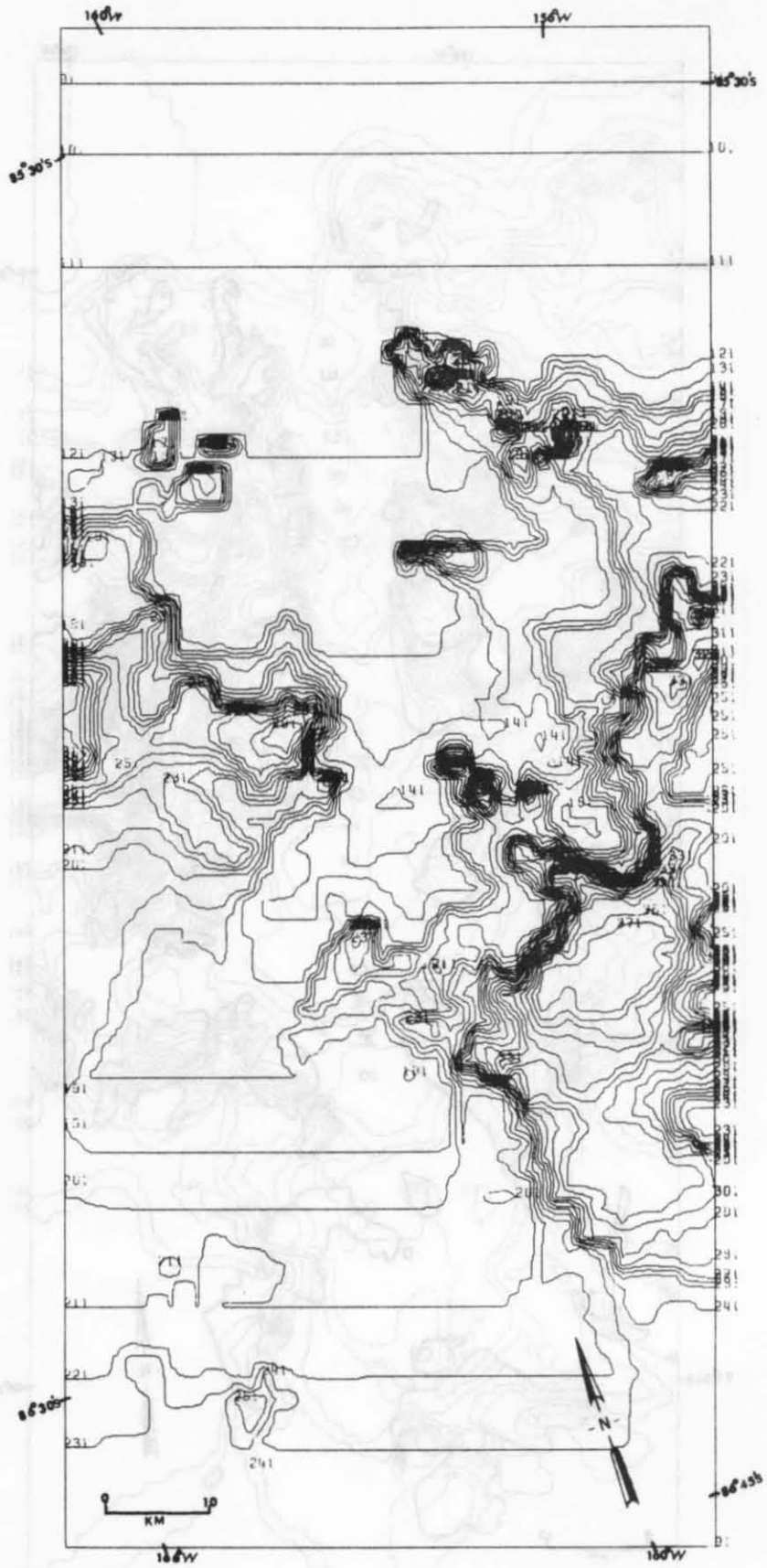

Figure 71. Shackleton Glacier area during Shackleton Glaciation.

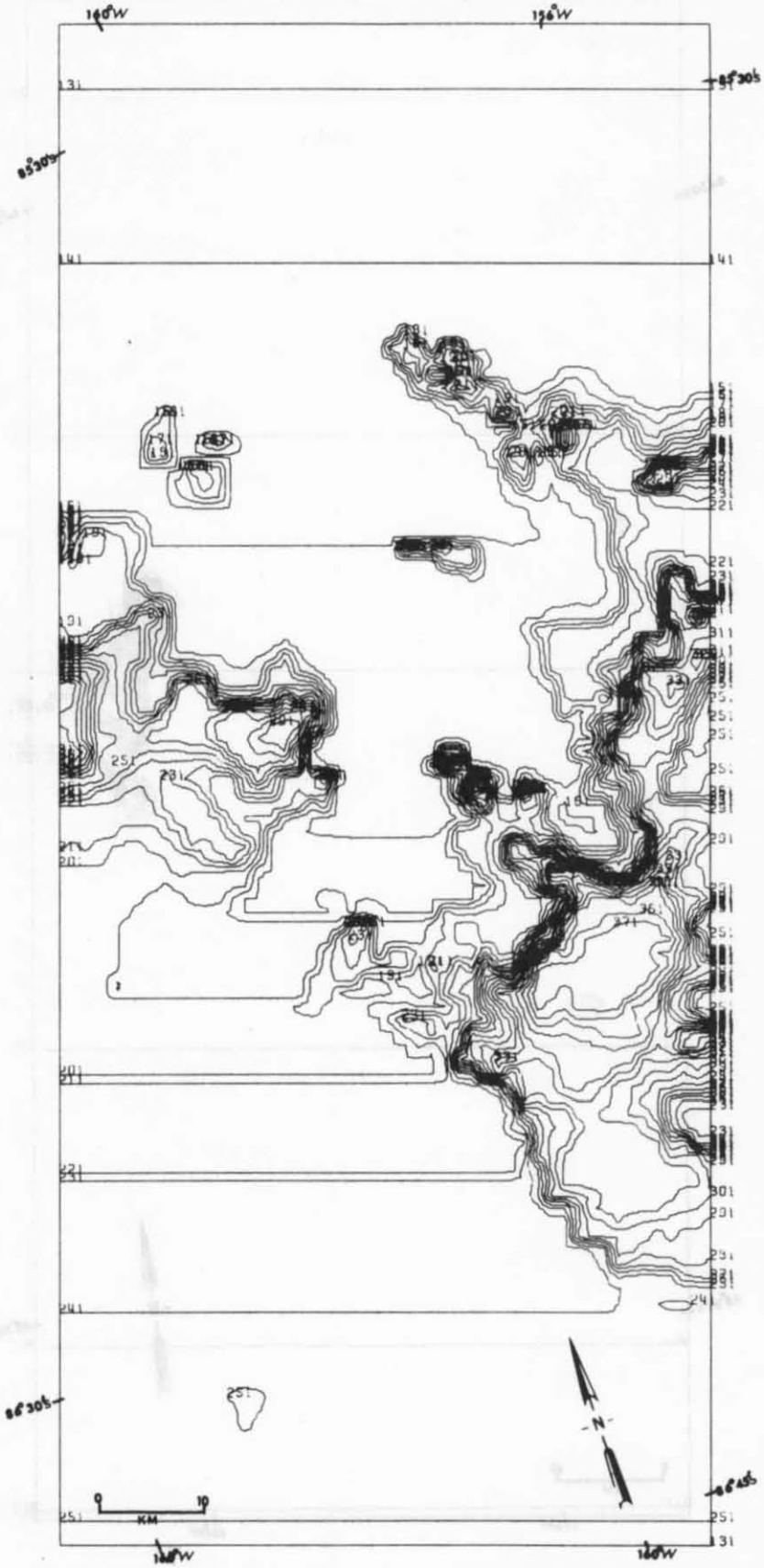

Figure 72. Shackleton Glacier area during Scott Glaciation.

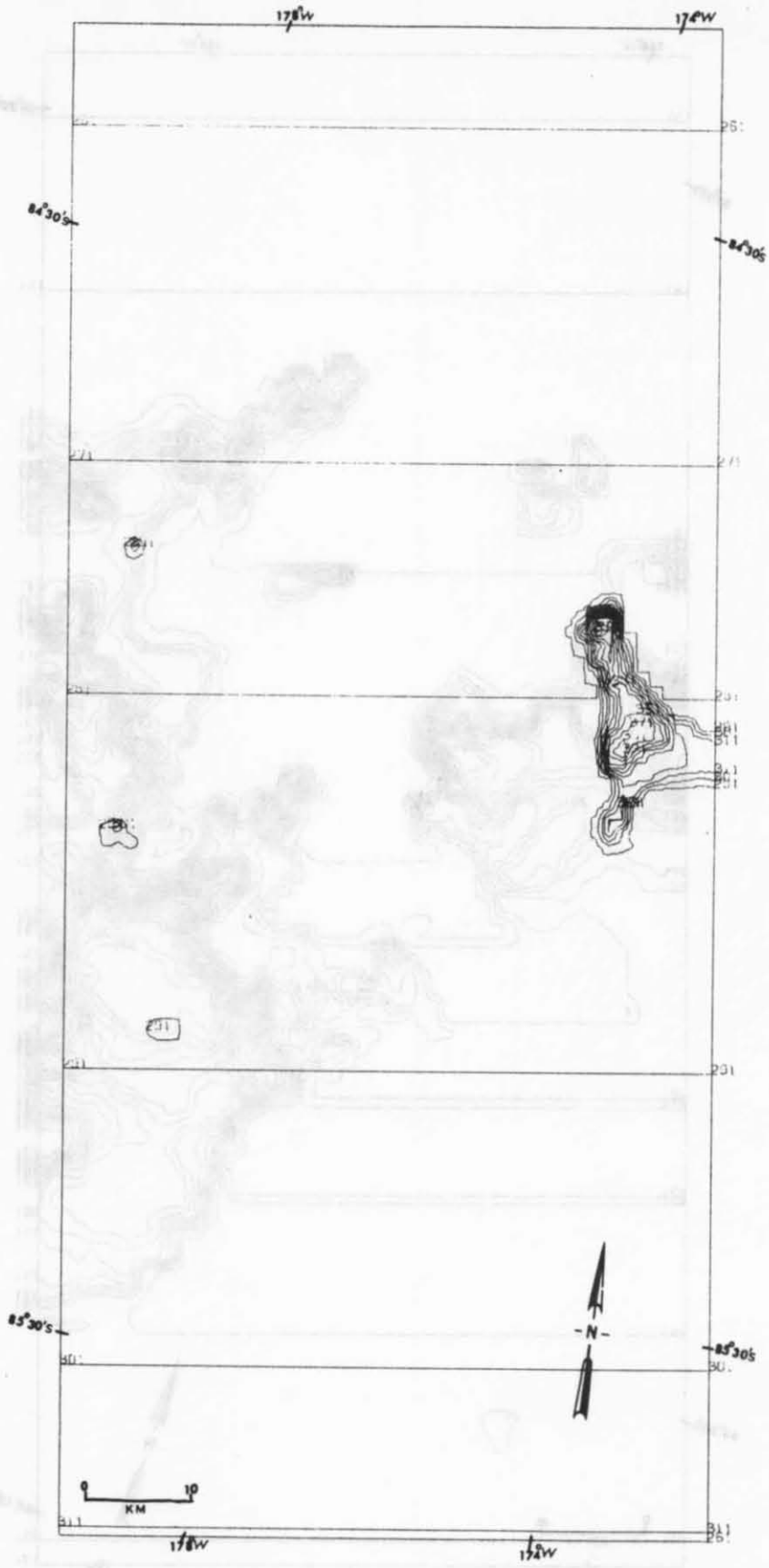

Figure 73. Shackleton Glacier area during Queen Maud Glaciation.

Table 17

Computer Developed Map Volumes Per Glaciation of Sample Outlet Glacier Area and Their Basins of Exudation

Locality	Area of Locality	Map Volume			
		Amundsen Glaciation	Shackleton Glaciation	Scott Glaciation	Queen Maud Glaciation
Scott Glacier Area	13,718.0 km^2	26,711.0 km^3	36,016.0 km^3	42,622.0 km^3	75,326.0 km^3
Amundsen Glacier Area	9,175.0	18,013.0	25,803.0	30,491.0	50,738.0
Shackleton Glacier Area	9,175.0	18,497.0	26,855.0	29,765.0	50,123.0

Table 18

Map Volumes Per Glaciation of Outlet Glaciers and Their Basins of Exudation in the Ross Ice Shelf Drainage System

Glaciation	*Map volume	Increase in ice volume compared to Amundsen Glaciation
Amundsen	386,130.0 km^3	
Shackleton	544,820.0	158,690.0 km^3
Scott	630,548.0	244,418.0
Queen Maud	1,074,210.0	688,080.0

*based on a map area of 194,830.0 km^2

Table 19

Ross Ice Shelf Area Ice Volumes Per Glaciation

Glaciation	*Area of grounded ice shelf	Average thickness of grounded ice above sea level	Volume of grounded ice
Shackleton	180,000.0 km^2	478.5 m	86,130.0 km^3
Scott	264,000.0	669.0	176,616.0
Queen Maud	820,000.0	1,624.0	1,331,680.0

*based on a present Ross Ice Shelf area of 490,000 km^2 (after Thiel, 1962)

The confluence of the grounding points determined from the Queen Maud Glaciation from the ice surface profiles related to the Ross Ice Shelf extension of the outlet glaciers of the Queen Maud Mountains indicates that the entire area of the present Ross Ice Shelf was filled with grounded ice during the Queen Maud Glaciation. Thus, the grounding line for the Queen Maud Glaciation is extended seaward of the present terminus of the Ross Ice Shelf and is thus determined from evidence further northwestward such as southern Victoria Land (i.e. Taylor, Wright, and Victoria Valleys).

The average thickness of grounded ice above sea level for each glaciation is computed from the extension of the ice surface profiles into the present Ross Ice Shelf area (Fig. 61). Grounded ice below sea level is not considered in these volume computations because it has a minimal effect in changing sea level.

Ice sheet volume changes

The ice volume increases related to former glaciations in the East Antarctic ice sheet portion of the Ross Ice Shelf drainage system (Table 20) are computed by multiplying the average increase in ice thickness per glaciation, relative to the present ice surface, by the area of this section of the ice sheet. The average increase in thickness is obtained from the elliptical ice surface profiles developed over the ice sheet (Fig. 61).

Ice volume changes for the Ross Ice Shelf drainage system and the Ross Ice Shelf are extrapolated over the present area of Antarctic grounded ice and ice shelves, respectively, yielding ice volume increases per glaciation for the former cover of Antarctic grounded ice (Table 21). This assumes that the glaciations in the Transantarctic Mountains which were used to determine ice volume changes throughout the Ross Ice Shelf drainage system and the Ross Ice Shelf also mark the major glacial events which affected the entire continent of Antarctica.

The amount of ice lost since the Queen Maud Glaciation, over the entire Antarctic continent, is approximately 19×10^6 cubic kilometers. This amount is larger than the values assumed for loss of ice since the glacial maximum in Antarctica determined by Suyetova (1970) of 1.65×10^6 cubic kilometers and Voronov (1965) of 12.0×10^6 cubic kilometers. In the latter cases, estimates of former ice volumes were based only on the development of one profile for a section of the continent extrapolated over the entire continent.

Interpretation of Glaciologic Reconstructions

Using the ice surface profiles developed for the ice shelf - outlet glacier - ice sheet continuum in the area of the Ross Ice Shelf drainage system and the Ross Ice Shelf allows the glaciologic reconstruction of the major glaciations affecting this area since the mid to late Pliocene.

Table 20

Ice Volume Increase Per Glaciation of the East Antarctic Ice Sheet Portion of the Ross Ice Shelf Drainage System

Glaciation	Average increase in ice thickness	*Ice volume increase compared to Amundsen Glaciation
Shackleton	92.5 m	144,670.0 km^3
Scott	192.1	300,444.0
Queen Maud	600.1	938,556.0

*based on a Ross Ice Shelf drainage system area of 1,750,000.0 km^2

(after Giovinetto & Robinson, 1962) minus outlet glacier and basin of exudation area.

Table 21

Composite Ice Volume Increases Per Glaciation

	Ice volume increase compared to Amundsen Glaciation		
	Shackleton Glaciation	Scott Glaciation	Queen Maud Glaciation
Ross Ice Shelf drainage system including	303,360.0 km^3	544,862.0 km^3	1,626,636.0 km^3
Ross Ice Shelf	389,490.0	721,478.0	2,958,316.0
*Former Antarctic grounded ice	3,621,669.0	5,796,136.0	19,569,315.0
(water equivalent)	(3,255.433.0	(5,210,000.0)	(17,590,396.0)

*based on a present Antarctic grounded ice area of 12,090,000 km^2 and a present Antarctic ice shelf area of 1,380,000^2 (after Thiel, 1962)

The Queen Maud Glaciation

The Queen Maud Glaciation, more than 4.2 million years old, encompasses the climax of a thick polar ice sheet over Antarctica. Based on the minimum ice surface profiles developed for this glaciation, the following is known about its extent.

Grounding line

The minimum value of the isostatically corrected grounding line associated with the Queen Maud Glaciation (Fig. 53) extended as much as 225 km north of the present terminus of the Ross Ice Shelf and was well within the region of the submarine valleys of the Ross Sea bottom proposed as glacially sculptured by Taylor (1930), Zhivago (1962), Guilcher (1963) and Lepley (1964). This grounding line is determined from: (1) coalescence of the grounding points of ice draining East and West Antarctica, (2) the northwestern extension of the grounded ice related to the Queen Maud Glaciation in southern Victoria Land, and (3) extrapolation of the grounding line developed in the Ross Sea embayment to within 50 km of the non-embayed coastline surrounding the remainder of the continent. A 50 km limit to the grounding line in non-embayed areas is used because factors such as the open ocean and steep continental shelves in this area would tend to exert a dominant influence on the extent of grounded ice seaward of this limit. Grounded ice during the Queen Maud Glaciation filled all of the major present ice shelf areas and probably extended seaward to connect presently isolated near shore islands. This is similar to the situation in West Antarctica at present.

Area of present outlet glaciers and their basins of exudation

Computer simulated maps (Figs. 65, 69 and 73) of the non-isostatically corrected ice surfaces related to the Queen Maud Glaciation in the areas of the present Scott, Amundsen, and Shackleton Glaciers indicate the fairly complete inundation by ice of this area during this glaciation. These maps, here referred to as "paleo-ice" maps, indicate: (1) a moderately featureless ice surface with (2) sparse nunataks in areas which at present are among the best exposed ice-free areas on the continent.

The broadly spaced ice surface contours on these "paleo-ice" maps are apparently unaffected by the underlying Scott, Amundsen, and Shackleton valleys. These broad, fairly featureless contours are further substantiated by a plot of the directional indicators (Fig. 29) related to the Sirius Formation till member deposited in the latter stages of the Queen Maud Glaciation.

Ice volume ratios (Table 22) of the Queen Maud Glaciation, compared to the Amundsen glaciation determined from Table 15, indicate the

increase in ice volume in these computer simulated areas by approximately 2.8 times. The fairly uniform increase ranging from 2.79 to 2.82 per glacier implies the uniform advance of an ice mass from the interior inundating the present coastal mountains.

Table 22 Ratio of outlet glacier ice volumes

Locality	Glaciation		
	Amundsen/ Shackleton	Amundsen/ Scott	Amundsen/ Queen Maud
Scott Glacier area	1/1.35	1/1.60	1/2.82
Amundsen Glacier area	1/1.43	1/1.69	1/2.81
Shackleton Glacier	1/1.45	1/1.61	1/2.79

The nunatak areas during the Queen Maud Glaciation were located closer to the present coast than they are currently. This indicates that the ice sheet during the Queen Maud Glaciation extended much further seaward than at present. Areas at present which contain nunataks similar to the Queen Maud Glaciation topographic relation occur as much as 200 to 250 km inland from the coast, i.e. the Grosvenor Mountains and Mount Howe.

Ice sheet

During the Queen Maud Glaciation the present area of the East Antarctic ice sheet portion of the Ross Ice Shelf drainage system (Fig. 61) was as much as 850 m thicker in the Transantarctic Mountains. Further inland the ice sheet tapered to 325 m thicker than present at the present ice divide. The isostatically corrected ice sheet surface at the present ice divide area was within 210 m of its present elevation, although the present irregularities throughout the ice sheet (Fig. 53) were probably far less pronounced due to this thickening.

Antarctic ice flow patterns

The effect of a thicker ice mass over the area of the present ice sheet and outlet glaciers and the extension of the grounding line during the Queen Maud Glaciation undoubtedly had a marked effect on the flow pattern of the East and West Antarctic ice sheets. Whereas the present Antarctic ice sheet flow pattern (Fig. 74) is subdivided into drainage basins, the flow pattern during the Queen Maud Glaciation may have resembled a more centrally radiating ice dome (Fig. 75) with present ice shelf areas totally grounded. Although conjectural, this Queen Maud Glaciation flow pattern would cause ice flowlines in Marie Byrd Land to flow roughly perpendicular to their present course.

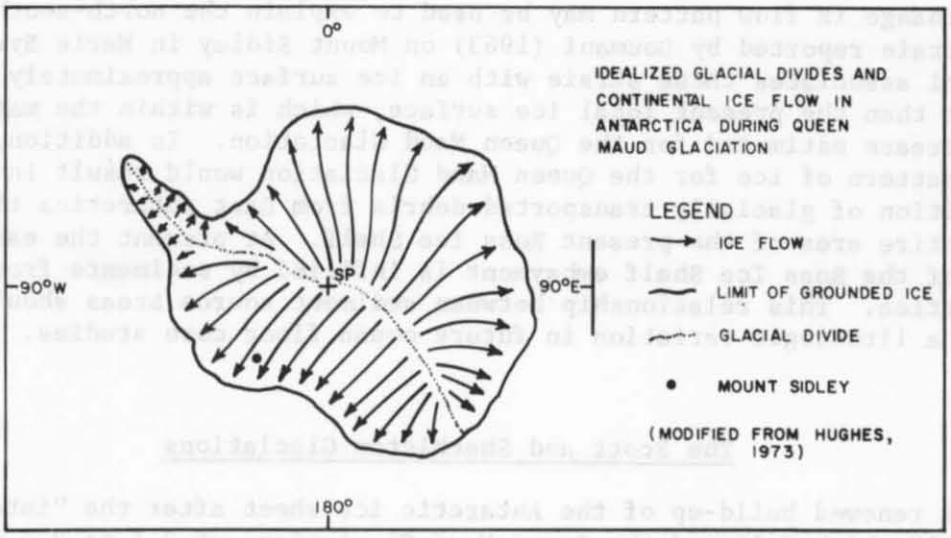

Figure 75. Flow pattern of Antarctic ice sheet during Queen Maud Glaciation.

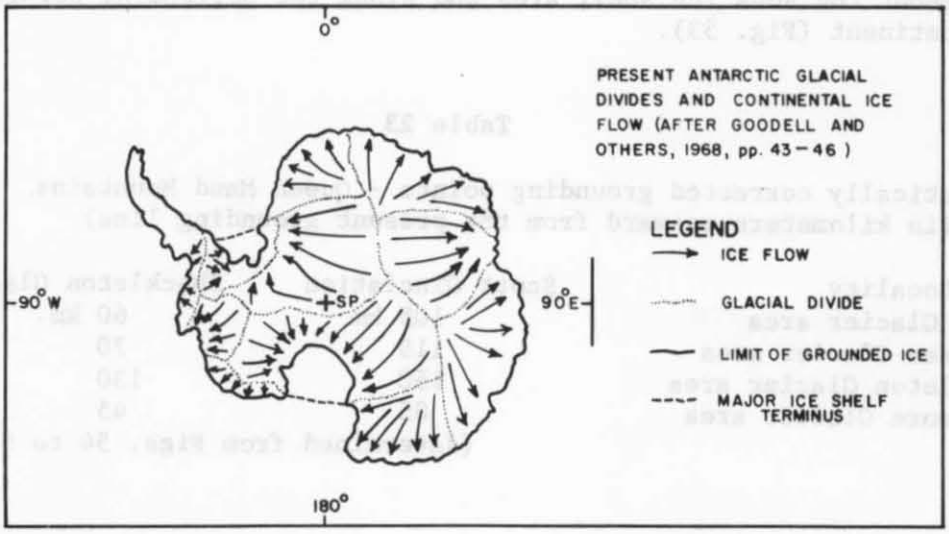

Figure 74. Flow pattern of present Antarctic ice sheet.

This change in flow pattern may be used to explain the north-south trending straie reported by Doumani (1963) on Mount Sidley in Marie Byrd Land. Doumani associates these straie with an ice surface approximately 500 m higher than the present local ice surface, which is within the magnitude of increase estimated for the Queen Maud Glaciation. In addition, the flow pattern of ice for the Queen Maud Glaciation would result in the deposition of glacially transported debris from East Antarctica throughout the entire area of the present Ross Ice Shelf. At present the eastern part of the Ross Ice Shelf embayment is infilled by sediments from West Antarctica. This relationship between sediment source areas should show up as a lithologic variation in future ocean floor core studies.

The Scott and Shackleton Glaciations

A renewed build-up of the Antarctic ice sheet after the "interglacial" which followed the Queen Maud Glaciation, at 2.1 to 2.4 million years ago, produced the Scott Glaciation. Following the retreat of the Scott Glaciation ice surface, a renewed build-up of the Antarctic ice sheet at somewhere between 1.6 m.y. to 49,000 years ago produced the Shackleton Glaciation. These two glaciations are treated together because they are quite similar in terms of glaciologic reconstruction except for the slightly greater extent of the Scott Glaciation.

Grounding lines

Average values of the isostatically corrected grounding points for glaciers in the Queen Maud Mountains (Table 23) and those in southern Victoria Land (Table 24) have been used to extrapolate grounding lines throughout the Ross Ice Shelf area and along the peripheral portions of the continent (Fig. 53).

Table 23

Isostatically corrected grounding points - Queen Maud Mountains
(in kilometers seaward from the present grounding line)

Locality	Scott Glaciation	Shackleton Glaciation
Scott Glacier area	105 km	60 km
Amundsen Glacier area	115	70
Shackleton Glacier area	150	130
Beardmore Glacier area	85	45

(determined from Figs. 54 to 57)

Table 24

Isostatically corrected grounded points - southern Victoria Land
(in kilometers seaward from the present coastline)

Locality	Scott Glaciation	Shackleton Glaciation
Taylor Valley	50 km	20 km
Wright Valley	60	35
Victoria Valley	35	25

(determined from Figs. 58 to 60)

The grounding lines of the Scott and Shackleton Glaciations are extremely similar in form with the only difference being the greater extent of the Scott Glaciation grounding line. Referring to Table 23, the seaward extent of the grounding points for both the Scott and Shackleton Glaciations can be seen to be a function of the size of the glacier, as is the case today. The greater the areal dimensions of the glacier, the less farther seaward it grounds. In order of decreasing size these glaciers are: Beardmore, Scott, Amundsen, and Shackleton. From this it can be concluded that a broad inland ice mass was being drained by these glaciers at the time of the Scott and Shackleton Glaciations. Smaller glaciers funnelled their drainage farther seaward. In addition, or by coincidence, the lowest value for distance seaward of a grounding point occurs at the most northwestern glacier, the Beardmore Glacier, well out of the restricted apex of the Ross Sea embayment.

Grounding points for the seaward extension of glaciers exiting through southern Victoria Land (Table 24) are remarkably consistent for each glaciation with the exception of the northernmost plot for the glacier exiting from Victoria Valley during the Scott Glaciation. Ice that invaded Taylor and Wright Valley was aided in its grounding by anchoring to Ross Island, whereas ice entering Victoria Valley glaciers was too far north of Ross Island (Fig. 53).

Area of present outlet glaciers and their basins of exudation

Non-isostatically corrected paleo-ice maps for the Scott (Figs. 64, 68 and 72) and Shackleton (Figs. 63, 67, and 71) Glaciations in the Scott, Amundsen, and Shackleton Glacier areas demonstrate the progressive uncovering despite readvances of the coastal portion of the Transantarctic Mountains. The Scott, Amundsen, and Shackleton valleys contained noticeably large outlet glaciers during these glaciations. Ice volume ratios (Table 22) determined from these paleo-ice maps compared to the Amundsen Glaciation result in increases in ice volume in these areas for the Scott Glaciation (approximately 1.60 to 1.69 times) and for the Shackleton Glaciation (approximately 1.35 to 1.45 times). The uniform ice volume ratios of the Queen Maud,

Scott, and Shackleton Glaciations, differing by no more than 0.10 from maximum to minimum outlet glacier ice volume ratio for each glaciation, indicate a broad and uniformly draining inland ice source during each of these glaciations. If the differences between the maximum and minimum outlet glacier ice volume ratios per glaciation (Table 25) are examined, the following can be determined in terms of the greatest ice volume per locality per glaciation:

Table 25 Ice volume maximum per glaciation per locality

Glaciation	Locality of greatest ice mass
Queen Maud	Scott Glacier area
Scott	Amundsen Glacier area
Shackleton	Shackleton Glacier area

This ice volume distribution implies a northward migration of the inland ice center or dome with decreasing ice volume over the continent. At present, the highest surface contour (4000 m contour, Fig. 53) lies close to the center of East Antarctica, or the Pole of Inaccessibility. Previous more extensive grounding would have increased the area of grounded ice and would have reoriented the center of the grounded ice sheet closer to the area of the present South Pole.

Ice sheet

Ice thicknesses over the present East Antarctic ice sheet portion of the Ross Ice Shelf drainage system (Fig. 61) during the Scott and Shackleton Glaciations were a maximum of 300 and 150 m thicker, respectively, than at present. The non-isostatically corrected elevation of ice at the ice divide by elliptical surface projection was less than 100 m higher than at present during both glaciations.

The Amundsen Glaciation

The present ice surface in the Ross Ice Shelf drainage system and the Ross Ice Shelf is related to the Amundsen Glaciation. This glaciation began less than 9490 years ago as a readvance following the retreat of glaciers during the Shackleton Glaciation. In the Queen Maud Mountains glacial deposits up to 20 m above present ice level mark the highest ice surface related to the Amundsen Glaciation. Marked by minor readvances the Amundsen Glaciation throughout the Transantarctic Mountains is now generally in a state of retreat.

Grounding line

The grounding line related to the Amundsen Glaciation forms the present coastline of Antarctica and coincides with the present coastal extent of the Transantarctic Mountains. Southward thickening of the

Ross Ice Shelf (Fig. 53) is demonstrated in Figures 60 to 54 along the coast of the Beardmore to Scott Glaciers. This thickening eventually coincides with the grounded West Antarctic ice sheet.

Area of present outlet glaciers and their basins of exudation

The computerized paleo-ice maps of the Scott, Amundsen, and Shackleton Glacier areas (Figs. 62, 66 and 70) show numerous tributaries joining these main outlet glaciers demonstrating the increasing importance of the local bedrock topography of the Transantarctic Mountains in diverting ice flow. Taylor, Wright, and Victoria Valleys (Figs. 58 to 60) presently form an ice-free depression encircled by the ice sheet to the west and the ice shelf and piedmont glaciers to the east. During previous glaciations the bedrock thresholds to the west were surmounted allowing the invasion of the East Antarctic ice sheet. While the ice sheet grew the piedmont glaciers expanded into the valleys from the east with the possible exception of the Taylor Valley area. An elevated beach at Marble Point on the southern Victoria Land coast near the eastern end of Wright Valley marks an isostatic rise of 16 m in the last 4,450 ± 150 years (Nichols, 1968), recording the most recent retreat of the Amundsen Glaciation along the coast.

Ice sheet

With time local bedrock topography has had an ever-increasing effect on the formation of the localized ice sheet. Studies by John (1972) in the South Shetland Islands to the north of West Antarctica indicate a more complicated recent glacial history than has been recorded in the Transantarctic Mountains of East Antarctica. East Antarctica, with only four major glaciations recorded since the mid to late Pliocene, appears to respond only to long-term and/or major causes of glacial fluctuation. The present disintegration of the West Antarctic ice sheet (Hughes, 1971) requires careful study because it may act as a small-scale example of the East Antarctic ice recession since the Queen Maud Glaciation and as an indication of the future of the East Antarctic ice sheet.

Effect of Antarctic Glaciations on Worldwide Sea Level

Using the water equivalent (21.36×10^6 cubic centimeters) and the corresponding sea level lowering capability (59 meters) of the present Antarctic ice sheet determined by Thiel (1962), the water equivalents noted in Table 21 of the former Antarctic glaciations can be used to determine their sea level lowering capability (Table 26).

Table 26

Sea level lowering capability of Antarctic glaciations

Glaciation	Sea level lowering capability	depth below present sea level
Queen Maud	108 m	49 m
Scott	73	14
Shackleton	68	9
Amundsen	59*	0

*(after Thiel, 1962)

Evidence of Tertiary sea levels is quite limited. Tanner (1968) estimates that during the Miocene to the Pliocene sea level was lowered 75 m, 68 m of which were glacio-eustatic. Tertiary sea-level information is far too limited to determine the effect of Antarctic glaciations on worldwide sea level lowering at this time. The results of Donn and others (1962), however, concerning Pleistocene sea level lowering give some implication of sea level lowering during "high" glacial times. They estimate a 137 to 160 m maximum sea level lowering during the Pleistocene and note the occurrence of worldwide submarine terraces at 142 to 154 m depth which date in excess of 30,000 years. The 49 m sea level depression beneath present sea level produced by the Queen Maud Glaciation is roughly one-third this estimated Pleistocene sea level depression. The Antarctic ice mass, therefore, was an extremely major glacio-eustatic factor during the Tertiary, based on the Pleistocene analogy.

Dates for the initiation of glaciation and for the maximum glaciation in the Northern Hemisphere and Antarctica are not synchronous. The oldest recorded date for the initiation of glaciation in the Northern Hemisphere is 3 million years (Berggren, 1970). The oldest recorded date for Antarctica is Eocene (Geitzenauer and others, 1968; Rex and Margolis, 1969). The maximum glaciation in Antarctica, or the Queen Maud Glaciation, ended prior to 4.2 million years ago. This glaciation pre-dates the earliest recorded initiation of Northern Hemisphere glaciation. Thus, prior to the initiation of Northern Hemisphere glaciation, the Antarctic ice mass had a marked effect on worldwide sea level. As sea level rose during the "interglacial" following the Queen Maud Glaciation the earliest record of Northern Hemisphere glaciation appears. This may imply that Antarctica has had and may still have a very major role in affecting the presence or absence of Northern Hemisphere glaciation.

SUMMARY OF THE GLACIAL HISTORY OF THE TRANSANTARCTIC MOUNTAINS

The Queen Maud Glaciation --more than 4.2 million years ago

Although glaciation in the Antarctic may have been initiated in the high mountain areas of the continent, the oldest Tertiary glacial deposits in the Transantarctic Mountains record a glaciation involving a thick, polar ice sheet, the Queen Maud Glaciation. This ice sheet had a volume of grounded ice approximately 1.8 times the present volume of grounded ice in Antarctica. It had a grounding line in the Ross Sea area which extended as much as 225 km north of the present terminus of the Ross Ice Shelf. The Transantarctic Mountains were inundated by this ice sheet, leaving only scattered nunataks. The area of the present East Antarctic ice sheet ice divide was up to 350 m higher at this time. The ice sheet related to this glaciation was thick enough to cause radiating ice flow throughout the entire continent from an ice dome centered approximately at the present South Pole. The local ice summit near the present South Pole (Fig. 53) may in fact be a remnant of this former more extensive ice dome.

In the Transantarctic Mountains basal melting in this ice sheet resulted in grooved and sculptured surfaces overlain by a deposit called the Sirius Formation. This deposit, correlated from the Queen Maud Mountains to southern Victoria Land, is composed of two members: (1) a till member composed primarily of lodgement till resulting from subglacial deposition overlain by (2) a stratified member composed primarily of ice-contact deposits. Both were deposited in the latter stages of the Queen Maud Glaciation.

'Interglacial' --more than 4.2 million years ago

A marked decrease in the volume of Antarctic ice followed the Queen Maud Glaciation. The ice cover at this time may have been similar to or less than the present Antarctic ice cover. An ameliorated climate during this interglacial caused the formation of: (1) drainage channels dissecting the Sirius Formation and (2) drainage channels at elevations between the level of the Queen Maud Glaciation ice surface and ice surfaces related to younger and lower level glaciations. During this time the removal of the portion of the Antarctic ice sheet covering Wright Valley allowed the entry of marine waters from McMurdo Sound and converted the valley into a fjord. This event is probably a correlative of the Pecten Marine Invasion (Webb, 1972; McSaveney and McSaveney, 1972) and sets the maximum date for the cessation of the Queen Maud Glaciation.

Scott Glaciation --2.1 to 2.4 million years ago

A renewed thickening of the Antarctic ice sheet following the interglacial dated by the Pecten Marine Invasion was accompanied by an increase in the volume, compared to the present Antarctic ice sheet, of approximately 1.25 times. The grounding line in the area of the present Ross Ice Shelf extended up to 150 km seaward of the present grounding line off the coast of the Queen Maud Mountains and up to 60 km seaward from the present coast of southern Victoria Land. The ice sheet in the area of the Transantarctic Mountains was funnelled into outlet glaciers and the ice thickness at the site of the present East Antarctic ice sheet ice divide was roughly equivalent to its present thickness. The center of the Antarctic ice sheet was located slightly north of the present South Pole along the 140° East Meridian.

Lateral moraines correlated from the Queen Maud Mountains (High Moraine) to southern Victoria Land mark the upper surface and retreat of the Scott Glaciation. The deposits comprising these lateral moraines are characterized by: (1) subdued morphology, (2) thickness ranging from 2 m to scattered erratics, (3) surficial clasts composed of only resistant lithologies (i.e. fine- to medium-grained dolerite) which are weathered to the ground and/or upstanding clasts which are cavernously hollowed and faceted, and (4) soils which contain: (a) an upper oxidized zone, (b) slight increases in clay and silt with depth, (c) increased salt content compared to younger morainic soils, and (d) a slight decrease in pH compared to younger morainic soils.

Semi-stratified deposits in the youngest portion of the High Moraine of the Scott Glaciation mark a moist period during the latter stages or at the end of this glaciation.

Shackleton Glaciation --less than 1.6 million years to 49,000 years ago

An increase in ice volume compared to the present East Antarctic ice sheet of 1.15 times accompanied the Shackleton Glaciation. This thickened the Antarctic ice sheet all over again producing a grounding line in the Ross Ice Shelf area up to 130 km seaward of the present coast of the Queen Maud Mountains. The grounding line extended up to 35 km seaward of the coast of southern Victoria Land. As during the Scott Glaciation, outlet glaciers funnelled through the Transantarctic Mountains, but the topographic influence of the subglacial valleys became more effective in diverting glacier flow during this glaciation. Although the thickness of the ice sheet at the ice divide remained the same as during the Scott Glaciation, the center of the ice sheet was situated still farther north along 140° East Meridian and closer to the center of the current East Antarctic ice sheet than during the previous glaciation.

Lateral moraines mark the surface of the Shackleton Glaciation in the Queen Maud Mountains (Middle Moraine) and in southern Victoria Land. These deposits are characterized by: (1) a slightly hummocky morphology including numerous recessional moraines, (2) a thickness of less than 2 m, (3) surficial clasts composed predominantly of resistant lithologies (i.e. similar to the High Moraine) and some less resistant granites, sandstones, shales, and siltstones with few if any clasts weathered to the ground and some limited cavernous hollowing and faceting, (4) soils which are ice-cemented at depth and contain lesser increases of clay and silt at depth than older soils, (5) soils with a slightly higher pH than older soils, and (6) soils with a decreased and oxidized zone compared to older soils.

Amundsen Glaciation --less than 9490 years ago

Although marked by a slight readvance, up to 20 m above the present ice surface in the Queen Maud Mountains, the Amundsen Glaciation coincides with the present configuration of the Antarctic ice sheet. Grounding lines of this glaciation form the present coastline of the Antarctic continent, outlet glaciers of the Transantarctic Mountains are at their lowest recorded level, and the Antarctic ice sheet is divided into several drainage basins.

Lateral moraines of the Amundsen Glaciation correlated from the Queen Maud Mountains (Low Moraine) to southern Victoria Land overlie and flank present ice surfaces and are composed of deposits which are: (1) extremely hummocky, (2) range in thickness up to 20 cm, (3) are underlain and cemented by a glacial ice core, (4) contain clasts which are angular and unweathered, and (5) lack any soil development.

APPENDIX A

Particle Size Distribution

APPENDIX A - Particle size distribution (physical disaggregation results) - Sirius Formation Sample

Sample Number	Location of Section	Position in Section (meters down from top)	(Member)	% of Total Sample		% of <2mm Fraction						
				(>4 mm) Pebble	(2-4 mm) Granule	(2-1 mm) Very Coarse Sand	(1-0.5 mm) Coarse Sand	(0.5-0.25 mm) Medium Sand	(0.25-0.125 mm) Fine Sand	(0.125-0.0625 mm) Very Fine Sand	(0.0625-0.002 mm) Total Silt	(<0.002 mm) Total Clay
24	Dominion	22	(t)	34.8	4.1	2.8	3.1	4.1	12.2	16.6	36.8	28.3
25	Range (B)	31	(t)	27.6	5.0	2.6	3.0	3.0	6.2	12.6	40.3	35.2
26		32	(t)	2.3	0.5	0.5	0.6	1.7	6.8	6.0	67.7	16.6
33	Otway Massif	0	(t)	12.5	10.5	14.1	13.1	12.7	9.8	4.8	23.8	21.3
42	Mt. Deaken	0	(t)	42.3	4.6	3.5	2.0	0.9	6.5	14.1	51.8	17.7
52A	Mt. Feather (A)	0	(t)	62.9	6.1	11.1	21.8	15.1	7.2	4.4	20.6	19.5
55	Mt. Feather (B)	17	(t)	11.3	5.9	11.6	17.9	21.4	13.5	7.1	13.1	17.3
59	Shapeless Mt.	0	(t)	13.8	2.7	2.1	3.1	5.7	10.9	18.9	38.6	26.3
61		0	(t)	6.2	5.0	6.1	12.2	13.8	12.4	14.3	22.3	25.5
61A		1	(t)	4.1	3.8	4.9	10.9	14.1	14.3	17.0	26.7	19.4
63	Carapace	0	(t)	30.8	3.5	3.1	6.2	8.1	9.1	7.9	33.2	32.1
75A	Coombs Hills (B)	0	(t)	5.5	6.0	6.6	6.4	9.9	11.4	7.5	28.1	31.1

(t) = till member
(s) = stratified member

APPENDIX A (continued) - Particle size distribution (thin section results) - Sirius Formation Samples

Sample Number	Location of Section	Position in Section (meters down from top)	(Member)	% of Total Sample								
				(>4 mm) Pebble	(2-4 mm) Granule	(2-1 mm) Very Coarse Sand	(1-0.5 mm) Coarse Sand	(0.5-0.25 mm) Medium Sand	(0.25-0.125 mm) Fine Sand	(0.125-0.0625 mm) Very Fine Sand	(0.0625-0.031 mm) Coarse Silt	(<.031 mm) Matrix
1	Bennett	5	(s)	0.0	0.0	1.4	2.9	10.5	7.6	5.7	8.1	64.0
3	Platform (A)	27	(t)	0.0	0.5	1.0	2.5	4.5	7.0	4.5	8.5	71.5
4		55	(t)	0.0	0.0	0.5	1.0	4.0	8.5	5.5	11.0	64.0
11A		84	(s)	0.5	1.0	0.5	1.0	2.0	4.0	8.5	5.0	72.5
12		100	(t)	0.0	0.5	0.5	1.6	4.0	7.5	6.5	8.0	72.5
13		110	(t)	0.0	0.0	0.0	6.0	9.0	13.0	8.0	9.0	55.0
14		125	(t)	0.0	0.0	1.0	3.5	6.0	5.5	6.0	10.5	67.5
17	Dominion	72	(t)	0.5	0.5	0.5	1.5	6.5	6.5	3.5	10.5	70.0
21	Range (A)	50	(t)	0.0	0.5	1.5	2.5	3.5	9.0	6.0	7.5	69.5
22		30	(t)	0.0	0.0	0.0	1.0	8.5	9.0	5.0	4.5	72.0
23		8	(t)	0.0	0.0	1.0	5.0	8.0	4.0	4.0	6.0	74.0
27	Dominion	41	(t)	0.0	0.0	0.0	1.0	4.0	8.0	12.0	9.0	66.0
29	Range (B)	66	(t)	0.0	0.0	0.0	0.0	3.0	4.0	12.0	1.0	80.0
35	Roberts Massif (A)	0	(t)	1.0	0.0	1.0	1.0	2.0	13.0	7.0	14.0	43.0
39	Mt. Wisting Area	0	(t)	0.0	0.0	1.0	3.0	13.0	9.0	10.0	7.0	57.0
32	Otway Massif	0	(t)	0.0	1.0	2.0	2.0	9.0	2.0	3.0	7.0	74.0
41	Mt. Deaken	0	(t)	2.0	0.0	1.0	2.0	4.0	3.0	8.0	10.0	71.0
42		0	(t)	0.0	2.0	1.0	0.0	5.0	10.0	21.0	21.0	40.0
43	Mt. Sirius	0	(t)	1.0	2.0	1.0	0.0	1.0	3.0	5.0	4.0	74.0

(t) = till member
(s) = stratified member

APPENDIX A (continued) - Particle size distribution (thin section results) - Sirius Formation Samples

Sample Number	Location of Section	Position in Section (meters down from top)	(Member)	% of Total Sample								
				(>4 mm) Pebble	(2-4 mm) Granule	(2-1 mm) Very Coarse Sand	(1-0.5 mm) Coarse Sand	(0.5-0.25 mm) Medium Sand	(0.25-0.125 mm) Fine Sand	(0.125-0.0625 mm) Very Fine Sand	(0.0625-0.031 mm) Coarse Silt	(<.031 mm) Matrix
44	Mt. Feather (A)	5	(t)	0.0	0.0	1.0	8.0	14.0	10.0	4.0	8.0	55.0
47		31	(t)	0.0	0.0	1.0	13.0	17.0	10.0	7.0	12.0	40.0
48		20	(t)	0.0	0.0	4.0	8.0	12.0	18.0	8.0	1.0	49.0
49		12	(t)	0.0	0.0	1.0	8.0	16.0	12.0	6.0	7.0	50.0
50		6	(t)	1.0	3.0	7.0	2.0	15.0	10.0	5.0	4.0	53.0
51		1	(t)	0.0	0.0	3.0	11.0	22.0	16.0	2.0	4.0	42.0
52		0	(t)	0.0	0.0	0.0	12.0	14.0	12.0	5.0	4.0	53.0
53	Mt. Feather (B)	21	(t)	0.0	2.0	3.0	8.0	22.0	12.0	8.0	8.0	37.0
54		19	(t)	0.0	1.0	5.0	6.0	14.0	16.0	3.0	14.0	41.0
55		17	(t)	0.0	0.0	3.0	3.0	26.0	12.0	2.0	3.0	51.0
59	Shapeless Mt.	0	(t)	0.0	0.0	1.0	2.0	7.0	10.0	14.0	5.0	61.0
62	Carapace Nunatak	0	(t)	0.0	0.0	0.0	3.0	10.0	6.0	2.0	3.0	76.0
66	Allan Nunatak	0	(t)	0.0	0.0	1.0	4.0	11.0	7.0	6.0	7.0	64.0
67	Coombs Hills (A)	0	(t)	0.0	0.0	0.0	7.0	26.0	11.0	2.0	3.0	51.0
69		29	(t)	0.0	0.0	1.0	4.0	12.0	10.0	8.0	1.0	64.0
73		47	(t)	0.0	1.0	0.0	1.0	20.0	10.0	7.0	4.0	57.0
74		70	(t)	0.0	0.0	1.0	4.0	19.0	16.0	3.0	4.0	53.0

(t) = till member
(s) = stratified member

Appendix A - Particle size distribution (physical disaggregation results)
Soil samples: High, Middle and Low Moraines

Sample Number	Collection Depth (cm)	% of Total Sample		% of < 2mm Fraction						
		(>4 mm) Pebble	(2-4 mm) Granule	(2-1 mm) Very Coarse Sand	(1-0.5 mm) Coarse Sand	(0.5-0.25 mm) Medium Sand	(0.25-0.125 mm) Fine Sand	(0.125-0.0625 mm) Very Fine Sand	(0.0625-0.002 mm) Total Silt	(<0.002 mm) Total Clay
Parent Material:		Beacon Sediments and Dolerite - Low Moraine								
80	0-4	41.4	16.1	23.3	12.2	8.4	6.5	2.6	20.3	25.6
81	0-3	15.9	14.1	11.0	18.6	15.1	8.6	5.1	16.4	24.9
82	0-4	12.6	10.6	9.7	14.8	17.3	14.0	7.6	12.7	24.2
83	0-4	18.2	7.8	8.4	8.4	9.4	9.6	8.3	30.5	25.3
84	0-3	4.3	5.8	9.7	20.5	26.9	11.4	5.4	10.3	17.1
85	0-4	17.4	2.7	13.5	24.6	17.1	12.5	7.6	12.5	14.0
86	0-5	33.4	14.2	25.6	21.9	13.0	7.0	2.8	14.1	14.7
87	0-4	33.2	9.1	7.0	9.4	9.4	8.4	6.1	34.6	24.2
88	0-6	54.7	5.7	6.0	5.1	10.2	12.0	10.1	34.9	24.7
89	0-8	58.8	2.4	1.9	0.9	0.3	0.5	1.5	66.1	27.8
90	0-5	60.2	21.0	41.3	11.5	4.2	1.9	0.3	17.4	22.8
Parent Material:		Beacon Sediments and Dolerite - Middle Moraine								
91	0-5	18.0	18.9	22.5	26.1	21.6	14.8	4.6	3.7	7.0
92	0-1	21.0	2.2	16.2	25.9	24.0	14.5	7.6	5.1	9.6
93	1-3	0.5	1.8	11.6	20.8	26.9	16.2	4.8	4.4	15.8
94	3-10	1.0	4.2	9.1	18.4	31.8	22.1	8.4	3.7	9.0
95	10-20	10.1	5.4	10.5	19.4	24.7	16.0	7.9	16.4	6.0
96	20-30	17.4	5.5	11.7	24.7	25.4	12.4	5.1	13.8	6.9
97	30-41	16.7	6.2	8.9	16.3	24.1	16.6	7.6	12.1	15.2

Appendix A - continued

Sample Number	Collection Depth (cm)	(>4 mm) Pebble	(2-4 mm) Granule	(2-1 mm) Very Coarse Sand	(1-0.5 mm) Coarse Sand	(0.5-0.25 mm) Medium Sand	(0.25-0.125 mm) Fine Sand	(0.125-0.0625 mm) Very Fine Sand	(0.0626-0.002 mm) Total Silt	(<0.002 mm) Total Clay
Parent Material:		Beacon Sediments and Dolerite - Middle Moraine - continued								
98	0-3	16.4	11.8	20.3	29.7	26.3	9.8	2.4	5.5	5.6
99	3-6	4.0	6.3	12.0	26.0	28.5	11.7	7.5	5.8	11.4
100	6-19	4.8	5.3	9.0	16.3	19.0	8.9	4.6	6.8	36.7
Parent Material:		Beacon Sediments and Dolerite - High Moraine								
101	0-5	35.5	10.5	12.2	8.6	8.9	10.8	7.9	25.1	25.6
102	0-2	49.4	4.8	5.4	3.9	5.0	9.2	9.8	44.7	19.8
103	2-5	21.0	15.6	18.6	14.3	12.7	11.9	5.6	16.7	18.8
104	5-13	38.0	11.4	13.7	11.0	10.4	8.5	5.3	24.9	25.8
105	13-20	52.2	10.8	13.4	7.9	6.8	6.0	2.9	33.2	27.8
106	20-30	46.1	15.4	18.2	8.8	5.6	4.0	2.3	29.0	31.3
107	30-40	43.3	19.6	23.8	11.0	6.4	4.3	1.7	24.6	26.7
108	40-50	59.2	14.1	20.5	9.5	5.3	3.7	1.2	29.2	29.2
109	50-60	58.6	14.8	16.1	6.6	3.7	2.6	1.0	33.1	35.7
110	60-70	50.8	18.1	23.3	9.0	4.6	3.1	1.0	26.8	40.0
111	1-3	15.4	9.3	11.3	13.1	25.2	16.1	6.9	13.1	15.2
112	3-9	10.7	9.2	6.9	11.7	16.9	11.6	6.0	11.3	36.2
113	9-20	4.9	8.5	13.1	15.1	19.2	13.5	7.8	14.5	18.2
114	20-30	37.5	8.7	16.3	13.4	10.5	6.2	3.4	22.6	25.9
115	30-65	27.4	6.7	9.0	7.4	6.9	8.5	7.4	32.8	26.1
116	1-2	19.9	2.3	5.5	8.1	9.4	10.2	8.9	25.7	33.0
117	2-7	10.0	4.7	9.8	15.2	19.0	11.8	7.3	27.1	10.5
118	7-18	11.6	11.5	11.5	12.3	13.8	8.4	4.2	19.0	29.2
119	18-29	10.4	8.5	11.7	25.0	25.6	9.6	3.4	15.2	8.6
120	0-2	61.4	7.2	12.4	16.2	9.9	6.2	6.1	20.9	29.4
121	2-5	19.8	10.8	8.7	10.4	11.2	10.8	4.7	24.0	26.8
122	5-10	18.1	4.7	4.1	6.3	7.4	9.5	10.2	33.5	30.1
123	10-20	30.8	6.4	6.0	8.5	7.9	10.8	17.4	28.8	28.5
124	20-30	22.6	6.4	5.2	6.1	5.8	7.9	8.8	34.1	32.0
125	30-40	21.3	4.2	3.9	2.7	2.9	7.6	10.0	36.8	36.8

Appendix A - continued

Sample Number	Collection Depth (cm)	(>4 mm) Pebble	(2-4 mm) Granule	(2-1 mm) Very Coarse Sand	(1-0.5 mm) Coarse Sand	(0.5-0.25 mm) Medium Sand	(0.25-0.125 mm) Fine Sand	(0.125-0.0625 mm) Very Fine Sand	(0.0625-0.002 mm) Total Silt	(<0.002 mm) Total Clay
Parent Material:		Metasediment with Granite and Dolerite - Low Moraine								
126	0-4	20.8	18.5	31.0	26.3	14.2	5.6	2.5	13.9	6.4
127	0-5	37.3	33.6	54.3	20.5	6.9	1.9	0.3	9.2	6.4
128	0-3	28.7	18.1	26.6	23.8	23.0	9.5	2.6	8.9	4.9
129	0-5	25.9	11.3	14.5	11.2	11.3	14.5	11.7	21.8	13.9
130	5-15	35.7	10.2	5.6	9.5	10.8	14.2	11.9	29.2	16.3
Parent Material:		Metasediment with Granite and Dolerite - Middle Moraine								
130	0-5	58.6	10.2	44.1	15.5	5.3	2.5	1.2	19.8	9.9
131	0-5	56.3	11.7	32.5	27.5	9.1	1.9	0.4	18.5	9.3
132	0-2	58.5	5.6	8.0	7.7	3.9	3.9	15.9	51.1	19.3
133	2-5	18.2	9.6	7.4	8.7	12.9	21.8	29.6	12.3	23.1
134	5-10	3.5	5.8	10.1	13.0	16.3	23.0	24.8	9.2	18.0
135	10-20	16.9	8.7	9.8	15.4	20.9	22.6	14.8	9.8	11.3
136	20-30	46.2	7.7	13.3	16.8	18.8	17.6	14.6	14.9	9.9
137	30-40	28.7	10.6	14.6	18.6	22.8	19.5	13.9	9.3	8.5
138	40-50	20.3	10.0	11.4	16.9	26.6	22.8	10.3	7.6	8.1
139	50-60	16.0	14.4	10.4	18.3	27.1	22.2	11.4	8.0	7.5
Parent Material:		Metasediment with Granite and Dolerite - High Moraine								
140	0-5	43.0	21.1	31.7	18.3	9.8	4.4	1.5	24.1	9.3
141	5-15	12.9	14.1	17.6	14.4	13.8	12.1	6.8	29.7	4.2
142	15-25	36.0	8.7	11.5	10.8	10.7	9.5	4.8	42.0	6.4
143	0-5	15.8	13.2	13.4	18.6	15.7	18.2	12.5	9.1	13.3

Appendix A - continued

Sample Number	Collection Depth (cm)	(>4 mm) Pebble	(2-4 mm) Granule	(2-1 mm) Very Coarse Sand	(1-0.5 mm) Coarse Sand	(0.5-0.25 mm) Medium Sand	(0.25-0.125 mm) Fine Sand	(0.125-0.0625 mm) Very Fine Sand	(0.0625-0.002 mm) Total Silt	(<0.002 mm) Total Clay
Parent Material:		Granite with Beacon and Dolerite - Low Moraine								
144	0-5	25.1	14.9	14.0	22.8	19.0	11.3	8.3	14.4	11.0
145	5-15	13.5	13.6	23.6	26.7	18.7	8.9	3.5	9.1	8.0
146	0-5	12.1	17.2	18.1	37.3	21.0	6.9	2.9	6.3	7.1
147	0-5	11.3	10.3	18.6	20.4	16.9	13.9	12.2	12.5	7.2
Parent Material:		Granite with Beacon and Dolerite - High Moraine								
148	0-2	36.1	0.1	15.3	15.0	8.3	5.6	4.7	21.6	28.1
149	2-10	8.6	15.9	27.2	24.3	12.5	7.4	5.0	12.3	11.2
150	10-20	31.2	10.4	11.3	16.2	12.1	9.7	5.4	27.3	14.1
151	20-30	10.9	17.1	29.1	21.2	11.3	7.0	5.0	16.7	9.9
152	30-40	34.0	18.6	19.2	21.8	10.0	5.3	3.8	18.2	21.2
153	40-50	47.8	14.4	28.2	17.7	6.9	2.9	1.4	21.2	20.4
154	50-60	29.9	19.4	34.3	21.9	8.3	3.5	2.0	22.8	6.5
155	60-70	42.9	20.6	20.9	23.3	11.3	5.9	2.6	23.1	11.4
156	70-80	15.6	17.1	30.6	26.7	13.8	6.3	4.1	13.1	5.5
Parent Material:		Dolerite - Low Moraine								
157	0-3	32.4	10.7	17.9	21.8	22.0	13.9	5.1	10.4	8.5
158	0-4	5.1	9.0	18.9	17.9	12.3	5.5	2.4	20.3	22.7
159	0-5	12.7	1.8	1.2	3.0	5.9	6.5	6.1	38.0	40.6
160	0-5	1.2	3.4	10.2	23.4	20.6	10.6	7.1	13.0	17.7
161	0-5	10.3	7.3	17.2	19.1	14.4	7.6	6.1	16.1	20.6

Appendix A - continued

Sample Number	Collection Depth (cm)	(>4 mm) Pebble	(2-4 mm) Granule	(2-1 mm) Very Coarse Sand	(1-0.5 mm) Coarse Sand	(0.5-0.25 mm) Medium Sand	(0.25-0.125 mm) Fine Sand	(0.125-0.0625 mm) Very Fine Sand	(0.0625-0.002 mm) Total Silt	(<0.002 mm) Total Clay
Parent Material:		Dolerite - High Moraine								
162	0-1	38.7	15.9	34.4	23.6	13.0	8.2	2.1	9.5	5.8
163	1-6	8.2	14.8	28.1	21.7	15.4	14.2	6.4	6.8	6.4
164	6-11	5.0	12.4	24.9	22.2	14.2	13.4	7.0	5.3	12.8
165	11-31	19.7	20.0	31.7	19.3	14.2	13.8	6.8	7.1	6.4
166	31-61	28.6	22.1	33.2	20.6	13.0	11.5	5.0	8.2	6.9

APPENDIX B

COMPUTER PROGRAMS

Combined use of the programs MAPPER, CONTUR and ICE LEVEL has allowed the development of the ice surface-bedrock topography maps used in this Report. These programs are written in FORTRAN IV level G for the IBM System 360. The MAPPER and CONTUR programs were made available to this author by the Ohio Department of Highways and are part of the Generalized Computer Assisted Roadway Selection System (GCARS) developed by Dr. A. Keith Turner of the Department of Civil Engineering at Purdue University (1972). Mr. Edward Janacek of the Ohio Department of Highways supervised the implementation of these programs and developed the program ICE LEVEL which interfaces with MAPPER and CONTUR and addresses itself to the adjustments in data required to simulate former ice surface topography.

In the following descriptions of these programs MAPPER and CONTUR are only briefly outlined based on the documentation available in the body of these programs and on the use of these programs in this text. The ICE LEVEL program is reproduced entirely and a description of it is incorporated in the program.

MAPPER

This program is capable of accepting either irregular or gridded data and implementing this data in the exercise of several subroutines.

Subroutine GRID interpolates a series of irregularly spaced three-dimensional data points and produces a gridded matrix by employing a weighted moving average.

Subroutine PRICON4 uses the gridded values developed in subroutine GRID or fed in directly as data in the preparation of contour maps on the printer. The maps are produced by linear interpolation within grid squares and can be displayed with any specified contour interval (maximum of 19 contour lines) and with alternate map displays, i.e. contour line may be printed, alternate contour bands may be printed, or all positions on the map may be printed. A frequency table accompanies each map and specifies percent area of the map within each contour interval.

Subroutine STATS provides statistical measures of the data arrays including: mean, variance, standard deviation, maximum and minimum values.

Subroutine HYPSO yields a measure of the relationship between area and altitude of each map equivalent to a hypsometric analysis (Strahler, 1952).

CONTUR

This program can produce a set of instructions for a CALCOMP plotter, yielding maps of different map scale and contour interval based on the gridded data used in the MAPPER program. These maps contain labeled titles and contour intervals.

```
C       ICE LEVEL PROGRAM
C       THIS PROGRAM IS DESIGNED TO PREPROCESS DATA DESTINED FOR THE
C       PLOTTER CONTOUR PROGRAMS MAPPER AND CONTUR.  THE PURPOSE IS TO
C       ALLOW ADJUSTING OF TERRAIN DATA TO REFLECT RISING ICE LEVELS.
C       THE EXISTING TERRAIN DATA IS IN THE FORM OF A RECTANGULAR GRID
C       OF N ROWS BY M COLUMNS, WHERE 1<N,M<101, WITH AN ELEVATION
C       VALUE AT EACH GRID INTERSECTION.
C       BY SPECIFYING TWO SETS OF (N,M) AND A SET OF SEARCH ELEVATION
C       LIMITS, THE PROGRAM WILL SCAN THE SPECIFIED GRID SUBSET, AND
C       WHENEVER AN ELEVATION WITHIN THE GRID SUBSET FALLS WITHIN THE
C       SEARCH LIMITS, IT IS REPLACED BY THE ICE LEVEL SPECIFIED.
C       IT IS THEREFORE POSSIBLE TO SIMULATE VARIOUS DIFFERENT ICE
C       LEVELS WITHIN A GRID SUBSET, AND TO DEVELOP CONTOUR MAPS OF
C       THE RESULTING SIMULATED TERRAIN.
C       AS MANY SUBSETS AS DESIRED MAY BE SELECTED FOR EACH RUN, AND
C       THEY MAY OVERLAP. THE ONLY RESTRICTION IS THAT EACH SUBSET
C       BE RECTANGULAR (AS IS THE CASE WHEN TWO SETS OF (N,M) ARE
C       GIVEN).
C       TO FACILITATE THE INTERFACE WITH MAPPER AND CONTOUR, THIS
C       PROGRAM HAS A DIRECT COPY FEATURE. IT WILL SIMPLY COPY
C       INPUT CARDS TO THE OUTPUT, UNLESS TOLD OTHERWISE. THIS
C       FEATURE ALLOWS CONTROL CARDS FOR MAPPER OR CONTUR TO BE
C       READ BY THE PROGRAM, AND IGNORED EXCEPT FOR BEING COPIED.
C       IN THIS WAY THE GRID OF DATA TO BE ALTERED MAY BE WITHIN
C       A GROUP OF CONTROL CARDS AND STILL BE PROCESSED.
C            THIS PROGRAM ONLY RECOGNIZES TWO CONTROL CARDS... *ARRAY,
C       SPECIFYING THAT AN ARRAY OF GRIDDED VALUES IS FORTHCOMING,
C       AND *ADJUST, SPECIFYING CHANGES TO THE GRID. ONLY ONE *ARRAY
C       CARD MUST APPEAR. THERE MAY BE ANY NUMBER OF ADJUST CARDS.
C            INPUT IS AS FOLLOWS....
C       (1) ANY NUMBER OF MAPPER OR CONTOUR CARDS WILL BE COPIED VERBATIM.
C       (2) COLS. 1-6 .... *ARRAY.
C       (3) COLS. 1-4 .... NO. OF ROWS, RIGHT JUSTIFIED.
C           COLS. 5-8 .... NO. OF COLS, RIGHT JUSTIFIED.
C       (4) COLS. 1-80  FORMAT OF ARRAY.
C       (5) ARRAY OR GRID, OF DATA... AS MANY CARDS AS NECESSARY.
C       (6) ADJUST CARDS, AS MANY AS DESIRED.
C         (A) COLS. 1-7 ... *ADJUST
C         (B) COLS. 1-4 ROW 1, RIGHT JUSTIFIED
C             COLS. 5-8 COL 1, RIGHT JUST
C             COLS. 9-12 ROW 2, RIGHT JUST
C             COLS. 13-16 COL 2, RIGHT JUST
C             COLS 21-30 LOW SEARCH ELEVATION, CODE DECIMAL POINT
C             COLS. 31-40 HIGH SEARCH ELEVATION, CODE DEC.PT.
C             COLS. 41-50 REPLACING ELEVATION, CODE DEC.PT.
C       (7) ANY NO. OF MAPPER OR CONTUR CONTROL CARDS....WILL
C           BE COPIED VERBATIM.
C       THIS PROGRAM PRINTS ON UNIT 6, READS ON UNIT 5, AND PUTS
C           OUTPUT CARDS ON UNIT 7.
        REAL ICELVL,MINLVL,MAXLVL
        INTEGER PRINTR, OUTPUT
        DIMENSION ARRAY (200,100),FMT(20),CARD(20)
        DATA ARR/'*ARR'/,ADJ/'*ADJ'/
        DATA INPUT/5/,PRINTR/6/,OUTPUT/7/
C
C       THIS IS WHERE THE COPY OPERATION TAKES PLACE
C
    5   READ(INPUT,100,END=999) CARD
        IF (CARD(1).EQ.ARR) GO TO 15
   10   WRITE (PRINTR,110) CARD
        WRITE (OUTPUT,100) CARD
        GO TO 5
```

```
C
C      THIS IS WHERE THE ARRAY IS READ
C
   15  READ (INPUT,120,END=999) NROWS,NCOLS
       READ (INPUT,100,END=999) FMT
       WRITE (PRINTR,130) NROWS,NCOLS,FMT
       DO 20 N=1, NROWS
       READ (INPUT,FMT,END=999) (ARRAY(N,M),M=1,NCOLS)
   20  WRITE(PRINTR,FMT)  (ARRAY(N,M),M=1,NCOLS)
C
C      THIS IS WHERE THE ADJUST CARDS ARE READ
C
   25  READ (INPUT,100,END=900) CARD
       IF(CARD(1).EQ.ADJ) GO TO 40
       WRITE(PRINTR,140)
       DO 30 N=1, NROWS
       WRITE (PRINTR,FMT) (ARRAY(N,M),M=1,NCOLS)
   30  WRITE (OUTPUT,FMT) (ARRAY(N,M),M=1,NCOLS)
       GO TO 10
   40  CONTINUE
C
C      THIS IS WHERE THE ADJUSTMENTS ARE READ AND PERFORMED
       READ (INPUT,150,END=900)NROW1,NCOL1,NROW2,NCOL2,
      X                        MINLVL,MAXLVL,ICELVL
       WRITE(PRINTR,160) NROW1,NCOL1,NROW2,NCOL2,MINLVL,MAXLVL,ICELVL
       DO 50 N=NROW1,NROW2
       DO 50 M=NCOL1,NCOL2
   50  IF(ARRAY(N,M).GE.MINLVL.AND.ARRAY(N,M).LE.MAXLVL)
     ?                  ARRAY(N,M)=ICELVL
       GO TO 25
  900  WRITE(PRINTR,140)
       DO 910 N-1,NROWS
       WRITE(PRINTR,FMT) (ARRAY(N,M),M=1,NCOLS)
  910  WRITE(OUTPUT,FMT) (ARRAY(N,M),M=1,NCOLS)
  999  STOP
  100  FORMAT (20A4)
  110  FORMAT (' ',20A4,10X,'COPIED VERBATIM')
  120  FORMAT (2I4)
  130  FORMAT (' ','THE INPUT GRID IS',I4,' ROWS BY',
     ?        I4,' COLUMNS,IN FORMAT ',20A4)
  140  FORMAT (' ','***** THE OUTPUT GRID FOLLOWS *****')
  150  FORMAT (4I4,4X,3F10.3)
  160  FORMAT (' ','SEARCH BETWEEN (ROW, COLUMN) (',I3,',',I3,') '.
     ?       'AND (ROW,COLUMN) (',I3,',',I3,') WITH SEARCH ',
     ?       '(MIN,MAX) (',F11.3,',',F11.3,')',/,
     ?        ' ',20X,'REPLACING ELEVATION IF SEARCH IS ',
     ?       'SATISFIED = ',F11.3)
       END
```

REFERENCES

Anderson, J.B. 1972. Nearshore glacial-marine deposition from modern sediments of the Weddell Sea. Nature Phys. Sci., v. 240, p. 189-192.

Barrett, P.J., 1969. Stratigraphy and petrology of the mainly fluviatile Permian and Triassic Beacon rocks, Beardmore Glacier area, Antarctica. Report 34, Institute of Polar Studies, The Ohio State University, Columbus, Ohio. 132 p.

Barrett, P.J., Elliot, D.H., Gunner, J. and Lindsay, J.F. 1968. Geology of the Beardmore Glacier area, Transantarctic Mountains. Ant. Jour. of the U.S., v. 3, no. 4, p. 102-106.

Barrett, P.J., Lindsay, J.F. and Gunner, J. 1970. Reconnaissance geologic map of the Mount Rabot Quadrangle, Transantarctic Mountains, Antarctica. U.S. Geological Survey Map No. 1.

Barrett, P.J., Grindley, G.W. and Webb, P.N. 1972. The Beacon Supergroup of east Antarctica (Review): in Adie, R.J., ed., Antarctic Geology and Geophysics, Universitetsforlaget, Oslo, p. 319-332.

Behling, R.E. 1971. Pedalogical development on moraines of the Meserve Glacier, Antarctica. (Unpub.) Ph.D. Dissertation, The Ohio State University, Columbus, Ohio. 216 p.

Behling, R.E. 1972. Calculated dates of selected glacial events in Wright Valley. Ant. Jour. of the U.S., v. 7, no. 6, p. 247-248.

Beitzel, J.E. 1971. Geophysical exploration in Queen Maud Land, Antarctica: in Crary, A.P., ed., Antarctic Snow and Ice Studies II, Ant. Res. Series v. 16. Amer. Geophys. Union, Washington, D.C., p. 39-88.

Bentley, C.R., Cameron, R.D., Bull, C., Kojima, K. and Gow, A.J. 1964. Physical characteristics of the Antarctic ice sheet: in Bushnell, V.C., ed., Ant. Map Folio Series, Folio 2, Amer. Geog. Soc.

Bentley, C.R. and Chang, Feng-Keng. 1971. Geophysical exploration in Marie Byrd Land, Antarctica: in Crary, A.P., ed., Antarctic Snow and Ice Studies II, Ant. Res. Series v. 16. Amer. Geophys. Union, Washington, D.C., p. 1-38.

Berggren, W.A. 1970. Late Pliocene-Pleistocene glaciation: in Davies, T.A., ed., Initial Reports of the Deep Sea Drilling Project, v. 12. Nat'l. Sci. Found., p. 953-963.

Black, C.A., Evans, D.D., White, J.L., Ensminger, L.E. and Clark, F.E. 1965. Methods of soil analysis: Part 1 and Part 2. Mono. no. 9, Am. Soc. Agron., Madison, Wisconsin. 1572 p.

Bull, C. 1971. Snow accumulation in Antarctica: in Quam, L., ed., Research in the Antarctic. Am. Assn. for the Adv. of Sci., Washington, D.C., p. 367-421.

Bull, C., McKelvey, B.C. and Webb, P.N. 1962. Quaternary glaciations in southern Victoria Land, Antarctica. Jour. of Glac., v. 4, no. 31, p. 63-78.

Calkin, P.E. 1964. Glacial geology of the Mount Gran area, southern Victoria Land, Antarctica. Geol. Soc. of Amer. Bull. 75, p. 1031-1036.

Calkin, P.E. 1971. Glacial geology of the Victoria Valley System, southern Victoria Land, Antarctica: in Crary, A.P., ed., Ant. Res. Series v. 16, Antarctic Snow and Ice Studies II. Amer. Geophys. Union, p. 363-411.

Calkin, P.E., Behling, R.E. and Bull, C. 1970. Glacial history of Wright Valley, southern Victoria Land, Antarctica. Ant. Jour. of the U.S., v. 5, no. 1, p. 22-28.

Claridge, G.G.C. and Campbell, I.B. 1968. Soils of the Shackleton Glacier region, Queen Maud Range, Antarctica. New Zealand Jour. of Sci., v. 11, no. 2, p. 171-218.

Crary, A.P. 1959. Oversnow traverses from I.G.Y. Little America Station. Nat'l. Acad. Sci., I.G.Y. Bull., no. 27, p. 11-15.

Crary, A.P., Robinson, E.S., Bennett, H.F. and Boyd, W.W. Jr. 1962. Glaciological regimen of the Ross Ice Shelf. Jour. Geophys. Res., v. 67, no. 7, p. 2791-2807.

Denton, G.H., Armstrong, R.L. and Stuiver, M. 1970. Late Cenozoic glaciation in Antarctica: The record in the McMurdo Sound Region. Ant. Jour. of the U.S., v. 5, no. 1, p. 15-22.

Denton, G.H., Armstrong, R.L. and Stuiver, M. 1971. The late Cenozoic glacial history of Antarctica: in Turekian, K.K., ed., The Late Cenozoic Glacial Ages, Yale University Press, New Haven, p. 267-306.

Donn, W.L., Farrand, W.R. and Ewing, M. 1962. Pleistocene ice volumes and sea-level lowering. Jour. of Geology, v. 70, no. 2, p. 206-214.

Doumani, G.A. 1963. Volcanics of the Executive Committee Range, Byrd Land. S.C.A.R. Proc., Cape Town, p. 666-675.

Doumani, G.A. and Minshew, V.H. 1965. General geology of the Mt. Weaver area, Queen Maud Mountains, Antarctica: in Hadley, J.B., ed., Ant. Res. Series v. 6, Geology and Paleontology of the Antarctic. Amer. Geophys. Union, p. 127-139.

Drewry, D.J. 1972. Subglacial morphology between the Transantarctic Mountains and the South Pole: in Adie, R.J., ed., Antarctic Geology and Geophysics, Universitetsforlaget, Oslo, p. 693-703.

Elliot, D.H. 1972. Aspects of Antarctic geology and drift reconstruction: in Adie, R.J., ed., Antarctic Geology and Geophysics, Universitetsforlaget, Oslo, p. 849-858.

Elliot, D., Barrett, P.J. and Mayewski, P.A. 1974. Reconnaissance geologic map of the Plunket Point Quadrangle, Transantarctic Mountains, Antarctica. U.S. Geological Survey Antarctic Map No. 4.

Everett, K.R. 1971. Soils of the Meserve Glacier area, Wright Valley, southern Victoria Land, Antarctica. Soil Science, v. 112, no. 6, p. 425-438.

Everett, K.R. and Behling, R.E. 1968. Chemical and physical characteristics of Meserve Glacier morainal soils, Wright Valley, Antarctica: on index of relative age?: in I.S.A.G.E. Symposium, Hanover, p. 459-460.

Ewing, M., Donn, W.L. and Farrand, W. 1960. Revised estimate of Pleistocene ice volume and sea-level lowering. Bull. Geol. Soc. of Amer., v. 71, no. 12, p. 1861.

Farrand, W.R. 1968. Postglacial isostatic rebound: in Fairbridge, R.W., ed., The Encyclopedia of Geomorphology, Rheinhold Book Corp., New York, p. 884-888.

Fleck, R.J., Jones, L.M. and Behling, R.E. 1972. K-Ar dates of the McMurdo volcanics and their relation to the glacial history of Wright Valley. Ant. Jour. of the U.S., v. 7, no. 6, p. 244-246.

Flint, R.F. 1971. Glacial and Quaternary Geology. John Wiley and Sons, Inc., New York, 892 p.

Folk, R.L. 1968. Petrology of Sedimentary Rocks. Hemphill's, Austin, 170 p.

Frakes, L.A. 1970. Marine geology of the Ross Sea (abstract), S.C.A.R. Proc., Oslo, p. 127.

Geitzenauer, K.R., Margolis, S.V. and Edwards, D.S. 1968. Evidence consistent with Eocene glaciation in a South Pacific deep sea sedimentary core. Earth and Planetary Sci. Letters, no. 4, p. 173-177.

German, R. 1968. Moraines: in Fairbridge, R.W., ed., The Encyclopedia of Geomorphology, Rheinhold Book Corp., New York, p. 710-717.

Giovinetto, M., Robinson, E.S. and Swithinbank, C.W.M. 1966. The regime of the western part of the Ross Ice Shelf drainage system. Jour. Glac., v. 6, no. 43, p. 55-68.

Goldthwait, R.P. 1971. Till--a Symposium. Ohio State University Press, Columbus, Ohio, 402 p.

Goodell, H.G., Watkins, N.D., Mather, T.T. and Koster, S. 1968. The Antarctic glacial history recorded in sediments of the Southern Ocean. Paleogeog., Paleoclim., Paleoecol., v. 5, no. 41, p. 41-62.

Grindley, G.W. 1963. The geology of the Queen Alexandra Range, Beardmore Glacier, Ross Dependency, Antarctica; with notes on the correlation of Gondwana sequences. New Zealand Jour. of Geol. and Geophys., v. 6, no. 3, p. 304-347.

Grindley, G.W. 1967. Geomorphology of the Miller Range, Transantarctic Mountains, with notes on the glacial history and neotectonics of East Antarctica. New Zealand Jour. of Geol. and Geophys., v. 10, no. 2, p. 557-598.

Guilcher, A. 1963. Continental shelf and slope (continental margin), in Hill, M.N., ed., The Sea, v. 3, John Wiley and Sons, New York, p. 281-311.

Gunn, B.M. and Warren, G. 1962. Geology of Victoria Land between the Mawson and Mulock Glaciers, Antarctica. Bull. of the Geol. Surv. of New Zealand, N.S., no. 71, 157 p.

Gunner, J.D. 1969. Petrography of metamorphis rocks from the Miller Range, Antarctica. Report no. 32, Institute of Polar Studies, The Ohio State University, Columbus, Ohio, 44 p.

Hamilton, W.B. 1969. Late Tertiary glaciation of Antarctica. Geol. Soc. of Amer., Prof. Paper 650-A, p. 214.

Harrison, P.W. 1957. A clay till fabric: its character and origin. Jour. Geol., v. 65, p. 275-308.

Heirtzler, J.R., Dickson, G.D., Herron, E.M., Pitman, W.C. III and LePichon, X. 1968. Marine magnetic anomalies, geomagnetic field reversals and motions of the ocean floor and continents. Jour. Geophys. Res., v. 73, no. 2119.

Hollin, J.T. 1962. On the glacial history of Antarctica. Jour. Glac., v. 4, p. 173-195.

Houtz, R. and Meijer, R. 1972. Structure of the Ross Sea shelf from profiler data (abstract): in Adie, R.J., ed., Antarctic Geology and Geophysics, Universitetsforlaget, Oslo, p. 745.

Hughes, T. 1971. Is the West Antarctic ice sheet disintegrating? I.S.C.A.P. Bull no. 1, Institute of Polar Studies, The Ohio State University, Columbus, Ohio, 77 p.

Hughes, T. 1973. Glacial permafrost and Pleistocene Ice Ages. Permafrost: North American Contribution [to the] Second International Conference, Yakutak, Siberia. Washington: National Academy of Science, 1973. p. 213-223.

John, B.S. 1972. Evidence from the South Shetland Islands towards a glacial history of West Antarctica. Instit. of British Geogr. Special Publ., no. 4, p. 75-92.

Johns, W.D., Grim, R.E. and Bradley, W.F. 1954. Quantitative estimations of clay minerals by diffraction methods. Jour. Sed. Pet., v. 24, p. 242-251.

Kaula, W.M. 1969. A tectonic classification of the main features of the Earth's gravitational field. Jour. Geophys. Res. v. 74, p. 4807-4826.

Krinsley, D. and Takahashi, T. 1962. Surface textures of sand grains - an application of electron microscopy: glaciation. Science, v. 133, no. 3546, p. 1262-1264.

LePichon, X. 1968. Sea-floor spreading and continental drift. Jour. Geophys. Res., v. 73, no. 3661.

Lepley, L.K. 1964. Submarine geomorphology of the eastern Ross and Sulzberger Bay, Antarctica. M.S. thesis, Texas A&M University.

Lindsay, J.F. 1969. Stratigraphy and sedimentation of Lower Beacon rocks in the central Transantarctic Mountains, Antarctica. Report 33, Institute of Polar Studies, The Ohio State University, Columbus, Ohio, 58 p.

Linkletter, G.O. 1972. Weathering and soil formation in the dry valleys of southern Victoria Land: a possible origin for the salts in the soils: in Adie, R.J., ed., Antarctic Geology and Geophysics, Universitetsforlaget, Oslo, p. 441-446.

Mayewski, P.A. 1972. Glacial geology near McMurdo Sound and comparison with the central Transantarctic Mountains. Ant. Jour. of the U.S., v. 7, no. 4, p. 103-106.

McElroy, C.T. 1969. Comparative lithostratigraphy of Gondwana sequences, eastern Australia and Antarctica: in Gondwana Stratigraphy, I.U.G.S. Symposium, Buenos Aires, p. 441-446.

McGregor, V.R. 1965. Notes on the geology of the area between the heads of the Beardmore and Shackleton Glaciers, Antarctica. New Zealand Jour. of Glac., v. 8, no. 2, p. 278-291.

McKelvey, B.C., Webb, P.N., Gorton, M.P. and Kohn, B.P. 1970. Stratigraphy of the Beacon Supergroup between the Olympus and Boomerang Ranges, Victoria Land, Antarctica. Nature, London, v. 227, no. 5263, p. 1126-1128.

McSaveney, M.J. and McSaveney, E.R. 1972. A reappraisal of the Pecten glacial episode, Wright Valley, Antarctica. Ant. Jour. of the U.S., v. 7, no. 6, p. 235-240.

Mercer, J.H. 1968. Glacial geology of the Reedy Glacier area, Antarctica. Geol. Soc. of Amer. Bull., v. 79, p. 471-486.

Mercer, J.H. 1972. Some observations on the glacial geology of the Beardmore Glacier area: in Adie, R.J., ed., Antarctic Geology and Geophysics, Universitetsforlaget, Oslo, p. 427-433.

Mirsky, A., Treves, S.B. and Calkin, P.E. 1965. Stratigraphy and petrography, Mount Gran area, Southern Victoria Land, Antarctica: in Hadley, J.B., ed., Geology and Paleontology of the Antarctic, Antarctic Res. Series, v. 6, Amer. Geophys. Union, p. 145-175.

Nichols, R.L. 1960. Geomorphology of Marguerite Bay area, Palmer Peninsula, Antarctica. Bull. Geol. Soc. Amer., v. 71, p. 1421-1450.

Nichols, R.L. 1961. Multiple glaciation in Wright Valley, McMurdo Sound, Antarctica (abstract): Tenth Pacific Science Congress, Honolulu, p. 317.

Nichols, R.L. 1966. Geomorphology of Antarctica: in Tedrow, J.F. ed., Antarctic Soils and Soil Forming Processes, Ant. Res. Series, v. 8, Amer. Geophys. Union, p. 1-46.

Nichols, R.L. 1968. Coastal geomorphology, McMurdo Sound, Antarctica. Jour. of Glac., v. 7, no. 51, p. 449-478.

Nichols, R.L. 1971. Glacial geology of Wright Valley: in Quam, L.O., ed., Research in the Antarctic, Amer. Assoc. for the Adv. of Sci., Washington, D.C., Publ. 93, p. 293-340.

Nye, J.F. 1959. The motion of ice sheets and glaciers. Jour. Glac., v. 3, p. 493-507.

Oliver, R.L. 1964a. The level of former glaciation near the mouth of the Beardmore Glacier: in Adie, R.J., ed., Antarctic Geology, Amsterdam, North-Holland Publ. Co., p. 138-142.

Oliver, R.L. 1964b. Geological observations at Plunket Point, Beardmore Glacier: in Adie, R.J., ed., Antarctic Geology, Amsterdam, North-Holland Publ. Co., p. 248-258.

Olson, E.A. and Broecker, W.S. 1961. LaMont natural radiocarbon measurements VII. Radiocarbon, v. 3, p. 141-175.

Paterson, W.S.B. 1969. The Physics of Glaciers: Pergamon Press, Oxford, 250 p.

Pessl, F. Jr. 1971. Till fabrics and till stratigraphy in western Connecticutt: in Goldthwait, R.P., ed., Till--a Symposium, The Ohio State University Press, Columbus, Ohio, p. 92-105.

Pettijohn, F.J. 1957. Sedimentary Rocks. Harper and Row Publ., 718 p.

Péwé, T.L. 1961. Multiple glaciation in the McMurdo Sound Region, Antarctica--A progress report: in Reports of Antarctic Geological Observations 1956-1960, I.G.Y. Glac. Report No. 4, p. 25-50.

Rex, R.W. and Margolis, S.V. 1969. Surface features on sand grains from Antarctic continental shelf and deep-sea cores. Ant. Jour. of the U.S., v. 4, p. 168.

Robin, G. deQ. 1964. Glaciology. Endeavor, v. 23, no. 89, p. 102-107.

Rutford, R.H. 1972. Glacial geomorphology of the Ellsworth mountains: in Adie, R.J., ed., Antarctic Geology and Geophysics, Universitetsforlaget, Oslo, p. 233.

Rutford, R.H., Craddock, C., White, C.M. and Armstrong, R.L. 1972. Tertiary glaciation in the Jones Mountains: in Adie, R.J., ed., Antarctic Geology and Geophysics, Universitetsforlaget, Oslo, p. 239-243.

Schwerdtfeger, W. 1968. The relation between terrain features, thermal wind, and surface wind over Antarctica. Ant. Jour. of the U.S., p. 190-191.

Strahler, A.W. 1952. Hypsometric (area-altitude) analysis of erosional topography. Bull. Geol. Soc. Amer., v. 63, p. 1117-1142.

Suyetova, I.A. 1970. Features of Pleistocene and present-day Antarctic ice cover (abstract). S.C.A.R. Proc., Oslo.

Tanner, W.F. 1968. Multiple influences on sea-level changes in the Tertiary. Paleogeog., Palioclim., Paleoecol., v. 5, no. 41, p. 165-171.

Taylor, G. 1930. Antarctic Adventure and Research, D. Appleton and Co., New York, 245 p.

Theil, E.C. 1962. The amount of ice on planet Earth. Ant. Res. Mono. No. 7, p. 172-175.

Turner, A.K. 1972. Contour plotting section of the G.C.A.R.S. roadway selection system: Ohio Dept. of Highways, Columbus,Ohio.

Ugolini, F.C. 1970. Antarctic soils and their ecology: in Holdgate, M.W., ed., Antarctic Ecology, Acad. Press, London, v. 2, p. 673-692.

Voronov, P.S. 1965. Attempt at a reconstruction of the Antarctic ice cap of the epoch of the Earth's maximum glaciation: Societ Ant. Exp. v. 3, Elsevier Publ. Co., Amsterdam, p. 88-93.

Wade, F.A., Yeats, V.L., Everett, J.R., Greenlee, D.W., LaPrade, K.E., and Shenk, J.L. 1965. The geology of the central Queen Maud Range, Transantarctic Mountains, Antarctica. Texas Tech. College Research Report Series, Antarctic Series No. 65-1, 54 p.

Webb, P.N., 1972. Wright fjord, Pliocene marine invasion of an Antarctic dry valley. Ant. Jour. of the U.S., v. 7, no. 6, p. 226-234.

Weertman, J. 1964. Profile and heat balance at the bottom surface of an ice sheet fringed by mountain ranges: in Publ. no. 61 of the I.A.S.H. Com. of Snow and Ice, p. 245-252.

Weertman, J. 1962. Mechanism for the formation of inner moraines found near the edge of cold ice caps, CRREL Report No. 94, 12 p.

Wilding, L.P. and Drees, L.R. 1966. Quantity estimations of clay minerals. The Ohio State University, Dept. of Agronomy (unpub. ms.).

Wilson, A.T. 1966. Variation in solar insolation to the South Polar Region as a trigger which induces instability in the Antarctic ice sheet. Nature, v. 210, p. 477-478.

Zhivago, A.V. 1962. Outlines of southern ocean geomorphology. Antarctic Research, Geophys. Mono. 7, Amer. Geophys. Union, p. 74-80.

TRANSANTARCTIC MTS.

EAST ANTARCTIC ICE SHEET

SOUTH POLE

BYRD LAND

MARIE

ROSS ICE SHELF

ROSS SEA

MOUNTAINS

SOUTH VICTORIA LAND

QUEEN MAUD MTS.

SCOTT GL.

AMUNDSEN GL.

SHACKLETON GL.

BEARDMORE GL.

TAYLOR V.

WRIGHT V.

VICTORIA V.

GROUNDING LINE
SHACKLETON GLACIATION

GROUNDING LINE
SCOTT GLACIATION

GROUNDING LINE
QUEEN MAUD GLACIATION

SCALE

50 0 100 200 300 400 500

KILOMETERS

LEGEND

- 3000 — c.i. = 500m — Present ice sheet elevation contours*
- Outline of present Ross Ice Shelf drainage system®
- Present inland margin of outlet glaciers and their basins of exudation*
- Present coastline* and grounding line
- D — D' Profiles (← along present ice flowlines*)
- 500 — c.i. = 100m — Present Ross Ice Shelf thickness•
- 600 — c.i. = 200m — Depth of ocean floor below sea level•
- Generalized present ice front*
- Former grounding lines (isostatically corrected)
- Computerized areas

Based on: *American Geographical Society Map of Antarctica (1970), ®Giovinetto and Robinson (1966), •Crary and others (1962), •Hughes (1972)

FIGURE 53